SECONDARY METABOLITES FROM ENDOPHYTIC FUNGI: ISOLATION, PURIFICATION, CHARACTERIZATION AND BIOASSAY.

A THESIS
SUBMITTED TO THE
UNIVERSITY OF PUNE

FOR THE DEGREE OF
DOCTOR OF PHILOSOPHY
IN
BIOTECHNOLOGY

BY
D. SREEKANTH

UNDER THE GUIDANCE OF
DR. M. I. KHAN

BIOCHEMICAL SCIENCES DIVISION
NATIONAL CHEMICAL LABORATORY
PUNE – 411008
INDIA

DECEMBER, 2008

DEDICATED TO MY MENTOR

Contents

Page no.

- **Acknowledgement** **i**
- **Certificate** **iv**
- **Declaration** **v**
- **Key to abbreviations** **vi- vii**
- **Abstract** **viii- xi**
- **Chapter 1:** **1- 39**

  General introduction
  References **32- 39**

- **Chapter 2:** **40- 66**

  Isolation, Screening, Morphological and Molecular characterization of taxol producing endophytic fungus.

  1. Summary 40
  2. Introduction 40- 41
  3. Materials 41- 43
  4. Methods 43- 50
  5. Results 51- 62
  6. Discussion 62- 63
  7. References 64- 66

- **Chapter 3:** **67- 87**

  Production, purification, characterization and bioassays of taxol and its precursor 10 DAB III.

  1 Summary 67
  2 Introduction 67- 68
  3 Materials 68
  4 Methods 68- 73
  5 Results 73- 83
  6 Discussion 83- 85
  7 References 85- 87

❖ **Chapter 4:** **88- 108**

Microbial transformation of 10 DAB III and side chain to biologically active taxanes.

1. Summary 88
2. Introduction 88- 89
3. Materials 89- 90
4. Methods 90- 94
5. Results 94- 105
6. Discussion 106- 107
7. References 107- 108

❖ **Chapter 5:** **109- 124**

Taxol-fluorescent conjugates: Synthesis and their applications.

1. Summary 109
2. Introduction 109
3. Materials 110
4. Methods 110- 113
5. Results 113- 120
6. Discussion 120- 122
7. References 122- 124

❖ **Chapter 6:** **125- 140**

Effect of Rhodamine-taxol conjugate on caveolin dynamics.

1. Summary 125
2. Introduction 125
3. Materials 126
4. Methods 126- 127
5. Results 127- 137
6. Discussion 138- 139
7. References 139- 140

❖ **Chapter 7:** **141- 151**

General Discussion and Conclusions
References 149- 151

❖ **Author's publication.** **152**

Acknowledgement

This thesis arose in parts out of the years of research that has been done since I came into **Dr. Khan's** group. Since then, I have worked with a great number of people whose contributions in assorted ways to the research and making of this thesis deserves special mention. It is a pleasure to convey my gratitude to them all in my humble acknowledgment.

In the first place I would like to record my gratitude to **Dr. Islam Khan** for his supervision, advice, and astute guidance from the very early stage of this research as well as giving me extraordinary experiences through out the work. Above all and the most needed, he provided me unflinching encouragement and support in various ways. His very true scientific intuition has made him a constant oasis of ideas, which exceptionally inspire and enrich my growth as a student, a researcher and as a scientist, which I want to be. His support at times which I was in needed will never be forgotten. I am indebted to him more than he knows.

Also, I gratefully acknowledge **Dr. Absar Ahmad** for his advice, supervision, and crucial contribution throughout, which made him a backbone of this research and so to this thesis. I am obliged to him for his invaluable guidance in the course of investigation. Without his support, completion of this work would not have been possible.

I would like to extend my sincere gratitude to **Dr. Sushma Gaikwad** for her valuable suggestions, kind help whenever required and for giving her precious time in constructing my thesis.

I would like to thank all my collaborators **Dr. Krishna Sastry, Dr. Dhiman Sarkar** and **Dr. Bashir Khan** for their help in conducting various experiments, allowing me to utilize their facilities and guiding me in choosing apt approaches during the course of investigation.

I am also grateful to **Mrs. Santakumari** for her ever ready help in conducting experiments on LC-MS and in analyzing them. I am very thankful to **Dr. Suresh** and to **Dr. Sumedha** for their suggestions and guidance.

My sincere thanks to Sampa and Neesar for their help in Cell culture work.

This thesis would not have been completed without the help of Dr. Raghupathi garu who has provided me sincere help involving chemical modifications. He has also helped me in the understanding of many concepts including NMR. I also cherish all those light moments I shared with him.

I would like to express my deepest love and gratitude to my seniors/ friends Dr. Anil Kumar, Dr. Atul Thakur, Dr. Feroz, Dr. Manish Arha, Dr. Manish Chandra, Dr. Rohini garu, Dr. Suresh, Dr. Shivshankar, Dr. Siddharth and Dr. Sucheta for their help in the course of investigation. I would always cherish the moments and the unlimited fun I shared with Dr. Satya, Dr. Nookaraju and Ambrish.

My sincere thanks to Natasha, Sunaina, Yogita, Kapil Kandelwal, Kapil, Satya, Praveen, Vivek and Sandya, my trainees who have helped me a lot in finishing my bench work and further my knowledge in many aspects.

It gives me a great pleasure to thank all my friends and lab mates Asad, Ashutosh, Avinash, Harish, Ravi, Shadab, Shabab, Prasad, Shahi, Nags, Late. Rohtas, Sajid, Jp, Madhurima, Sameer, Rodu, Noor, Arun, Raju, Rishi, Somesh, Ashish, Ashif, Mayank, Santosh, Maggie, Bhuvan, Nishant, Raman, Rajendhar, Shivswaroop, Sreekar, Mujahid, Vicky, Meera, Ramya, Pankaj, Prashanth, Preeti and Vivek for making my stay in NCL memorable and enjoyable.

I will always treasure the memories I gathered from my P-group members Atul Kumar, Ansary, Dip-T, Geeta, Sarvanan I, Sarvanan A, Shivendroo, Daisy and Swat Cat.

I have no words to extend my thanks to my best buddy **Sush** for his support in my thick and thin days. He has been a constant support, inspiration and strength in many aspects of my life. Probably I will run short of adjectives to praise him, in one word I can say that I cannot ask for any better human being like him. Same is for my pal **Punu**, she has given me a never ending support and been on my side in every

instance. She has made my stay more comfortable with her presence. I will treasure the laughs, fights and tears I have shared with them till my last breath.

My warm love and sincere thanks to my **Father, Mother, Aunt, Sister, Brother** and **Brother-in-law** for their never ending support, uncountable sacrifices they have made and the struggle that they have gone through for my studies. What ever I am today is because of them. I also thank my relatives who have been a supportive for me. I extend my love and thanks to my wife **Swapna**, for her continuous support, being very understanding and helping me to fight back in all odd situations. I thank God for blessing me with such a wonderful life partner.

Lastly, I thank the Head, Division of Biochemical Sciences and Director, NCL, Pune for allowing me to work at NCL. I Thank CSIR to for financial support.

Thanks to the Almighty for whatever he has given me.

December 2008. **Sreekanth Dasari**

CERTIFICATE

This is to certify that the work incorporated in the thesis entitled "**Secondary metabolites from endophytic fungi: Isolation, purification, characterization and bioassay**" submitted by **D. Sreekanth** for the degree of Doctor of Philosophy was carried out under my supervision at the Biochemical Sciences Division, National Chemical Laboratory, Pune. Materials obtained from other sources have been duly acknowledged in the thesis.

Date:

Dr. M. I. Khan
(Research guide)

DECLARATION

I hereby declare that the thesis entitled, "**Secondary metabolites from endophytic fungi: Isolation, purification, characterization and bioassay**" has been carried out in the Biochemical Sciences Division, National Chemical Laboratory, Pune under the guidance of **Dr. M. I. Khan**. The work is original and has not been submitted in part or full by me for any other degree or diploma to any other University. I further declare that the materials obtained from other sources have been duly acknowledged in the thesis.

D. Sreekanth

Date:
Place: Biochemical Sciences Division,
National Chemical Laboratory (NCL),
Pune – 411008, India.

ABBREVIATIONS

µg	Microgram
µL	Micro liter
BSA	Bovine serum albumin
CDI	N,N' Cardonyldiimidazole
CdS	Cadmium sulphate
CIEIA	Competitve inhibition enzyme linked immuno assay
CMA	Corn meal agar
DAB	Deacetyl baccatin
DMF	Demethyl formamide
DMSO	Dimethyl sulphoxide
DNA	Deoxyribonucleic acid
dNTP	Deoxyribonucleotide triphosphate
E. coli	*Escherichia coli*
EDTA	Ethylenediaminetetraacetic acid
ESI-MS	Electron Spray Ionization Mass spectrophotometery
FBS	Fetal bovine serum
FITC	Fluorescene isothiocyanate
g/ gm	Grams
GFP	Green fluroscent protein
HBT	Hydroxyl benzo triazol
HPLC	High Performance Liquid Chromatography
IC_{50}	50 % inhibitory Concentration
IPTG	Isopropyl-beta-D-thiogalactopyranoside
ITS	Internal Trascription spacer regions
Kb/Kbp	Kilo base pairs
Kd/Kda	Kilo Daltons
LB(A)	Luria Bertani (Agar)
LC-MS	Liquid chromatography Mass spectrophotometery
MALDI-TOF	Matrix Assisted Laser Dissorption Ionization Time of Flight
mg	Milli gram

MIC	Minimum Inhibitory Concentration
min(s)	Minute(s)
mL	Milli liter
mM	Milli molar
MTT	3-(4,5-dimethylthiazol-2-yl)-2,5-diphenyltetrazolium bromide
ng	Nanogram
nm	Nano meter
nM	Nano molar
OD	Optical density
SDS-PAGE	Sodium Dodecyl sulfate Polyacrylamide gel electrophoresis
OMA	Oat meal agar
PBS	Phosphate buffered saline
PDA	Potato dextrose agar
SMQ	Sterile Milli Q water
TAE	Tris acetic EDTA buffer
TBS-Cl	Tertiary Butyl Silisyl- Chloride
TE	Tris EDTA buffer
TEMED	Tetramethylethylenediamine
TIRFM	Total ineternal reflection fluroscence microscopy
TLC	Thin layer chromatography
UV	Ultra violet
X-gal	5-bromo-4-chloro-3-indolyl-β-D-galactoside

ABSTRACT

Drug-resistance of pathogens causing fatal diseases has increased in recent years, which is a prime aspect to be addressed by researchers. Evidently, scientists have provided the public health cause with many effective drugs and vaccines, but the battle against these witty microbes is still far from over. Diseases caused by microbes (bacteria, viruses, fungi, protozoans and prokaryotes) such as respiratory infections, HIV/ AIDS, tuberculosis and malaria and diseases such as cancer account for many infections deaths. These microbes obtained resistance to many of the first-line drugs used for the treatment. Resistance to these first-line drugs has forced to change the treatment to more expensive second- or third-line agents. If resistances to these drugs also emerge, we would run out of treatment options.

An intensive search for newer and more effective agents to deal with these problems is now underway. One such renewable source apart from the medicinal plants is endophytic microbes, which reside in the tissues between living plant cells. Some of the interesting compounds produced by endophytic microbes are taxol, cryptocin, cryptocandin, jesterone, oocydin, isopestacin, the psuedomycins and ambuic acid. The reason endophytes mimic the chemistry of their respective hosts and make the same bioactive natural products or derivatives has been attributed to the possible intergeneric-genetic exchange between higher plants and the endophytic microbe.

Usually the host-endophyte associations are symptom-less, as the latter do not interfere with the host biological or physiological affairs. In some cases, especially in grasses, it is observed that secondary metabolites produced by the inhabitant endophytes show beneficial effects on the growth of the host. Plants infected by some endophtyes which produce alkaloids have also been found to be pest-resistant. In turn the host provides nutrition, protection and improved dissemination of the endophytes (via seeds). Thus, endophytes and their metabolites have proven to be a potential source of novel biology and chemistry to assist in helping solve not only human health, but plant and animal health problems also.

Chapter I: General Introduction.

This chapter gives a general introduction to endophytes and their secondary metabolites. Further, a detailed survey of literature regarding taxol, its history, sources of its production, its application and biotechnological aspects of microbes producing it will be summarized.

Chapter II: Isolation, Screening, Morphological and Molecular characterization of taxol producing endophytic fungus.

The endophytic fungal population was explored from different tissues of *Taxus baccata* growing at higher altitudes of West Bengal, India. The isolated fungal population represented different genera, which were screened for taxol production using immunoassay (CIEIA) technique. The culture AAT-TS-4_1 that produced taxol was identified as *Gliocladium* sp. on the basis of its cultural as well as morphological characters, ITS and 18S rRNA sequence analysis. Kinetics of taxol production as a function of culture growth was also investigated.

Chapter III: Production, purification, characterization and bioassays of taxol and10 DAB III.

Out of the forty fungal cultures screened, one fungus *Gliocladium* sp. was found to produce taxol and 10DAB III (10 Deacetyl baccatin III). These compounds were purified by TLC, column chromatography, HPLC and characterized using UV-Spectroscopy, ESI-MS, MS/MS and proton NMR. One liter of *Gliocladium* sp. culture yielded 10 µg of taxol and 65 µg of 10 DAB III. The purified taxol from the fungus showed cytotoxicity towards cancer lines; HL-60 (leukemia), A431 (epidermal carcinoma) and MCF-7 (breast cancer). Antibacterial activity of taxol, 10DAB III and baccatin III against different pathogenic bacteria was also determined.

Chapter IV: Microbial transformation of 10 DAB III and side chain to biologically active taxanes.

Microbial transformation of 10 DAB III and side chain (N-benzoyl-(2R, 3S)-3-phenylisoserine) to biologically active taxanes using a taxol producing fungus *Gliocladium* sp was carried out. The transformed compound was purified by TLC and HPLC. The purified compound has similar chromatographic and spectroscopic properties as that of taxol. However further characterization with the help of MALDI-TOF and LC-MS lead to the conclusion that the compound obtained is 10 Deacetyl

paclitaxel. 10 Deacetyl paclitaxel showed affinity to tubulin, the prime target of many taxanes and was immunologically detected using taxane antibodies. Cytotoxicity of the compound was determined against A431 and THP1 cancer cell lines.

Chapter V: Taxol-fluorescent conjugates: Synthesis and their applications**.**

Taxol was chemically derivatized accordingly to couple with FITC, Rhodamine and CdS nanoparticles. Two different strategies were employed to synthesize taxol with free amino group and with free carboxyl group. All the conjugates were purified by preparative TLC and HPLC and further characterized by spectroscopic and fluoremetric techniques. Cytotoxicity of all the intermediate compounds and conjugates was determined by MTT assay. All the conjugates purified were immunologically estimated and further used for different microscopy purposes. CdS-taxol conjugate was treated on different cell lines and fluorescence microscopy was done to exploit the fluorescence properties of CdS. A detailed study on CdS-taxol conjugate using fluorescence microscopy was done.

Chapter VI: Effect of Taxol –Rhodamine conjugate on caveolin dynamics**.**

Caveolin-1, a marker protein of caveolae is found to be induced by taxol. However, as reported earlier taxol binds to microtubules but not to caveolin, thus the role of it's over expression when treated with taxol in MCF-7 is not clear. Thus we tried to understand the caveolin dynamics on HeLa cells transfected (transient) with GFP when treated with Taxol-Rhodamine conjugate by Total internal reflection microscopy. Experiments were also done on 293T cell line, which has very low expressions of caveolin. To understand the localization of Rhodamine-taxol conjugate and Caveolin-1-GFP on HeLa cells, confocal imaging was done at different time intervals.

Chapter VII: General Discussion and Conclusions**.**

This chapter deals with the general discussion of the results obtained from all the working chapters. Endophytes from Indian yew tree *Taxus baccata* were explored for taxol producing nature. Out of 40 fungal strains obtained, one fungus identified as *Gliocladium* sp was found to produce taxol and 10 DAB III in culture medium. Taxol concentrations increased with increase in incubation time i.e 21 days old culture yielded a maximum of 10 µg/ lit of taxol and 65 µg/ lit of 10 DAB III, while taxol was even

detected in 2 days old culture. Fungal taxol and 10 DAB III were detected immunologically using taxol and taxane antibodies. Taxol ESI-MS spectrum showed peak at *m/z* 854 attributing to M+H ion, while 10 DAB III showed peak at *m/z* 545 attributing to M+H ion. Proton NMR of fungal taxol was similar as that of the reported plant taxol. Fungal taxol showed cytotoxicity against HL 60, MCF 7 and A431 cell lines.

Microbial transformation of 10 DAB III and side chain using fungus *Gliocladium* sp yielded biologically active taxane. Purification by prep-TLC and HPLC yielded compound which showed affinity to microtubules and was detected immunologically using taxane antibodies. LC-MS and MALDI-TOF analysis showed peak at *m/z* 811 attributing to M+ ion of 10 Deacetyl paclitaxel. 10 Deacetyl paclitaxel showed cytotoxicity against THP 1 and A431 cell lines.

Taxol was successfully derivatized into 7, succinyl taxol and to 2' 1, 6-diaminoheaxane taxol to couple with fluorescent molecules such as FITC, Rhodamine and CdS nanoparticles. All the conjugated and intermediates showed cytotoxicity against cancer cell lines. Biochemical characterization of the conjugates was done by spectroscopic and fluoremetric analysis. Further, conjugates were used for *in vivo* based on microscopy.

Taxol- Rhodamine treatment on HeLa cells transfected with GFP (transiently) showed sudden recruitment of caveolin 1 and the withdrawal of the same with the increase in time (Kiss and run dynamics). It was also observed that most of the Rhodamine-taxol signals were intense at the sites where Caveolin-1- GFP was high on the HeLa cell surface. The most important out come of this work where we observed that there was no Rhodamine-taxol dynamics on the surface of 293T cell line which shows very poor expression of caveolin. This behavior of Rhodamine-taxol conjugate on 293T cell line gives us a lead to understand the requirement of caveolin1 for the up take of drug. The recruitment and withdrawal dynamics of caveolin seen on the surface of HeLa cell line also suggests its requirement of taxol up take. Further localization of Caveolin-1- GFP and Rhodamine-taxol conjugate was observed by confocal microscopy.

Chapter 1

General Introduction

Drug resistance to many deaths causing diseases has increased in recent years, which is a prime aspect to be addressed by researchers. Evidently, scientists have provided the public health cause with many effective drugs and vaccines, but the battle against these witty microbes is still far from over. Diseases caused by microbes such as bacteria, viruses, fungi, protozoans and prokaryotes include respiratory infections, HIV/ AIDS, tuberculosis and malaria and incurable/ dreadful diseases such as cancer account for many infections and deaths. These microbes have attained resistance to many of the first line drugs used for their treatment. Resistance to these first line drugs has forced a change to more expensive second or third line agents. If resistance to these drugs also emerges, we would run out of treatment options. Research in the fronts of improving infection control, exploiting nature for more effective drug discovery and using drugs more appropriately against the disease causative agents needs to be initiated.

1. Secondary metabolites: Lead for novel drug discovery

Secondary metabolites are naturally derived metabolites and/or by-products from microorganisms, plants, or animals (Baker et al, 2000). These metabolites have been explored and exploited for human use for thousands of years, and plants have been investigated as a source of compounds used for medicine. As evident, the Chinese use more than 5,000 plants and their products in their traditional medicine (Bensky et al, 1993). History also shows that now-extinct civilizations had also discovered the benefits of medicinal plants. In fact, nearly 3,000 years ago, the Mayans used fungi grown on roasted green corn to treat intestinal ailments (Buss et al, 2000). More recently, the Benedictine monks (800 AD; FIG 1) began to apply *Papaver somniferum* as an anesthetic and pain reliever like the Greeks had done for years before (Grabely et al, 1999). Many people, in past times, realized that leaf, root, and stem concoctions had the potential to help them. Even though an understanding of the chemical nature of bioactive compounds in these complex mixtures and how they functioned remained a mystery, these plant products, in general, enhanced the quality of life, reduced pain and suffering, and provided relief,

Until Pasteur discovered that fermentation is caused by living cells that people seriously began to investigate microbes as a source for bioactive natural products. Then, scientific serendipity and the power of observation provided the impetus to Fleming to usher in the antibiotic era via the discovery of penicillin from the fungus *Penicillium notatum*. After which, array of bioactive metabolites were isolated form micro organisms including fungi, bacteria and actinomycetes. These include the isolation of anti-cancerous, anti-oxidants, anti-fungal, anti-bacterial, anti-viral, anti-insecticidal and immnosuppressant compounds.

FIG 1: An ancient painting depicting a man in search of traditionally used Chinese medicinal plants and herbs (by **Li Shizhen**).

2. Plants: A potential source for bioactive molecules

Plants supply most of the active ingredients of traditional medicinal products, and plant extracts have long been used in screening programmes in pharmaceutical companies and university institutes. It might be thought that most of the plant kingdom has been thoroughly examined in the search for biologically active molecules. However, this is unlikely to be the case. There are estimated to be ~250,000 species of plants in the world and probably ~10% of these have been tested for some type of biological activity (Verpoorte, 1998). In traditional medicine systems in countries such as India and China (Baker et al 2000; Chang et al, 1986; Dev, 1999), plants have formed the basis for novel drug discovery. The use of plants in the traditional medicine of many other cultures has been extensively documented (Kapoor, 1990). These plant based systems continue to play an essential role in health care, and it has been estimated by the World Health Organization that approximately 80% of the world's inhabitants rely mainly on traditional medicines for their primary health care (Schultes et al, 1990; Arvigo et al, 1993). Plant products also play an important role in the health care systems of the remaining 20% of the population, mainly residing in developed countries. In a study it has been shown that at least 119 chemical substances, derived from 90 plant species, can be considered as important drugs that are in use in one or more countries (Schultes et al, 1990). Of these 119 drugs, 74% were discovered as a result of chemical studies directed at the isolation of the active substances from plants used in traditional medicine.

Examples of traditional medicine providing leads to bioactive natural products abound. Suffice it to point to some recent confirmations of the wealth of this resource. Artemisinine (qinghaosu) (FIG 2) is the antimalarial sesquiterpene from a Chinese medicinal herb *Artemisia annua* (Wormwood) used in herbal remedies since ancient times (Arvigo et al, 1993; Farnsworth, 1985). Forskolin (FIG 2) is the antihypertensive agent from *Coleus forskohlii* Briq. (Labiatae), a plant whose use was described in ancient Hindu Ayurvedic texts (Clark, 1996; Bhat et al, 1977). The ginkgo tree, mentioned in Chinese medicinal books from 2800 B.C. and used in antiasthmatic and antitussive preparations, produces the ginkgolides, unusual diterpenes containing a tertiary butyl group (FIG 3). Their involvement in the clinical efficacy of ginkgo tree extracts was reported in 1987 (Kinghorn, 1987).

Castanospermine, a tetrahydroxyindolizidine alkaloid isolated from the Australian plant *Castanospermum australe* (FIG 3), inhibits replication of the human immunodeficiency virus (HIV) (Hamburger, 1991).

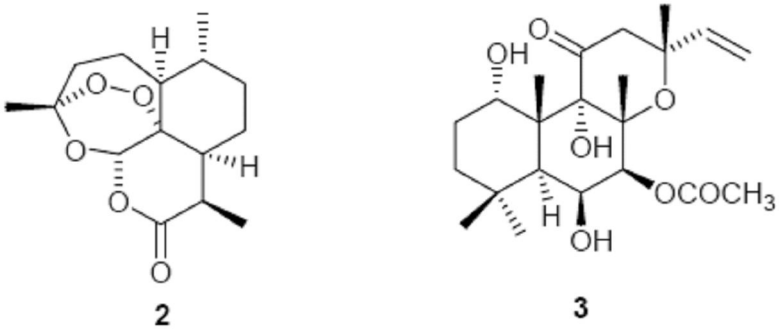

2 **3**

Figure 2: Artemisinin (**2**) and forskolin (**3**)

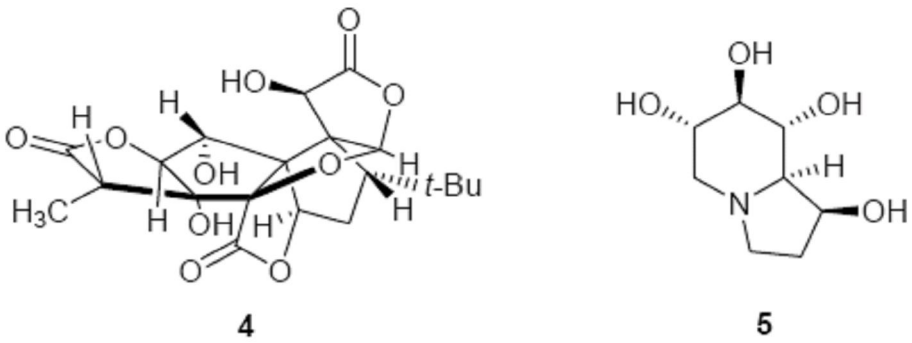

4 **5**

Figure 3: A ginkgolide (**4**) and castanospermine (**5**)

3. Microbes: As a rich source of bioactive molecules

Fleming in 1929 discovered the serendipitous penicillin from the filamentous fungus, *Penicillium notatum,* and he discovered the broad therapeutic use of this agent in the 1940s. This ushered a new era in medicine, the so-called Golden Age of Antibiotics (Mann, 1994). This discovery promoted the intensive investigation of nature as a source of novel bioactive agents, and microorganisms have proved to be a prolific source of structurally diverse bioactive metabolites which have yielded some of the most important products of the pharmaceutical industry.

This lead to discover more novel compounds including antibacterial agents, such as the penicillins (from *Penicillium* species), cephalosporins (from *Cephalosporium cryptosporium*), aminoglycosides, tetracyclines, and other polyketides of many structural types (from the *Actinomycetales*); immunosuppressive agents, such as the fungal metabolites, the cyclosporins, and rapamycin (from *Streptomyces* species); cholesterol-lowering agents, such as mevastatin (compactin) and lovastatin (from *Penicillium* species); and anthelmintics and antiparasitic drugs, such as the ivermectins (from *Streptomyces* species) (Buss and Waigh, 1995).

Cancer chemotherapeutic agents were also discovered which include members of the anthracycline, bleomycin, actinomycin, mitomycin, and aureolic acid families (Newman and Cragg, 2005). Some of them in these proved to be clinically important which include daunomycin-related agents, daunomycin itself, doxorubicin, idarubicin, and epirubicin; the glycopeptidic bleomycins A2 and B2 (Blenoxane®); the peptolides exemplified by d-actinomycin; the mitosanes such as mitomycin C; and the glycosylated anthracenone, mithramycin. Most of these compounds were isolated from various *Streptomyces* species (Foye, 1995).

The epothilones, isolated from the *Myxomycetales* (gliding bacteria) have drawn the eyes of many researchers as a potential antitumor agents due to their mechanism of action being the same as that of paclitaxel (vide infra) though having, at first glimpse, quite a different topology (Wartmann and Altmann 2002). Other microbially derived drugs which have gained importance include the indolocarboxazoles, represented by staurosporine and its simple derivative UCN-01, which is in Phase I clinical trials (Dancey and Sausville 2003; Newman et al 2002), and the geldanamycin derivatives, represented by 17-allylamino-geldanamycin (17-AAG), which is also in Phase I trials (Kamal et al 2003; eliakoff et al 2003).

4. Endophytic fungi: A source for novel bioactive secondary metabolites

Endophytic microorganisms are found virtually in every plant on earth. These organisms reside in the living tissues of the host plant and participate in a variety of relationships ranging from symbiotic to pathogenic. Since the discovery of endophytes in Darnel,

Germany, by Freeman 1904, various investigators have defined endophytes in different ways, usually dependent on the perspective from which the endophytes were being isolated and subsequently examined. Bacon and White 2000, give an inclusive and widely accepted definition of endophytes: "Microbes that colonize living, internal tissues of plants without causing any immediate, overt negative effects". While the symptomless nature of endophyte occupation in plant tissue has prompted focus on symbiotic or mutualistic relationships between endophytes and their hosts, the observed biodiversity of endophytes suggests they can also be aggressive saprophytes or opportunistic pathogens.

Fungal endophytes of grasses produce a variety of ergot alkaloids, loline alkaloids, lolitrems, growth hormone and paramine alkaloids both *in vitro* and *in vivo*. (Clay and Schardl, 2002). In *Claviceps*, ergot alkaloids are confined to sclerotium. In contrast, the alkaloids can be isolated from whole parts of the infected plant. Hardy et al 1986 and Lyons et al 1986 found that the presence of alkaloids in infected plants varied in different plant parts (leaf blades, sheaths, flowering culms) at different times of the year and alkaloid concentrations were higher in young than old leaves and in leaf sheaths, then in leaf blades in case of plants infected with endophytes (Bacon et al, 1986; Bush et al, 1982 and Yates et al, 1985). Bacon et al (1975) for the first time demonstrated that endophytic fungus of grass grown in synthetic medium produced precursors of auxin *in vitro*. *In vitro* auxin production by endophytic fungus of grass was also reported by Porter et al (1985).

Cryptosporiopsis cf. *quercina* Petr. is the imperfect stage of *Pezicula cinnamomea* (DC.) Sacc, a fungus commonly associated with hardwood species in Europe. This fungus and the related species occur as endophytes in many parts of the world. It was isolated as an endophyte from T*ripterygium wilfordii*, a medicinal plant native to Eurasia, (Strobel. et al, 1999). On petriplates, *C. quercina* demonstrated excellent antifungal activity against some important human fungal pathogens (*Candida albicans* and *Trichophyton* sp.). Since infections caused by such fungi are a growing health problem, especially among AIDS patients and those who are otherwise immuno-compromised, new antimycotics are needed.

A unique antimycotic, termed cryptocandin was isolated and characterized from *C. quercina*. This bioactive compound is related to known antimycotics, the echinocandins and the pneumocandins and was also active against a number of plant pathogenic fungi, including *Sclerotinia sclerotioum* (Lib.) De Bary and Botrytis cinerea Pers.: Fr. Cryptocandin is currently being considered for applications against several of the fungi that cause human diseases.

Cryptocin, a tetramic acid, is also produced by *C. quercina*. This unusual compound possesses potent activity against *Pyricularia oryzae Cavara* and a number other plant pathogenic fungi (Li et al, 2000). It was ineffective against a general array of human pathogenic fungi. Nevertheless, with the minimum inhibitory concentrations of 0.39 ug/ ml against *P. oryzae*, this compound is being examined as a natural chemical control agent for rice blast. Given the general interest on the part of the public and on the industry to develop safer and more environmentally compatible plant disease control agents, perhaps endophytic fungi do serve as a reservoir of untapped biologically based compounds that may also help in agriculture field.

Biologically important compounds from endophytic fungi will be found only when assay systems will be devised to allow biologically guided fractionation of the culture extracts. Despite an obscure role to either the endophyte or the host-endophyte relationship in most cases, one or more bioactive compounds are still produced. Such is the case of subglutinols A and B, which are immuno- suppressive compounds produced by *Fusarium subglutinans*, an endophyte of *Tripterygium wilfordii* (Lee et al, 1995). The compounds have mean inhibitory concentration (IC_{50}) values of 0.1 µM in the mixed lymphocyte reaction assay. In the same assay system, cyclosporin is roughly as potent as the subglutinols. These compounds are being examined more thoroughly for their ability to serve as immunosuppressive agents.

A perfect example of a suitable bioassay system developed for finding novel bioactive products is Merck Co. - a unique system that allowed the isolation of a molecule dubbed L-783. This compound is a quinone produced by a plant - associated fungus (*Pseudomassaria sp.)* isolated from a plant collected in an African rain forest near

Kinshasa, in the Democratic Republic of Congo (Anonymous, 1999). It lowers blood glucose levels in diabetic mice, thus mimics the action of the polypeptide hormone, insulin. However, unlike insulin it is, not destroyed by enzymes in the digestive tract and can be given orally.

The search for novel endophytes and their associated secondary products should also be directed towards plants that commonly serve native populations for medicinal purposes. It is conceivable that these plants have microbes that mimic the chemistry of the irrespective host plants and make the same bioactive natural products or derivatives that are more active than those of their respective hosts. This is exemplified in the case of taxol from yews and that being produced by a series of endophytes from yews as well as other plant sources. Thus, if a microbial source for a medicinally important substance can be found, then its supply is better guaranteed than its sole source from one or more obscure, rare or difficult to cultivate higher plants. A thorough comprehensive study should be made of the endophytes of each of the medicinally important plants in the world.

An array of medicinally important compounds which can be used in the treatment of many diseases have been reported. Of all the diseases listed, anticancerous compounds has caught much focus. Identification of potential secondary metabolites which can be used for the treatment of cancer has gained importance.

5. Cancer

Clinically, cancer is the name given to a large family of diseases, may be a hundred or more, which vary in the age of onset, rate of growth, state of cellular differentiation, diagnostic detectability, invasiveness, metastatic potential, and response to treatment and prognosis. Cancer occurs when cells become abnormal and keep dividing and forming new cells without any control or order. All organs of the body are made up of cells. Normally, cells divide to form new cells only when the body needs them. If cells divide when new ones are not needed, they form a mass of excess tissue, called a tumor. Tumors can be benign (not cancer) or malignant (cancer). The cells in the malignant tumors can damage and invade nearby tissues and organs.

Both internal and external factors play some role in the promotion and initiation of carcinogenesis. External factors such as exposure to chemicals (tobacco smoke, benzene, asbestos, vinyl chloride, polychlorinated biphenyls etc.), UV-radiation, and viruses [hepatitis B virus (HBV), human papillomavirus (HPV), human immunodeficiency virus (HIV), and human T-cell leukemia/lymphoma virus-I (HTLV-I)] are linked to most types of cancer. Physiological factors like hormones, immune conditions, mutations due to metabolism and inherited mutations also increase the chance of contracting cancerous diseases; which account to internal factors. The American Cancer Society has estimated about 1,444,920 new cancer cases to be diagnosed in the US in 2007. In the same year, 559,650 cancer patients had been expected to die in America, the statistics translating to more than 1500 deaths per day. Cancer is the second leading cause of death in the US next to coronary heart disease. Breast cancer cases (31%) are the highest among adult females while prostate cancer (31%) is found to be the highest in adult males. Leukemia accounts for 31.5% of cancer cases (American Cancer Society, Cancer Facts and Figures, 2007).

5.1. Cancer treatment and anticancer compounds

The economic burden, loss of human life and the suffering due to cancer have triggered a concerted effort to fight against this serious public health problem. Although significant advances have been made in the lines of early detection, preventive measures and medical treatment of this disease, much more effort is needed to reduce the alarming rate of cancer incidence and the emergence of new multi-drug resistant cancers (MDR). The treatment of cancer patients involves a combination of surgery, radio therapy, chemotherapy, hormone therapy, biological therapy and targeted therapy. For solid tumors the prior two methods are used classically. Chemotherapy is imperative and the only approach possible for strewn cancers like leukemia and lymphomas. The ultimate goal of cancer chemotherapy is to kill the cancer cells without killing the normal cells of the patient. This requires the development of selective drugs that can kill malignant tumor cells or render them benign. The advances in molecular and cell biology of cancer have contributed to the rationalization of chemotherapy and the resulting drug resistance in cancer on a molecular basis (Boyle and Costello 1998).

Based on a mechanistic approach, the current anticancer chemotherapeutic agents can be classified (Espinosa, 2003) as 1) cytotoxic agents, 2) antibody targeting agents, 3) anti–

hormonal agents, 4) signal transduction inhibition agents, 5) Ras-inhibition agents, 6) cell cycle modulation agents, 7) apoptosis inducing agents, 8) angiogenesis inhibition agents, and 9) anti–invasion agents (Boyle and Costello, 1998). Cytotoxicity reduces proliferative drive to the tumour, but lacks discrimination between effects on tumour and normal tissue, has cell-cycle dependency and is susceptible to induced drug resistance. These agents are further subdivided as tubulin binding (Paclitaxel, Vincristin, Vinblastine and Colchicin), DNA intercalating (Doxorubicin), antifolates (Methotrexate), alkylating agents (Cisplatin), and topoisomerase inhibitors (Etoposide) (FIG 4).

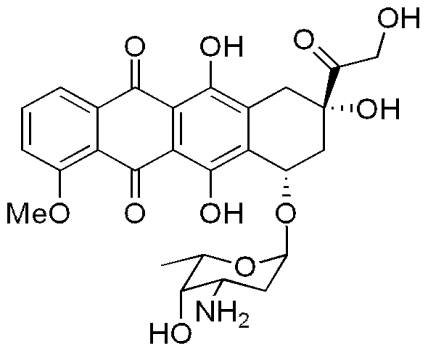

Doxorubici

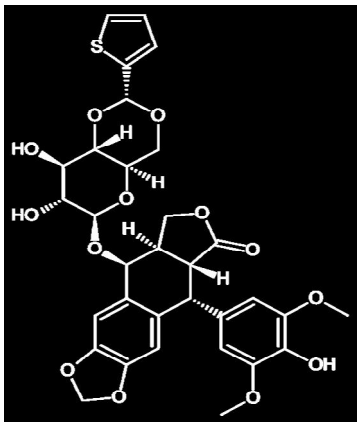

Teniposide

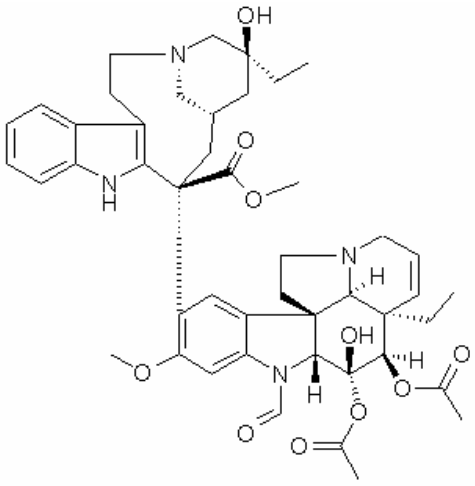

Vincristin

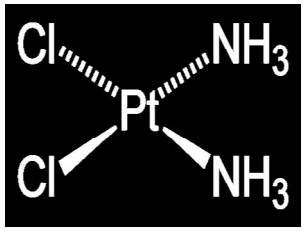

Cisplatin

Contd…

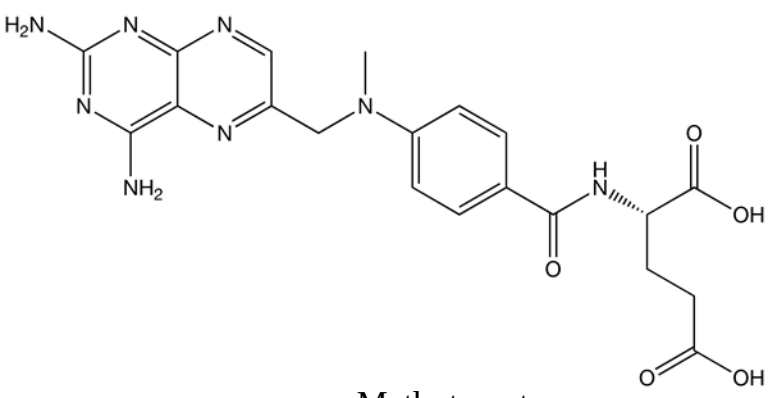

Methotrexate

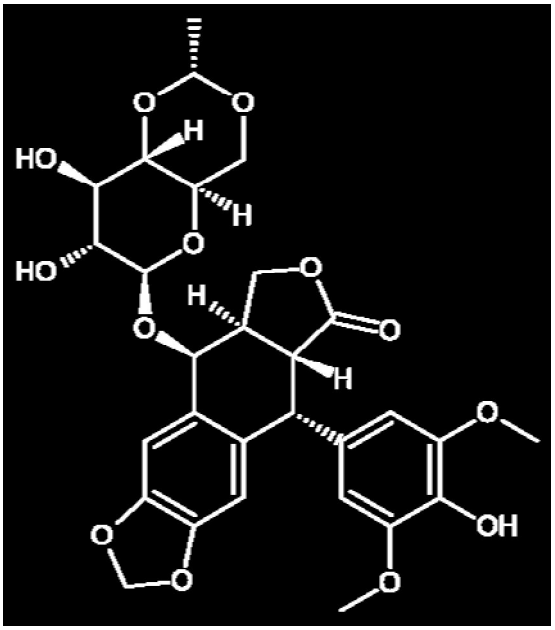

Etoposide

FIG 4: Some of the drugs which gained much attention in the treatment of cancer.

Among cytotoxic anticancer agents, tubulin-binders have attracted greater interest due to the fact that these drugs intervene in the finely tuned (α-/β-) tubulin-microtubule equilibrium. The microtubule system is essential for a number of cellular functions including mitosis and cell replication, maintenance of cell shape, cellular transport, and motility; hence these drugs follow an important mechanism to act as anticancer agents (Wilson and Jordan, 1995). The formation of microtubules and their depolymerization is a dynamic process which can be interrupted by both stabilization of microtubules and inhibition of polymerization. Some compounds shift this equilibrium to one or the other side and thereby abrogate the biological functions of microtubules. Taxanes and epothilones induce polymerization of microtubules, whereas colchicin, combretastatin A-4 and the vinca alkaloids inhibit the polymerization of tubulin dimers (Kaufmann et al, 2007). Of these tubulin-binders, the most commonly known and extensively studied drug is taxol.

5. 2. History of Development of Paclitaxel as an Anticancer Drug

The diterpenoid natural product paclitaxel[a] (Taxol™), first discovered in the 1960's has proved to be the most important and interesting anticancer drug introduced in the last ten years (FIG 6). Discovery of the cytotoxic activity now known to be due to paclitaxel was made in 1962, when a collection of the stem and bark of *Taxus brevifolia* Nutt. in Washington State was extracted and analysed for bioactivity; the extract from *T. brevifolia* was found to have activity against certain leukemias, a carcinosarcoma and showed considerable cytotoxicity in the 9KB assay. Paclitaxel was isolated from this extract (as well as extracts from other *Taxus* species; *T. cuspidata* and *T. baccata* (FIG 5)) in 1967.

FIG 5: *Taxus baccata* growing in West Bengal, India.

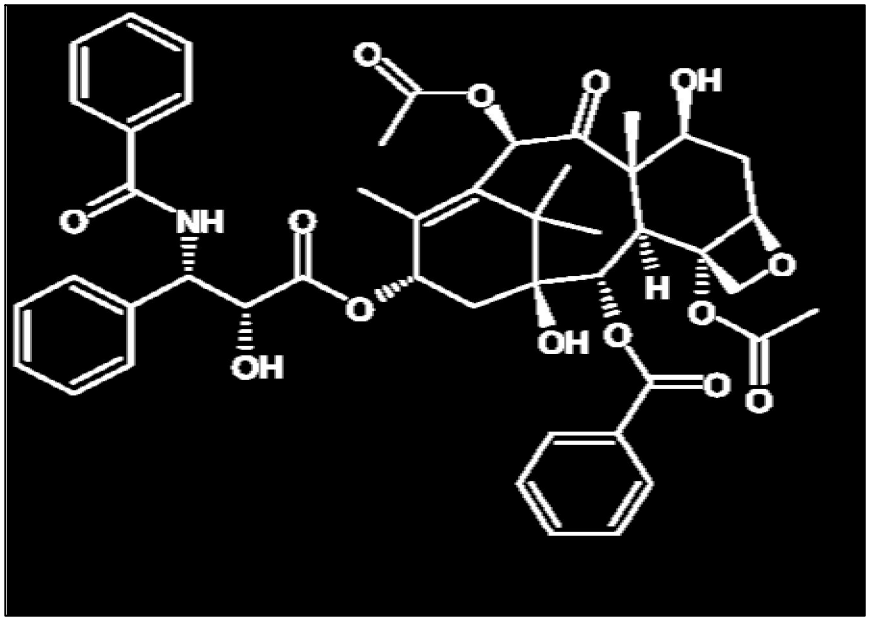

FIG 6: Paclitaxel

The structure was elucidated by a combination of X-ray studies of two degradation (base-catalysed methanolysis) products. The intact molecule was characterised spectrally (IR, UV, ^{1}H-NMR) and analytically (mass spectrum; *m/z* 853.9), and was published in 1971 (Wani et al, 1971). Taxol completed preclinical formulation and toxicology studies in 1982 and entered Phase I clinical trials in 1984, and into Phase II trials in 1985. It was approved by USFDA for clinical use in 1992 for drug-refractory ovarian cancer, and in 1994 for breast cancer.

5.3. Mechanism of action

Interest in paclitaxel as a potential drug candidate was increased significantly when Susan Horwitz reported in 1979 that it had a previously unknown mechanism of action, in that it promoted the assembly of the proteins α- and β-tubulin into microtubules (FIG 7). The binding of taxol to assembly of microtubules is non-covalent and reversible. A schematic representation of the effect of paclitaxel on the tubulin polymerization process is shown below.

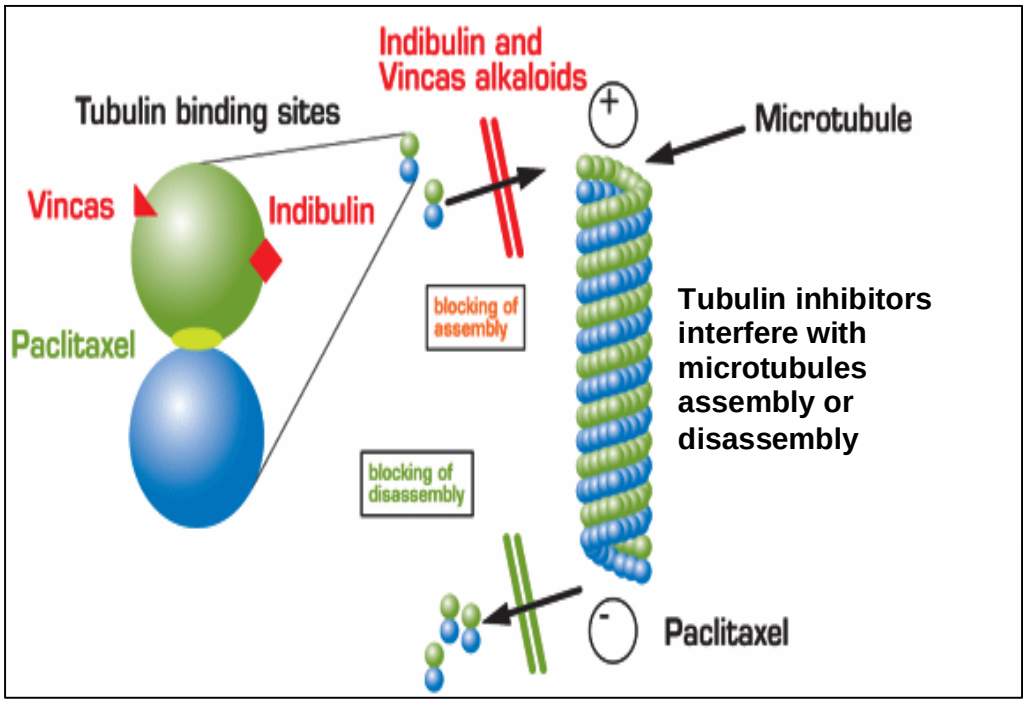

FIG 7: Tubulin dynamics in presence of anti mitotic agents paclitaxel and Vinca-alkaloids.

As described in the earlier section, microtubules are required for chromosome segregation and for other operations such as intracellular transport and positioning of cellular organelles, and all of these activities require that the microtubules be in dynamic equilibrium with monomeric tubulin molecules. Several compounds, including the clinically used drugs vinblastine (Velban™) and Vincristine (Oncovin™), known to operate as spindle poisons, prevent the assembly of tubulin monomers into microtubules or induce tubulin paracrystals (Na and Timasheff, 1982), but paclitaxel was the first compound in which the activity was linked to the promotion of microtubule assembly (FIG 8).

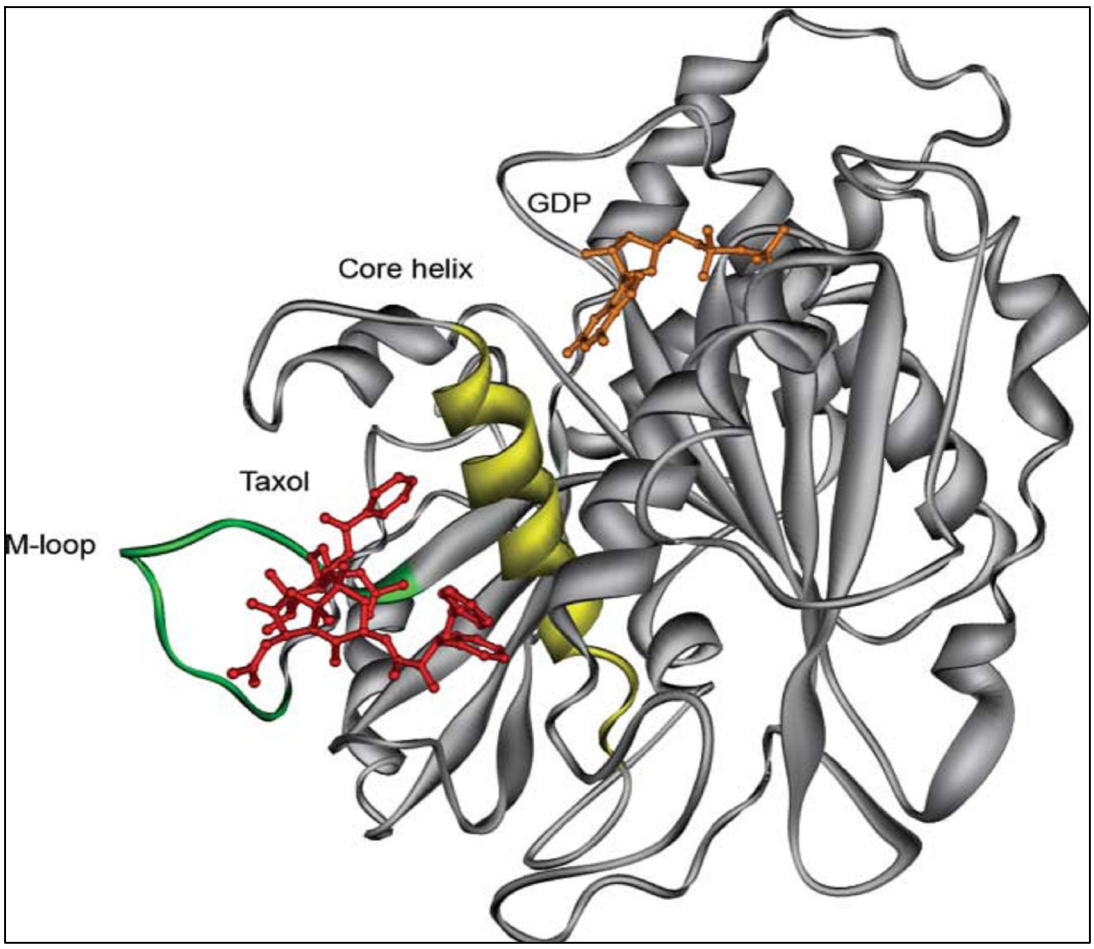

FIG 8: Paclitaxel conformation in tubulin-bound state.

Microtubule-associated proteins (MAPs) like MAP2 and tau are known to stabilise microtubules both *in vitro* as well as *in vivo*. Paclitaxel is thought to mimic the MAP tau, which is involved in stabilisation of microtubules in neuronal processes, in a qualitatively indistinguishable manner. This is consistent with the idea that antimitotic drugs mimic the actions of natural regulatory substances (Wilson and Jordan, 1995). Thus, paclitaxel can eliminate the requirement for microtubule-associated proteins in microtubule formation. In cancer cells, the cytotoxicity of paclitaxel represents both inhibition of cell proliferation and cell death. Paclitaxel binds to the assembled microtubule with a stoichiometry of approximately 1 mole of the drug to 1 mole of tubulin dimer and stabilizes it against dissociation. This binding occurs in the absence of any cofactors, and the resulting disruption of the equilibrium between tubulin and microtubules also disrupts cell division and ultimately leads to cell death by apoptosis (Horwitz 1984, 1992). The drug blocks cells in the G2/M phase of the cell cycle. In a lower concentration range (few nM), paclitaxel stabilizes the spindle formation during mitosis, thereby blocking mitosis. This mitotic block leads to the inhibition of cell proliferation and the induction of apoptosis. In a higher concentration range (few μM), paclitaxel mainly increases the polymerization of microtubule and stimulates the formation of microtubule bundles, which block entry into S phase. This inhibition of S phase entry leads to the inhibition of cell proliferation and the induction of necrosis (Yeung et al, 1999).

Methods like photoaffinity labeling, fluorescence spectroscopy, fluorescence resonance energy transfer (FRET), electron crystallographic studies and NMR studies have been applied to determine the location of the binding site of paclitaxel on tubulin (Snyder et al, 2001). It has been proposed that all the subunits of the microtubule at the steady state are GTP-tubulin-paclitaxel, but they are formed through two different pathways: either from paclitaxel binding to a tubulin subunit before GTP hydrolysis (high affinity binding) or paclitaxel binding to a tubulin subunit after GTP hydrolysis (low affinity binding). Since paclitaxel exists in chloroform, and presumably in polar solvents also, as a population of different conformations, it is possible that relatively weak association of paclitaxel with tubulin may be due in part to the presence of a large number of non-productive conformers (Kingston, 2001).

Some investigators have researched upon the dependence of paclitaxel sensitivity on a functional spindle assembly checkpoint (Sudo et al, 2004). When paclitaxel stabilizes microtubules and interferes with the dynamic changes that occur during formation of the mitotic spindle, the spindle assembly checkpoint is activated to arrest cells at mitosis. The induction of dysfunctional spindle assembly checkpoint by knocking down checkpoint genes *Mad2* and/or *BubR1* results in resistance to paclitaxel. Thus, a functional spindle assembly checkpoint is essential for paclitaxel-sensitivity.

Recent research has shed light upon a second mechanism through which paclitaxel mediates apoptotic cell death, independent of mitotic arrest (Fan, 1999; Wang, 2000). The protein Bcl-2 (product of the proto-oncogene *Bcl-2* and the guardian protein for microtubules, Haldar et al, 1997) has been identified as a second paclitaxel-binding protein (Rodi, 1999), along with similar anti- apoptotic proteins like Bcl-x_L belonging to the same family (Poruchynsky et al, 1998). In cancer cells, Bcl-2 dimerizes with a pro-apoptotic molecule Bax, inhibiting its function and hence making it difficult for the cancerous cells to undergo apoptosis. In the presence of paclitaxel however, Bcl-2 undergoes dose-dependent hyperphosphorylation at serine residues (Scatena, 1998) which leads to a loss of the Bcl-2 anti-apoptotic function (of dimerizing with pro-apoptotic molecules) and the cells then execute apoptosis. It has also been shown that Bcl-2 phosphorylation in the presence of paclitaxel is linked to the tubulin-assembly activity of the drug and it has thus been proposed that paclitaxel-promoted assembly of microtubules leads to Raf-1 activation and Bcl-2 phosphorylation and hence to apoptosis (Blagosklonny, 1997).

Apart from *bcl-2*, a number of apoptosis-associated genes or regulatory proteins have been reported to be regulated by paclitaxel. These include genes that may act as effectors of apoptosis, such as the interleukin-1b (IL-1b) converting enzymes family of proteases (Ibrado et al, 1997) and genes that may act as mediators of signal transduction, such as $p21_{waf}$, TNF-α, c-*raf*-1 and BID (Ding et al, 1990). Also, the transcription factor NF-κB is known to be regulated by presence of paclitaxel in cells (Huang et al, 2000). NF-κB plays an important role in coordinating the control of apoptotic cell death. It normally resides in the cytoplasm as an inactivated form by forming a complex with IκB-α (the cytoplasmic inhibitor of NF-κB).

Upon certain stimulations, IκB-α is rapidly phosphorylated and degraded, allowing NF-κB to translocate to the nucleus, where it participates in transcriptional regulation of numerous genes. Paclitaxel down-regulates IκB-α through modulation of IκB kinase (IKKβ) activity, which in turn promotes the nuclear translocation of NF-κB and its DNA binding activity and regulation of apoptosis-associated genes. From these findings, it is possible that paclitaxel induces apoptosis via a gene-directed process, i.e., paclitaxel may directly induce or modulate gene expression, which in turn triggers the apoptotic process (Moos and Fitzpatrick, 1998). Apoptosis has been reported to occur by both caspase-dependent (Park et al, 2004) and independent mechanisms. The caspase-independent pathway involves induction of apoptosis by paclitaxel employing a calpain-mediated mechanism (Piñeiro et al, 2007).

Another novel and significant activity of paclitaxel involves favourable molecular interactions with DNA (Krishna et al, 1998). Paclitaxel binds to DNA through the taxane ring system, the association occuring in the DNA groove through the eight-membered taxane core ring, with the three phenyl rings pointing away and is similar to that proposed for paclitaxel-tubulin interaction. In the bound form, paclitaxel inhibits DNA dependent DNA synthesis. In spite of these significant findings, the studies have been conducted *in vitro* and the biological (*in vivo*) significance of these interactions needs to be proven experimentally.

5.4. Clinical use

Paclitaxel being highly insoluble in water, a formidable formulation problem for it to act as an effective drug existed. The solubility problem has been successfully overcome with a formulation in ethanol and Cremophor EL (polyoxyethylated castor oil, a surfactant), and this has its own pros and cons. The high levels of Cremophor can lead to hypersensitivity reactions but, there is some evidence that Cremophor has a pharmaceutical effect in addition to its surfactant properties, and may act to reverse multidrug resistance (MDR) in cancer. The other formulations of paclitaxel include coupling to albumin as the delivery agent (Trade name: Abraxane which obtained USFDA approval in 2005). Numerous other techniques for administration of paclitaxel like DHA-paclitaxel, PG-paclitaxel, and tumor-activated Taxol prodrugs are currently

being researched in an effort to reduce the side effects of Taxol[b] treatment, and increase effectiveness of the drug.

The clinical trials of Taxol were limited by the supply of the drug, but gave the first clear evidence of activity with clinically relevant responses in ovarian and breast cancer reported in 1989 (Mc Guire) and 1991 (Holmes) respectively. Paclitaxel and its semisynthetic analog docetaxel (Taxotere™) are now used (either as single agents or in combination with other drugs such as cisplatin) for the treatment of ovarian cancer, breast cancer, non-small-cell lung cancer, head and neck cancer and AIDS-related Kaposi's sarcoma (Crown, 2000) FIG 9.

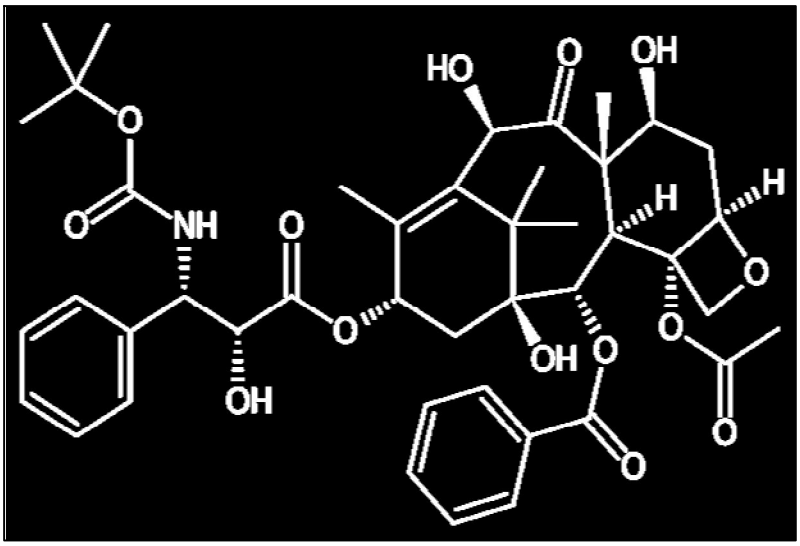

FIG 9: Docetaxel

Paclitaxel is used to treat a number of other human tissue-proliferating diseases as well. It has been demonstrated to be a lipopolysaccharide mimetic in murine macrophages (Doherty et al, 1998). This action is effective in eliciting parasite killing. For instance, the malarial parasite *Plasmodium falciparum* and the leishmaniasis parasite *Leishmania major* have been shown to be killed by it. It is also used for the prevention of restenosis (recurrent narrowing) of coronary stents. A paclitaxel coating locally delivered to the wall of the coronary artery limits the growth of neointima (scar tissue) within stents (Heldman et al, 2001).

Paclitaxel has been shown to protect primary neurons against amyloid-induced toxicity. Since neurons do not divide, paclitaxel does not affect them in the same way as normally dividing cells and tumor cells. Instead, microtubule-binding drugs have other effects in nerve cells similar to the function of the protein tau. Tau binds microtubules, essential structures in axons in nerve cells. Mutations in the tau gene cause neurons to lose their ability to send and carry signals over time. When the misfolded proteins aggregate and form fibrils that accumulate in different parts of the brain, the normal physiology is disrupted and neurodegenerative disease progression starts. This happens when the cell's proteosome is not working properly, causing such effects as cell death, oxidative stress, and in this case impaired axonal transport, which is linked to many neurodegenerative diseases. Impaired axonal transport of proteins and other cargoes needed to maintain synapses can cause nerve cell loss with subsequent dementia, Parkinsonism or weakened motor skills in peripheral muscles, and later on muscle atrophy. The protein tau, like paclitaxel (or other taxanes), is required to stabilize the microtubule. Microtubule-stabilizing drugs may help slow down the development of the neurofibrillary pathology that leads to the loss of neuronal integrity in Alzheimer‘s disease (Michaelis et al, 1998).

5.5. The Chemistry of Paclitaxel, Structure-Activity Relationship and the Paclitaxel Pharmacophore

Taxol is a member of the class of taxane diterpenoids, which contains more than 300 identified taxoids with the basic ring system as shown below (FIG 10).

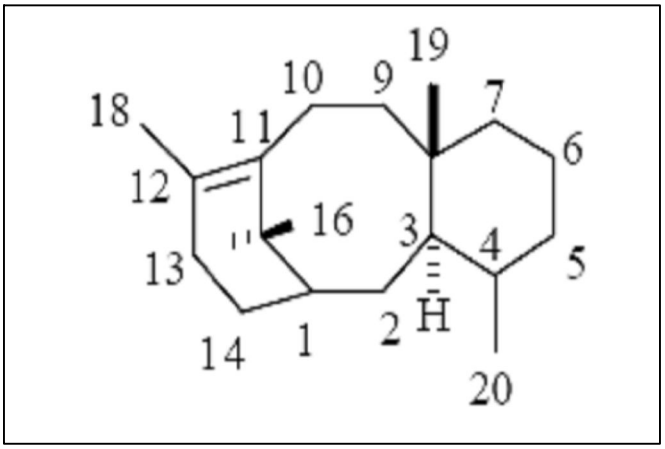

FIG 10: The basic structure involved in taxanes.

Structurally, it can be viewed as the N-benzoyl-β-phenylisoserine ester of diterpenoid baccatin III with a very characteristic oxetane ring. It has a complex and unusual diterpene carbon skeleton, with eleven stereogenic centers and elaborated functional groups. The structure of paclitaxel can be roughly divided into four parts, the 'northern hemisphere', oxetane ring, 'southern hemisphere' and the celebrated side chain (Kingston 2000).

The northern hemisphere of paclitaxel comprises of C-10 acetyl, the C-11-C-12 double bond and C-7 hydroxy along with C-6. The oxetane ring is a very unique and extremely important group in the molecule. It is clearly not involved in any covalent binding to tubulin, since taxol can be exchanged with labeled taxol on tubulin. The southern hemisphere comprises of the C-14 and C-1 to C-5. The structure of taxol differs from that of many known members in having a complex phenylisoserine side chain esterifying the C-13 position. Many paclitaxel analogs with modified side chains have been prepared in studies to find improved analogs of the drug, and few have been found to be as effective as the *N*-benzoyl phenylisoserine side chain, e.g. Docetaxel. In non-polar solvents such as chloroform, paclitaxel seems to exist primarily in a set of open conformations in which the side chain is oriented away from the 2-benzoyl group (Snyder et al, 2001), but in polar aqueous solvents it adopts a set of hydrophobically collapsed conformations in which the 3'phenyl group is oriented towards the 2-benzoyl group.

The structure of a molecule dictates its activity and hence defines the function. In order to determine this correlation, paclitaxel was subjected to chemical modifications of different groups. Alterations in the northern hemisphere of paclitaxel appear to have less impact on its activity, although these changes can still be important therapeutically as some altered compounds have been shown to enhance biological activity. Changes to the southern hemisphere exert a major effect on the activity of the drug. This is the case for changes at C-1, C-2 and C-4. Opening of the oxetane ring essentially eliminates paclitaxel's cytotoxicity and tubulin assembly. The C-4 acetate function that exists in the oxetane ring is necessary for activity and H-bond acceptor properties and the rigidification of the paclitaxel ring system by the oxetane ring plays a role in stabilizing

the paclitaxel-tubulin complex. Changes in the side chain have also been made by several investigators, and it is expected that future second-generation paclitaxel analogues will have modifications both on the side chain and on the taxane ring system. Based on these studies, a representation of the structure-activity relationship of paclitaxel is shown in figure 11.

A pharmacophore is the ensemble of steric and electronic features that are necessary to ensure the optimal supramolecular interactions with a specific biological target structure and to regulate its biological response. It does not represent a real molecule or a real association of functional groups, but a purely abstract concept that accounts for the common molecular interaction capacities of a group of compounds towards their target structure. Thus, by studying various drugs exhibiting activity similar to paclitaxel, a common pharmacophore that unites paclitaxel, nonataxel, the epothilones, eleutherobin, and discodermolide, and rationalizes the extensive structure-activity relationship data pertinent to these compounds can be deduced. Insights from the common pharmacophore have enabled the development of a hybrid construct with demonstrated cytotoxic and tubulin-binding activity (Ojima et al, 1999) and will help in creating new and improved paclitaxel analogs.

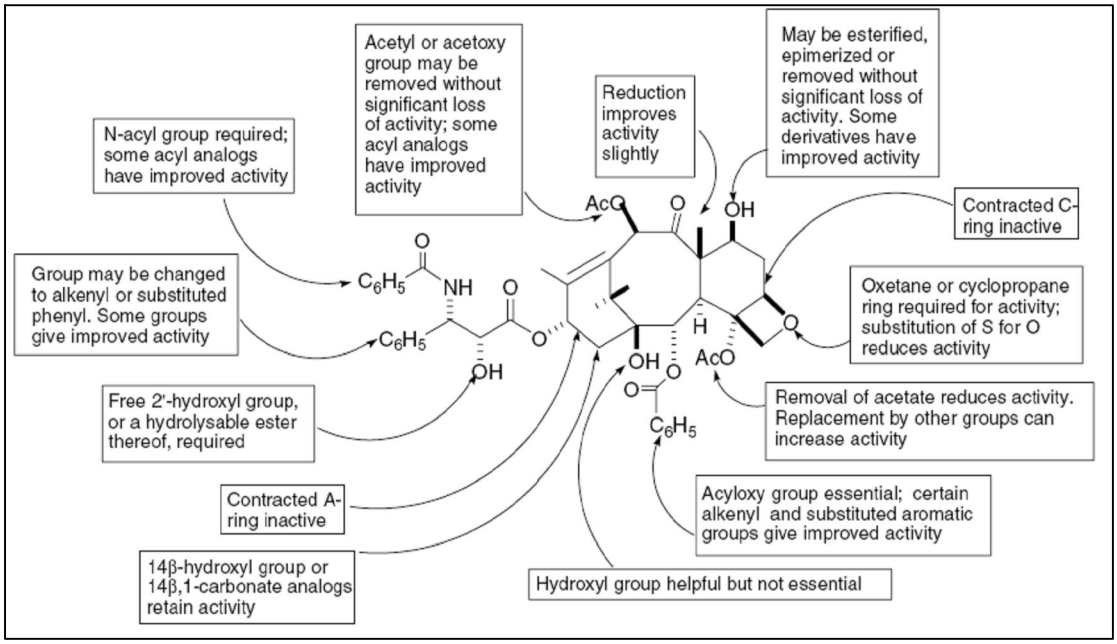

FIG 11: Structure Activity relationship of paclitaxel

5.6. Paclitaxel supply crisis and its solution

At the time of recognition of the clinical activity of paclitaxel, as described in the earlier sections, it was only available in low yield from the bark of *T. brevifolia* and this was a major impediment to its development as a drug, creating a crisis in its supply. Serious environmental concerns were raised on the prospects of large-scale logging needed to supply paclitaxel to the clinical market as this tree is relatively uncommon. The various options for increasing the supply included increased harvesting of *T. brevifolia* bark, the isolation of paclitaxel from a renewable resource such as yew needles/leaves, total laboratory synthesis (six methods reported until now) (Nicolaou, 1994), semi synthesis from other more abundant taxoids in yew (eg; baccatin III, 10-deacetyl baccatin III) (Gebetta et al, 1998), and production through plant tissue culture (Robert et al, 1997). Many studies of paclitaxel production from endophytes of *Taxus* sp. have also been reported (Page et al, 1999; Caruso et al, 2000).

5.7. Chemical synthesis:

The first two total synthesis of paclitaxel appeared in the literature in 1994 by Holton and Nicolaou, practically at the same time. Later followed by Danishefsky's group (1996); Wender, who reported the shortest total synthesis of paclitaxel to date which was accomplished in thirty seven steps; Kuwajima and Mukaiyama also reported total laboratory synthesis of paclitaxel. The semi-synthesis approach involves use of the relatively more abundant taxoids from needles of trees of the *Taxus* sp. and the synthetically produced β–lactam side-chain. The two entities are then linked together by Holton's efficient coupling to yield reasonable quantities of paclitaxel (FIG 12).

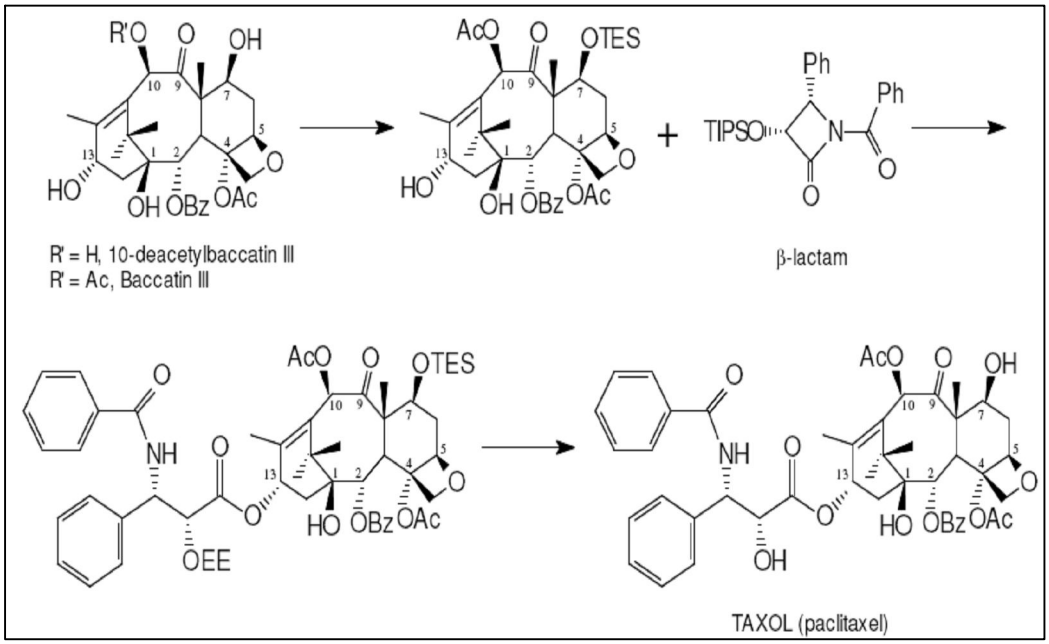

FIG 12: Holton semisynthesis of paclitaxel from 10-DAB III and synthetic β-lactam precursor of side chain. Triisopropylsilyl (TIPS); Triethylsilyl (TES); Ethoxyethyl (EE).

5.8. Cell culture

Plant cell cultures are considered one of the most promising approaches to provide a stable supply of paclitaxel and taxanes. These cultures originate from either embryo or needle explants which are cultured on callus induction media and eventually transferred to suspension culture media. Several attempts have been made to produce cell cultures from different *Taxus* sp. (Zhong, 2004), and various elicitors (like methyl jasmonate) have been used to increase the productivity and the release of paclitaxel into culture medium. However, recalcitrant behaviour of *Taxus* sp. under *in vitro* conditions delimits the production of paclitaxel on a commercial scale. Hence, efforts have been focused also on the isolation and cultivation of paclitaxel-producing endophytic fungi associated with yew.

5.9. Endophytes

An endophyte is a bacterial, actinomycete or fungal microorganism, which spends the whole or part of its life cycle colonizing inter- and/or intra-cellularly inside the healthy tissues of the host plant. The reason why some endophytes produce certain

phytochemicals originally characteristic of the host might be related to a genetic recombination of the endophyte with the host that occurs in evolutionary time. It does seem apparent that the production of certain bioactive compounds by the endophyte *in situ* may facilitate the domination of its biological niche within the plant or even provide protection to the plant from harmful invading pathogens. This is a concept that was originally proposed as a mechanism to explain why the endophytic fungus *T. andreanae* may be producing paclitaxel (Stierle et al, 1993). Thus, if endophytes can produce the same rare and important bioactive compounds as their host plants, this would not only reduce the need to harvest slow-growing and possibly rare plants but also preserve the world's ever-diminishing biodiversity. Furthermore, it is recognized that a microbial source of a valued product may be easier and more economical to produce, effectively reducing its market price (Strobel and Daisy, 2003). Later, several other species of fungi were discovered to produce paclitaxel: *Pestalotiopsis* sp. (Strobel et al, 1996), *Periconia* sp. (Li et al, 1998), *Tubercularia* sp., *Seimatoantlerium nepalense*, *Sporormia minima* and a *Trichothecium* sp.

Thus, for the foreseeable future, the supply of paclitaxel must continue to rely upon biological methods of production and improvements to this biosynthetic process in yew or derived cell cultures requires a full understanding of the paclitaxel biosynthetic pathways.

5.10. Biosynthetic pathway for paclitaxel production

The supply crisis of paclitaxel underlines the need to understand and modify the paclitaxel biosynthetic pathway, in order to manipulate the step(s) which result in decreased production of the drug**.** Improving the biological production of paclitaxel thus depends on a thorough understanding of the biosynthetic pathways and on defining the associated enzymes, as well as the genes that encode them. The improved flux through slow steps by over-expression of the corresponding genes in transgenic cells is expected to raise the production titres of this medicinally useful taxane diterpenoid to commercially significant levels.

The paclitaxel biosynthetic pathway (FIG 13) is predicted to consist of twenty steps from the primary isoprenoid precursors, isopentenyl diphosphate and dimethylallyl diphosphate (Chau, 2004). More than half of the enzymes and genes involved in this

pathway have been defined. There are at least nine cytochrome P450 mediated oxygenations and five acyl-CoA dependent acylations in the biosynthetic pathway. Typical of plant secondary metabolism (Schuler, 1996), cytochrome P450-mediated oxygenations play a major role in paclitaxel biosynthesis. A report by Croteau and Walker (2006) has ascertained the role of taxane-metabolizing cytochrome P450s and the identification of the family of cytochrome P-450 genes responsible for the nine oxygenation steps *en route* to paclitaxel.

The pathway begins with the formation of the universal precursor of diterpenoids, geranylgeranyl diphosphate (GGPP), by GGPP synthase from the C5 isoprenoid precursors, isopentenyl diphosphate and dimethylallyl diphosphate (Croteau and Walker, 2001). This parental taxane is functionalized by a series of eight cytochrome P450-mediated oxygenations, two subsequent CoA-dependant acetylations, a benzoylation, oxetane ring formation, and oxidation at the C-9 to the late intermediate baccatin III, to which the C13-side chain is appended (derived by transfer from β-phenylalanoyl CoA, followed by 2'-hydroxylation and N-benzoylation) to complete the pathway to produce paclitaxel.

There are three committed early steps in the pathway, namely the cyclization of the universal diterpenoid precursor geranylgeranyldiphosphate to taxa-4(5), 11(12) diene, the cytochrome P450-catalyzed hydroxylation of the diene at C-5 to taxa-4(20), 11(12)-dien-5α-ol, and the acetyl CoA dependent esterification of the alcohol to acetate ester.

Biosynthesis of taxanes in *Taxus* involves several oxidation steps catalyzed by cytochrome P450 oxygenases. The order of oxygenation steps has yet to be fully elucidated, although predictions have been made based on a survey of the oxygenation patterns of the naturally occurring taxoids and on biochemical studies on the early pathway steps (Suffness, 1995).

The proposed oxygenation order begins with C5 and C10, then C2, C9, and C13 (exact order uncertain), followed by C7, and finally C1. Four acylations, catalyzed by acetlytransferases, occur late in the paclitaxel biosynthetic pathway after these eight taxane ring oxygenations have taken place. C5-acetylation appears to be the earliest acylation on the paclitaxel pathway, and this acyl group is predicted to play a role in the

formation of the oxetane ring. Several biosynthetic mechanisms have been proposed for formation of the oxetane D-ring, with the most favoured involving the epoxidation of the 4(20)-double bond of the 5α-acetate, followed by a rearrangement in which the α-acetoxy group migrates from C-5 to C-4, accompanied by the oxirane-to-oxetane ring expansion. Next is the acetylation of 10-deacetylbaccatin III to baccatin III. The schematic representation is as given in figure 14.

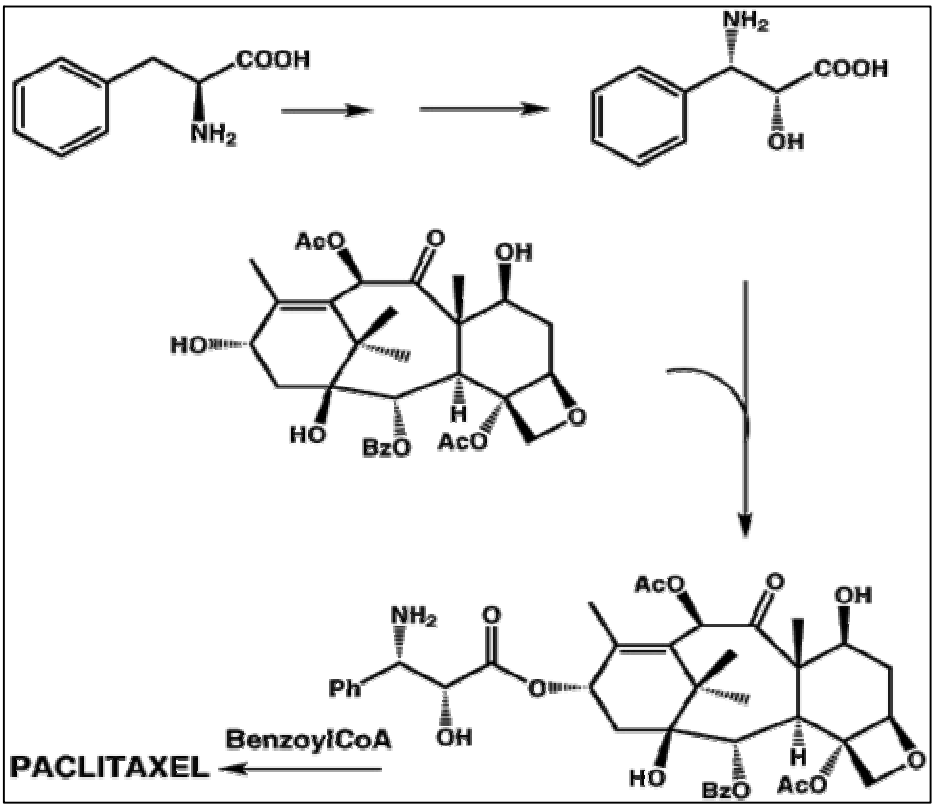

FIG 13: A very simplified approach of paclitaxel biosynthesis can be considered to be comprised of the conversion of phenylalanine to phenylisoserine and its subsequent "coupling" with *baccatin III*. The resulting intermediate can be foreseen to undergo benzoylation yielding paclitaxel. The biosynthesis of the main core of the molecule has been suggested to be initiated by the cyclisation of geranylgeranyl diphosphate.

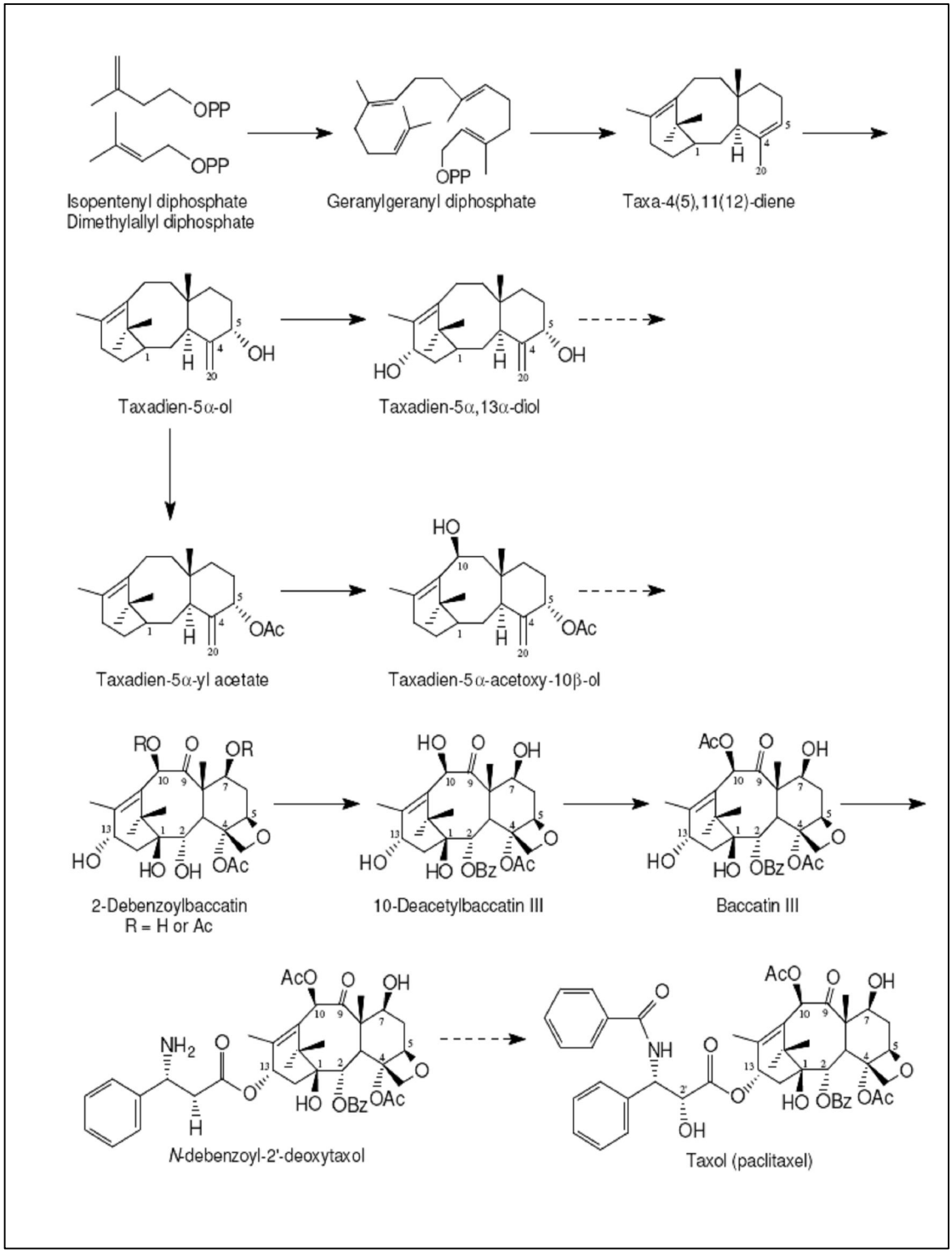

FIG 14: Schematic representation of taxol biosynthetic pathway.

Based on cell-free enzyme studies and the specificity of the recombinant enzymes, the biosynthesis of the side chain of paclitaxel appears to occur in three sequential steps, the 2'-hydroxylation of β-phenylalanine, followed by attachment of phenylisoserine to baccatin III and then N-acylation (Fleming et al, 1994); as represented in FIG 15. The biosynthetic origin of the side chain is determined to be phenylalanine *via* β-phenylalanine from an aminomutase reaction. The benzoyl group is also formed *via* β-phenylalanine and possibly via phenylisoserine but not *via* cinnamic acid (Croteau, 2001; Fleming, 1993). Thus, the paclitaxel side chain does not append as an intact N-benzoylphenylisoserine moiety.

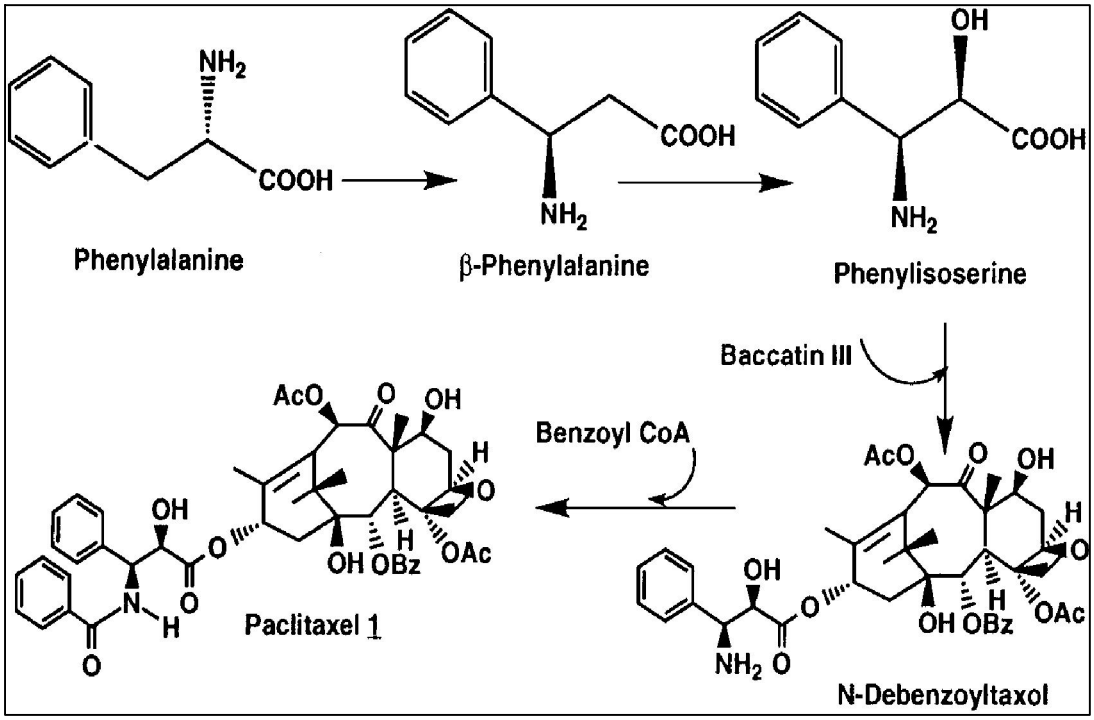

FIG 15: The most important steps involved in the biosynthesis of taxol.

There are at least six cytochrome P450-mediated reactions which have yet to be elucidated. These include the oxygenations C-1, C-2, C-7, C-9 and C-2' and the C-4, C-20-epoxidation. Additionally, the oxidation of the C-9-hydroxyl to the carbonyl has not yet been biochemically described but precedents in the biosynthesis of other natural products suggest that this step may also be cytochrome P450-mediated (*via* the ketone

hydrate). Also, another reaction that has yet to be elucidated is the proposed C-4, C-20-epoxide ring expansion/C5-acetate migration thought to be involved in oxetane ring formation. Furthermore, the CoA ligases for activation of the respective acyl groups have yet to be described (Chau, 2004).

A combination of classical biochemical and molecular methods, including cell-free enzyme studies and differential-display of mRNA-reverse transcription polymerase chain reaction (RT-PCR) combined with random sequencing of a cDNA library from induced *Taxus* cells, led to the discovery of six novel cytochrome P450 taxoid hydroxylases (Kaspera, 2006). In addition to generation of gene libraries, differential display libraries and EST libraries, some genes have been isolated through classical homology-based approaches (Rupasinghe and Schuler, 2006). Two groups of gene families encoding acyltransferases and cytochrome P450 oxygenases have been isolated. The genes of paclitaxel biosynthesis for the branch-point enzyme geranylgeranyl diphosphate synthase, taxadiene synthase (the committed step); several cytochrome P450 taxoid hydroxlases and C13-side chain transferase, N-benzoyltransferase, taxoid C2-O-benzoyltransferase, C10-O-acetyltranferase and C5-O-acetyltransferase have been isolated. Genes encoding the acyl and aroyltransferases have been cloned by several strategies employing cDNA libraries derived from transcripts isolated from *Taxus* cell cultures induced with methyl jasmonate for increased paclitaxel production. These approaches, in addition to the random sequencing of an EST library from similarly induced *Taxus* cells, have now yielded a family of 16 closely related acyltransferase clones, which have been characterized by heterologous functional expression in *Escherichia coli* or *Saccharomyces cerevisiae*. The recent acquisition of this family of presumptive taxoid acyl/aroyltransferase clones has provided the opportunity to broaden the search for genes relevant to taxoid metabolism, with immediate focus on those responsible for the origin of acetylated taxoids and with a long term view to manipulate these genes so as to suppress side-routes and promote pathway flux towards paclitaxel (Walker, 2001; Walker, 2002).

This manipulation can be achieved by over expression of genes controlling slow steps to increase the production titers of desirable taxoids; while suppressing, by antisense technology, the production of undesired taxoids. Both approaches would improve flux to

the desired end-product and simplify downstream purification processes. Also, redirection of the pathway for the production of novel taxanes with a greater range and potency and decreased side-effects, such as those associated with the formulation vehicles needed to deliver these drugs, cumulative neurotoxicity and acquired resistance is a potential area to work upon (Jennewein 2001). Genetic manipulation of transcription factors for the global up-regulation of the pathway, and improved efficiency of the intracellular metabolite trafficking and extracellular secretion machinery, can also be anticipated to improve production yields and the ease of drug isolation from the medium.

Although paclitaxel and its precursors for semisynthesis are the most important taxoids, an examination of a compendium of the naturally occurring taxoids reveals a large assortment of other compounds possessing positionally different acylation patterns and a variety of acyl and aroyl substitutions. The latter functional groups include acetyl, propionoyl and butyroyl and their hydroxylated and methylated derivatives, tigloyl and benzoyl esters and amino acid derivatives, such as cinnamoyl, aminophenylpropanoyl (Winterstein's acid), and phenylisoserinoyl esters, as well as glycosyl groups. Paclitaxel bears acetate groups at C-4 and C-10, a benzoate at C-2 and the unusual N-benzoylphenylisoserine side chain appended at C-13 (C2-benzoate, C13-side chain and C4-acetate being important pharmacophores in promoting tubulin binding). However, taxoids bearing acetate groups variously at C-1, C-2, C-5, C-7, C-9, C-10 and C-13 positions are far more abundant than paclitaxel and its congeners. The rationale for the production of such a vast assortment of acetylated taxoids is unknown. Some of these metabolites may be relevant intermediates, or may simply represent the consequence of promiscuous acyltransferase activity, while others may play a role in plant defence in possessing antifeedant and antifungal activities and toxicity towards mammals (Daniewski, 2001). It is clear that *Taxus*, both intact plants and derived cell cultures, direct considerable pathway flux to the production of acetylated taxoids other than paclitaxel and any approach to improving the production yields of paclitaxel and its immediate precursors must take into account these apparently diversionary taxoid biosynthetic side-routes.

In this course of investigation, endophytes from *Taxus baccata* growing in the higher altitudes of West Bengal, India were isolated and screened for the production of taxol and its precursor molecules. Further, fungus producing taxol was identified based on morphological and molecular characters. Biotransformation of taxol precursors into bioactive taxanes was also done using the same fungus. Further taxol was modified to couple with fluorescent labels including CdS nanoparticles and *in vivo* and *in vitro* studies were done on different mammalian cell lines.

6. References

1. American Cancer Society. *Cancer Facts and Figures 2007*. Atlanta: American Cancer Society. 1-56.
2. Arvigo R and Balick M. 1993. Rainforest Remedies. Lotus Press, Twin Lakes.
3. Bacon CW and White JF. 2000. Physiological adaptations in the evolution of endophytism in the *Clavicipitacaeae*. In Microbial Endophytes (CW Bacon and JF White, eds): 237-261. Marcel Dekkar, New York.
4. Bacon CW, Porter JK, Robbins JD. 1975. Toxicity and occurrence of *Balansia* on grasses from toxic fescue pastures. Appl Microbiol. 29:553–556.
5. Baker D, Mocek U and Garr C. 2000. Natural products vs. combinatorials: a case study, p. 66–72. *In* S. K. Wrigley, M. A. Hayes, R. Thomas, E. J. T. Chrystal, and N. Nicholson (ed.), Biodiversity: new leads for pharmaceutical and agrochemical industries. The Royal Society of Chemistry, Cambridge, United Kingdom.
6. Baker, U. Mocek, C. Garr. 2000. *Biodiversity: New Leads for Pharmaceutical and Agrochemical Industries* (Eds.: S. K. Wrigley, M. A. Hayes, R. Thomas, E. J. T. Chrystal, N. Nicholson), The Royal Society of Chemistry, Cambridge, UK, pp. 66-72.
7. Beliakoff J, Bagatell R, Paine-Murrieta G, Taylor C W, Lykkesfeldt A E, Whitesell L. 2003. Clin. Cancer Res. 9. 4961–4971.
8. Bensky D and Gamble A. 1993. Chinese herbal medicine. Materia medica, new ed. Eastland Press Inc., Seattle, Wash.
9. Bhat SV, Bajwa BS, Dornauer H, de Souza NJ, Fehlhaber HW. 1977. Tetrahedron Lett. 1669-72.

10. Blagosklonny MV, Giannakakou P, El-Deiry WS, *et al.* 1997. Raf-1/bcl-2 Phosphorylation: A Step from Microtubule Damage to Cell Death. Cancer Res. 57: 130-135.
11. Boyle FT and Costello GF. 1998. Cancer Therapy: a move to molecular level. Chem. Soc. Rev. 27: 251-261.
12. Bush, L. P., P. L. Cornelius, R. C. Buckner, D. R. Varney, R. A. Chapman, P. B. Burrus II, C. W. Kennedy, T. A. Jones and M. J. Saunders. 1982. Association of N-acetyl loline and N-formyl loline with *Epichloe typhina* in tall fescue. Crop Sci. 22:941.
13. Buss AD and. Waigh R D. 1995. In *Burgers Medicinal Chemistry and Drug Discovery*, 5th ed., Vol. 1, M. E. Wolff (Ed.), pp. 983–1033, John Wiley, New York.
14. Buss T and Hayes MA. 2000. Mushrooms, microbes and medicines, p. 75–85. *In* S. K. Wrigley, M. A. Hayes, R. Thomas, E. J. T. Chrystal, and N. Nicholson (ed.), Biodiversity: new leads for pharmaceutical and agrochemical industries. The Royal Society of Chemistry, Cambridge, United Kingdom.
15. Caruso M, Colombo AL, Fedeli L, Pavesi A, Quaroni S, Saracchi M, Bentrella G. 2000. Isolation of endophytic fungi and actinomycetes taxane producers. Ann. Microbiol. 50**:** 3-13.
16. Chang HM, But PPH. 1986. Pharmacology and Applications of Chinese Materia Medica, vol. 1 & 2, World Scientific Publishing, Singapore.
17. Chau M. 2004. Molecular Cloning and Characterisation of 3 Enzymes involved in the taxol/taxoid biosynthesis: Taxoid 2α-hydrolase, Taxoid 7β-hydrolase, and Taxoid 5α-O-Acetylttransferase. *Ph. D Thesis*, Washington State University.
18. Clark M. 1996. Pharm. Res. 13: 1133-1144.
19. Clay K, Schardl C. 2002. Evolutionary origins and ecological consequences of endophyte symbiosis with grasses. American Naturalist 160: 99–127.
20. Crown and Leary MO'. 2000. The taxanes: an update. Lancet. 355: 1167-1168.
21. Dancey J and Sausville E A. 2003. *Nature Rev. Drug Discov.* 2,296–313.
22. Daniewski M *et al.* 2001. Synthesis and antifeedant properties of *N*-benzoylphenylisoserinates of *Lactarius* sesquiterpenoid alcohols. *Phytochemistry* 58: 775-787.

23. Daniewski WM, Gumulka M, Anczewski W, Masnyk M, Bloszyk E, Gupta KK. 1998. Why the yew tree (*Taxus baccata*) is not attacked by insects. Phytochemistry 49: 1279–1282.
24. Danishefsky SJ, Master JJ, Young WB. 1996. A total synthesis of Taxol. J. Am. Chem. Soc. 118: 2843-2859.
25. Dev. 1999. *Environ. Health Perspect.* 107: 783-789.
26. Ding AH, Porteu F, Sanchez E, Nathan CF. 1990. Shared actions of endotoxin and taxol on TNF receptors and TNF release. Science. 248: 370–372.
27. Doherty TM, Sher A, Vogel SN. 1998. Paclitaxel (Taxol)-Induced Killing of *Leishmania* major in Murine Macrophages. Infection and Immunity. 66: 4553-4556.
28. Espinosa P, Zamora J, Feliu, *et al.* 2003. Classification of anticancer drugs: A new system based on therapeutic targets. Cancer Treatment Reviews. 29: 515-523.
29. Fan. 1999. Possible mechanisms of paclitaxel-induced apoptosis. Biochem. Pharmacol. 57: 1215-1221.
30. Farnsworth NR, Akerele O, Bingel AS, Soejarto DD, Guo Z. 1985. Bull. WHO. *63*: 965-981.
31. Fleming E, Mocek U, Floss HG. 1993. Biosyntthesis of taxoids: mode of formation of the taxol side chain. *J. Am. Chem. Soc*. 115: 805-807.
32. Fleming PE, Knaggs AR, He XG, *et al.* 1994. Biosynthesis of taxoids. Mode of attachment of the Taxol side chain. *J. Am. Chem. Soc.* 116: 4137-4138. *Products Isolation: Separation Methods for Antimicrobials, Antiviral and Enzyme.*
33. Foye W O. 1995. *Cancer Chemotherapeutic Agents*, American Chemical Society, Washington, DC.
34. Freeman EM. 1904. Philos. Trans. R. Soc. Lond. [Biol]. 196, 1.
35. Gebetta B, Orsini P, Peterlongo F, Appendino G. 1998. Paclitaxel analogues from *Taxus baccata*. Phytochemisrty. 47 (7): 1325-1329.
36. Grabley S and R Thiericke (ed.). 1999. Drug discovery from nature, p.3–33. Springer-Verlag. Berlin, Germany.
37. Haldar S, Basu A and Croce CM. 1997. Bcl-2 Is the Guardian of Microtubule Integrity. Cancer Res. 57: 229-233.
38. Hamburger M, Marston A, Hostettmann K. 1991. Adv. Drug. Res. 20: 167-215.

39. Hardy TN, Clay K, Hammond Jr AM. 1986. Leaf age and related factors affecting endophyte-mediated resistance to fall armyworm (Lepidoptera: Noctuidae) in tall fescue. Environmental Entomology. 15: 1083–1089.
40. Heldman L, Cheng G, Jenkins, *et al.* 2001. Paclitaxel stent coating inhibits neointimal hyperplasia at 4 weeks in a porcine model of coronary restenosis. *Circulation* 103, 2289-2295. *Inhibitors, Journal of Chromatography Library* (Eds.: G. H. Wagman, R. Cooper), vol. 43, chapter 13, Elsevier, Amsterdam (1989).
41. Holmes et al., 1991. "Phase II Trail of Taxol, an Active Drug in the Treatment of Metastatic Breast Cancer," J. Natl. Cancer Inst. 83: 1797-1805.
42. Holton RA, Somoza C, Kim HB, Liang F, Biediger RJ, Boatman PD, Shindo M, Smith CC, Kim S, Nadizadeh H, Suzuki Y, Tao C, Yu P, Tang S, Zhang P, Murthi KK, Gentile LN, Liu JH. 1994. First total synthesis of Taxol. J. Am. Chem. Soc. 116: 1597-1600.
43. Horwitz SB. 1992. Mechanism of action of Taxol. Trends Pharmacol. Sci. 13: 134–136.
44. Huang Y, Johnson KR, Norris JS, *et al.* 2000. Nuclear Factor-κB/IκB Signaling Pathway May Contribute to the Mediation of Paclitaxel-induced Apoptosis in Solid Tumor Cells. Cancer Res. 60: 4426-4432.
45. Ibrado AM, Liu L, Bhalla K. 1997. Bcl-$X_L$overexpression inhibits progression of molecular events leading to paclitaxel-induced apoptosis of human acute myeloid leukemia HL-60 cells. Cancer Res. 57: 1109–1115.
46. Jennewein S, Rithner CD, Williams R. 2001. Taxol biosynthesis: Taxane 13α-hydroxylase is a cytochrome P450-dependent monooxygenase. Proc. Natl. Acad. Sci. USA. 98: 13595-13600.
47. Kamal A, Thao L, Sensintaffar J, Zhang L, Boehm M F, Fritz L C, Burrows F J. 2003. Nature 425, 407–410.
48. Kapoor D. 1990. *CRC Handbook of Ayurvedic Medicinal Plants*, CRC Press, Boca Raton.
49. Kaspera and. Croteau R. 2006. Cytochrome P450 oxygenases of Taxol biosynthesis *Phytochem Rev.* 5: 433–444.
50. Kinghorn D. 1987. *J. Nat. Prod. 50*: 1009-1024.
51. Kingston G.I. 2001. Taxol, a molecule for all seasons. Chem. Commun. 867–880.

52. Kingston I. 2000. Recent advances in chemistry of taxol. Journal of Natural Products. 63: 726-734.
53. Krishna G, Kumar DV, Khan B. M, *et al.* 1998. Taxol-DNA interactions: fluorescence and CD studies of DNA groove binding properties of taxol. *Biochimica et.* Biophysica Acta. 1381: 104-112.
54. Kusama H, Hara R, Kawahara S, Nishimori T, Kashima H, Nakamura N, Morihira K, Kuwajima I. 2000. J. Am. Chem. Soc. 122: 3811.
55. Lee J, Lobkovsky E, Pliam NB, Strobel GA, Clardy J. 1995. Subglutinols A and B: immunosuppressive compounds from the endophytic fungus *Fusarium subglutinans*. J. Org. Chem. 60: 7076-7077.
56. Li JY, Sidhu RS, Ford E, Hess WM, Strobel GA. 1998. The induction of taxol production in the endophytic fungus *Periconia sp*. from *Torreya grandifolia*. J. Ind. Microbiol. 20**:** 259–264.
57. Li JY, Strobel GA, Harper JK, Lobkovsky E, Clardy J. 2000. Cryptocin, a potent tetramic acid antimycotic from the endophytic fungus *Cryptosporiopsis cf. quercina*. Org. Lett. 2: 767-770.
58. Lyons PC, Plattner RD, Bacon CW. 1986. Occurrence of peptide and clavine ergot alkaloids in tall fescue grass. Science. 232: 487–489.
59. Manfredi JJ and Horwitz SB. 1984. Taxol: an antimitotic agent with a new mechanism of action. *Pharmacol. Ther.* 25: 83-125.
60. Mann J. 1994. *Murder, Magic, and Medicine,* pp. 164–170, Oxford University Press, New York.
61. Matthew Suffness. 1995. *Taxol: science and applications.* Published by CRC Press. Patel. Tour de Paclitaxel: Biocatalysis for Semisynthesis. *Annu. Rev. Microbiol.* 98 (1998) pp. 361-395.
62. McGuire WL, Clark GM, Dressler LG, Owens M, Pounds G, Oldaker T. 1989. Prediction of relapse or survival in patients with node negative breast cancer by DNA flow cytometry. N EngI J Med. 320:627-632.
63. Michaelis ML, Ranciat N, Chen Y, *et al.* 1998. Protection Against ß-Amyloid Toxicity in Primary Neurons by Paclitaxel (Taxol) J. Neurochem. 70: 1623-1627.
64. Moos J and Fitzpatrick FA. 1998. Taxane-mediated gene induction is independent of microtubule stabilization: Induction of transcription regulators and enzymes that modulate inflammation and apoptosis. Proc. Natl. Acad. Sci. USA. 95. 3896–3901.

65. Mukaiyama T, Shiina I, Iwadare H, Saitoh M, Nishimura T, Ohkawa N, Sakoh H, Nishimura K, Tani Y, Hasegawa M., Yamada K, Saitoh K. 1999. Chem. Eur. J. 5: 121.
66. Na and S. N. Timasheff. 1982. In vitro vinblastine-induced tubulin paracrystals J. Biol. Chem. 257: 10387-10391.
67. Newman D J and. Cragg G M. 2005. In *Drug Discovery, Therapeutics, and Preventive Medicine*, L. Zhang, A. Fleming, A. L. Demain (Eds.), Humana Press, Totowa, NJ.
68. Newman D J, Cragg G M, Holbeck S, Sausville E A. 2002. *Curr. Cancer Drug Targ.* 2,279–308.
69. Nicolaou KC, Yang Z, Liu JJ, Ueno H, Nantermet PG, Guy RK, Claiborne CF, Renaud J, Couladours EA, Paulvannan K, Sorensen EJ. 1994. Total synthesis of taxol. Nat. 367: 630-634.
70. Ojima S, Chakravarty T, Inoue, *et al.* 1999. A common pharmacophore for cytotoxic natural products that stabilize microtubules. Proc. Natl. Acad. Sci. USA. 96: 4256-4261.
71. Page M and Landry N. 1996. Bacterial mass production of taxanes with *Erwinia*. US P5561055; Chem Abt. 125. P 245821.
72. Park SJ, Wu CH, Gordon JD, *et al.* 2004. Taxol Induces Caspase-10-dependent Apoptosis. Biol. Chem. 279: 51057-51067.
73. Pineiro D, Martin ME, Guerra N, *et al.* 2007. Calpain inhibition stimulates caspase-dependent apoptosis induced by taxol in NIH3T3 cells. Exptal cell res. 313: 369-379.
74. Porter JK, Bacon CW, Cutler HG, Arrendale RF, Robbins JD (1985) *In vitro* auxin production by *Balansia epichloe.* Phytochemistry 24:1429-1431.
75. Poruchynsky MS, Wang EE, Rudin CM, *et al.* 1998. Bcl-xL is Phosphorylated in Malignant Cells following Microtubule Disruption. Cancer Res. 58: 3331-3338.
76. Robert SC and Shuler ML. 1997. Large-scale plant cell culture. Current Opinion in Biotechnology. 8: 154-159.
77. Rodi DJ, Janes RW, Sanganee HJ *et al.* 1999. Screening of a library of phage-displayed peptides identifies human bcl-2 as a taxol-binding protein. J. Mol. Biol. 285: 197-203.

78. Rupasinghe S and Schuler MA. 2006. Homology modeling of plant cytochrome P450s. Phytochem Rev. 5: 473-505.
79. Scatena D, Stewart ZA, Mays D, *et al*. 1998. Mitotic Phosphorylation of Bcl-2 during Normal Cell Cycle Progression and Taxol-induced Growth Arrest J. Biol. Chem. 273: 30777-30784.
80. Schiff PB and Horwitz SB. 1979. Promotion of microtuble assembly in vitro by taxol. Nature. 277: 665–667.
81. Schuler MA. 1996. The role of cytochrome P450 monooxygenases in plant-insect interactions. Plant Physiol. 112: 1411–1419.
82. Schultes E and Raffauf RF. 1990. *The Healing Forest*, Dioscorides Press, Portland.
83. Snyder JP, Nettles JH, Cornett B, *et al.* 2001. The binding conformation of Taxol in β-tubulin: A model based on electron crystallographic density. *Proceedings of the National Academy of Sciences, USA*. 9: 85312-85316.
84. Stierle A, Strobel G and Stierle D. 1993. Taxol and Taxane Production by *Taxomyces andreanae*, an Endophytic Fungus of Pacific Yew. Science. 260: 214-216.
85. Strobel G and Daisy B. 2003. Bioprospecting for Microbial Endophytes and Their Natural Products. Microb and Mole boil rev. 67: 491–502.
86. Strobel G, Yang X, Sears J, *et al.* 1996. Taxol from *Pestalotiopsis microspora*, an endophytic fungus of *Taxus wallichiana*. Microbiology. 142: 435–440.
87. Strobel GA, Miller RV, Miller C, Condron M, Teplow DB and Hess WM. 1999. Cryptocandin, a potent antimycotic from the endophytic fungus *Cryptosporiopsis cf. quercina*. Microbiology. 145:1919-1926.
88. Sudo T, Nitta M, Saya H and Ueno NT. Dependence of paclitaxel sensitivity on a functional spindle assembly checkpoint. Cancer Res 2004; 64:2502–8.
89. Suffness M**.** 1995. Taxol, science and applications. CRC Press, Boca Raton, Fla.
90. Verpoorte R. 1998. Exploration of nature's chemodiversity: the role of secondary metabolites as leads in drug development. Drug Discovery Today. 3: 232–238.
91. Walker R and Croteau. 2001. Taxol biosynthetic genes. *Phytochemistry.* 58: 1–7.
92. Walker R, Long and Croteau R. 2002. The final acylation step in Taxol biosynthesis: Cloning of the taxoid C13-side-chain N-benzoyltransferase from *Taxus. Proc. Natl. Acad. Sci. USA.* 99: 9166-9171.

93. Wang H, Wang HS and Soong YK. 2000. Paclitaxel-induced cell death: where the cell cycle and apoptosis come together. *Cancer* (N. Y.). 88: 2619-2628.

94. Wani C, Taylor HL, Wall ME *et al*, 1971. Plant Antitumor Agents. VI. The Isolation and Structure of Taxol, a Novel Antileukemic and Antitumor Agent from *Taxus breoifolia*. Journal of the American Chemical Society. 1: 2325-2327.

95. Wartmann M and. Altmann K H. 2002. *Curr. Med. Chem. Anti-Cancer Agents* 2,123–148.

96. Wender PA and David BR. 1992. Toward the Synthesis of the Taxol C, D Ring System: Photolysis of a-Methoxy Ketones Tetrahedron. 48. 7033-7048.

97. Wilson and Jordan. 1995. Microtubule dynamics: taking aim at a moving target. Chemistry & Biology. 2: 569-573.

98. Yates SG, Plattner RD and Garner GB. 1985. Detection of ergopeptine alkaloids in endophyte infected, toxic K-31 tall fescue by mass spectrometry/ mass spectrometry. J. Agric. Food Chem. 33:719.

99. Yeung K, Germond C, Chen X, *et al.* 1999. The Mode of Action of Taxol: Apoptosis at Low Concentration and Necrosis at High Concentration. *Biochemical and Biophysical Research Communications.* 263: 398-404.

100. Young DH, Lichelotti EL, Swindell CS, Krauss NE. 1992. Antifungal properties of taxol and various analogues. Experientia 48:882–885.

101. Zhong JJ. 2004. Plant cell culture for production of paclitaxel and other taxanes. *J Biosci Bioeng*. 94: 591-599.

Chapter 2

Isolation, Screening, Morphological and Molecular characterization of taxol producing endophytic fungus.

1. Summary

The endophytic fungal population was explored from different tissues of *Taxus baccata* growing at higher altitudes of West Bengal, India. The isolated fungal population represented different genera, which were screened for taxol production using immunoassay (CIEIA) technique. The culture AAT-TS-4$_1$ that produced taxol was identified as *Gliocladium* sp. on the basis of its cultural as well as morphological characters and also by ITS and 18S rRNA sequence analysis. Kinetics of taxol production as a function of culture growth was also investigated.

2. Introduction

It is seen that endophytic microbial populations can easily adapt their physiology in order to establish themselves in the plant host tissues. These physiological changes can result in production of useful metabolites which could be exploited for human use. Taxol is one such metabolite that was first isolated from the bark of Western yew, *Taxus brevifolia* (Wani et al, 1971) and later on from other geographically diverse *Taxus* species. This anti-microtubule drug is used for the treatment of a broad range of human tumors including ovarian and metastatic breast cancer (Croom et al, 1995). Apart from cancer treatment, its applications in rheumatoid arthritis, malaria, Alzheimer's disease and Autosomal Dominant Polycystic Kidney Disease (ADPKD) (Croom et al, 1995) have been reported.

The use of *Taxus* sp. for taxol production is ecologically unsuitable as it requires sacrificing the mature trees. Over the past few years, other renewable sources have been found which account for the commercial scale taxol production, such as needles (leaves) (Witherup et al, 1990), plant tissue culturing of *Taxus* species (Robert et al, 1997) and synthesis from readily available 10-deacetylbaccatin III (Gebetta et al, 1998). But none of them could meet the high demand for the drug. A novel method for the production of taxol by a cheaper industrial fermentation method has come from the discovery of

endophytic fungi belonging to different genera that produce taxol. Apart from fungi, some bacteria (Page et al, 1999) and actinomycetes (Caruso et al, 2000) that produce taxol have also been discovered. India has a large wealth of medicinal plants with an abundance of *Taxus baccata,* hence a screening programme was initiated to isolate endophytic microorganisms from *Taxus baccata* that could produce taxol.

3. Materials

Taxus baccata was brought from West Bengal, India. Taxol Immunoassay kit was bought from Hawaii Biotech, Hawaii (USA). PCR buffer and Taq polymerase was from Bangalore Genei, India. dNTPs were from Sigma. Restriction enzymes and pGEM T vector were from Promega (USA). Secondary antibodies- enzyme conjugates were from CAL TAG Laboratories, San Francisco, USA. PCR primers from MWG, Bangalore. Gel elution kit was from Axygen, USA. p-nPP (p-nitro phenyl phosphate) was from Sigma. All other chemicals and solvents were from Qualigens, Himedia and Merck (HPLC grade).

3.1. Potato Dextrose Agar (PDA)

Potato	250 gm
Dextrose	20gm
Agar	20gm
Distilled Water	1000 mL

3.2. Modified Taxol Medium (MM)

Soya Peptone	10 gm
Glucose	40 gm
Sodium Acetate	1 gm
Sodium Benzoate	50 mg
Distilled Water	1000 mL

3.3. Luria Bertani Broth (LB)

Bactotryptone	10 gm
Yeast extract	5 gm
NaCl	10 gm
Distilled Water	1000 mL
pH adjusted to 7.2 using NaOH.	

3.4. S7 media

Glucose	1 gm
Sucrose	3 gm
Fructose	6 gm
Sodium acetate	1 gm
Soya peptone	1 gm
Manganese chloride	5 mg
Magnesium sulphate	3.6 mg
Cupric nitrate	1 mg
Calcium nitrate	6.8 mg
Ferric chloride	2 mg
Biotin	1 mg
Thiamine	1 mg
Pyridoxal	1 mg
Calcium pantothenate	1 mg
L- phenylalanine	5 mg
Sodium benzoate	100 mg
Phosphate buffer (pH 6.8) 1 M	1 mL
Distilled Water	1000 mL

3.5. Buffers used for the Immunoassay

3.5.1. 1 M Sodium phosphate buffer pH 7.0

100 mL of 1 M of NaH_2PO_4 (15.6 gm in 100 mL)

100 mL of 1 M of Na_2HPO_4 (17.8 gm in 100 mL)

Adjust the pH of NaH_2PO_4 with Na_2HPO_4.

3.5.2. 50 mM (PBS) Phosphate buffer saline (pH 7.0)

1 M PB was diluted to make 50 mM

0.15 M NaCl,

0.02 % (w/v) NaN_3.

3.5.3. Blocking buffer

50 mM PBS

1 % BSA and 0.02 % (w/v) NaN_3

3.5.4. Sample diluting buffer

PBS- 0.25 % (w/v) BSA, 0.05 % (v/v) Tween– 20, 20 % (v/v) Methanol and 0.02 % NaN_3.

3.5.5. Antibody diluting buffer

PBS- 0.25 % (w/v) BSA, 0.05 % (v/v) Tween– 20 and 0.02 % NaN_3

3.5.6. Wash buffer

50 mM Tris HCL, pH 7.0, 0.15 M NaCl, 0.05 % (v/v) Tween- 20 and 0.02 % NaN_3.

3.5.7. Enzyme Substrate buffer

25 mM Tris, pH 9.5, 0.15 M NaCl, 5 nM $MgCl_2$ and 0.02 % NaN_3.

4. Methods

4.1. Isolation of endophytic fungi from *T. baccata.*

Endophytic fungi were isolated from the bark, stem and needles of *T. baccata* obtained from West Bengal, India. The samples were cut into small pieces approximately (0.5 cm X 0.5 cm) and surface sterilized with 0.01% mercuric chloride ($HgCl_2$) solution for 1 min and washed thoroughly with sterile distilled water (Bills, 1996; Janardhanan et al, 1991; Ahmad, 1991; Moutia and Dookuna, 1999). The outer bark was teased apart with the help of sterilized sharp blade in order to obtain inner bark (stem). Residual water on the sample surface was removed by soaking on sterile blotting paper. Small pieces of stem and needles were placed on the surface of Potato Dextrose Agar (PDA) poured into Petri dishes. After 10-15 days, fungi were observed growing from the stem and needle fragments in the plates. Individual hyphal tips of the various fungi were removed from the PDA plates and placed again on PDA and incubated at room temperature for at least 10-15 days. Each fungal culture was checked for purity and transferred to agar slants by hyphal tip as well as single spore isolation method (Strobel et al, 1996; Ahmad, 1991). From the fungal population only the slow growing and unusual fungi were considered for further study. Stock cultures were maintained by subculturing at monthly intervals. After growing at a pH of 7 and 25 ^{o}C for 7 days the slants were maintained at 15 ^{o}C. From an actively growing stock culture, sub-cultures were made on fresh slants and after 7 days of incubation at pH 7 and 25 ^{o}C, these were used as the starting material for fermentation experiments.

4.2. Screening of endophytic fungi for taxol production

Production of taxol by the forty endophytic fungi isolated from different plant parts of *Taxus baccata* was studied by a two stage fermentation procedure. In the first stage, these fungi were grown in submerged culture and in the second stage they were grown as stationary culture. These fungi were grown in 500 mL Erlenmeyer flasks containing 100 mL modified mycological medium (Stierle et al, 1993). The flasks were inoculated with agar plugs, containing mycelium from 7 days old slants. The inoculated flasks were incubated at 25-27 ^{0}C on a rotary shaker (240 rpm) for 5 days. These cultures were used as seed cultures (First stage). For taxol production, 10 mL seed cultures were transferred to 500 mL flasks containing 100 mL modified S7 medium (Stierle et al, 1993). The flasks were incubated at 25-27 ^{0}C for 21 days as stationary culture (Second stage). After 3 weeks of incubation the culture was harvested and passed through four layers of muslin cloth to separate the mycelial mat from the culture filtrate. Both the culture filtrate & mycelia were lyophilized to dryness, extracted thrice with equal volumes of chloroform: methanol (9:1). The extracts were pooled and dried with anhydrous sodium sulphate and concentrated at 40 ^{0}C *in vacuo* to yield crude extract. A small amount of crude extract was dissolved in methanol and then used for screening of taxol positive cultures with the help of the immunoassay technique.

4.3. Immunoassay

Taxol in the crude extracts was detected with the help of an enzyme immunoassay kit (Indirect competitive enzyme linked immunoassay (CIEIA), Hawaii Biotechnology group, Hawaii), according to the procedure described by the manufacturers (Grothus et al, 1995). It was seen that most of the chloroform extracts were not completely soluble in methanol. In brief the assay was performed as described below:

The assay was performed by coating Taxol –BSA coating antigen at a dilution of 1/100 in 50 mM PBS (100 µL/ well) in a 96-well microtiter plate and incubated for an hour. The unbound antigen was removed by washing the plate with wash buffer (50 mM Tris HCL, pH 7.0, 0.15 M NaCl, containing 0.05 % (v/v) Tween- 20 and 0.02 % NaN_3). The non specific sites were blocked with 1 % (w/v) BSA in PBS (200 µL/ well) for one hour. After washing the unbound BSA, the solid phase bound taxol was incubated with samples prepared in sample diluting buffer (PBS with 1 % BSA, 20 % methanol, 0.02 % Tween- 20) at a dilution of 1/100, (50 µL/ well) and a specific antitaxol monoclonal

antibody at a dilution of 1/100 in antibody diluting buffer (PBS containing 0.25 %BSA, 0.05 % Tween- 20 and 0.02 % NaN_3) (50 µL/ well) and the plate was incubated for one hour at 37 ^{0}C. For plotting a standard curve, the solid phase bound taxol was incubated with standard taxol (25 µL of the standard taxol was serially diluted in 8 wells, wherein the 8th well does not receive any standard taxol) and specific anti-taxol monoclonal antibody at a dilution of 1/100 was added (50 µL/ well) and plate was incubated for about one hour at 37 ^{0}C. The taxol in the sample competes with solid phase bound taxol for binding to the monoclonal antibody. The monoclonal antibody bound to the taxol was detected by an enzymatic reaction in which alkaline phosphatase conjugated goat anti-mouse IgG secondary antibody at a dilution of 1/1000, (100 µL/ well) was incubated for an hour at 37 ^{0}C. The unbound secondary antibody was washed and the substrate p-nitrophenylphosphate (1 mg/ mL) (200 µL/ well) was added and incubated till the color appeared. The inhibition of color development was proportional to the concentration of free taxol present in the samples. The amount of taxol in each sample was calculated from an inhibition curve plotted by using different concentrations of standard taxol supplied with the kit. This technique was used to screen for taxol in each of the fungal extracts. The assay is sensitive to about 1 ng/ mL. Screening of fungal isolates for taxol production, studies on culture conditions inducing taxol production, taxol content in mycelia & culture filtrate and the amount of taxol produced in growth phase of the fungus were performed using the same kit.

4.4. Production of taxol by fungal strain AAT-TS-4$_1$

The fermentation parameters were as described above. The flasks were incubated at 27 ^{0}C for different (2, 5, 10, 15 and 21 days) time intervals as stationary culture (Second stage). After 2, 5, 10, 15 and 21 days of incubation the culture was harvested and passed through four layers of muslin cloth to separate the mycelial mat from the culture filtrate. Culture filtrate & mycelia were lyophilized to dryness, extracted thrice with equal volumes of chloroform: methanol (9:1) each time. Similarly taxol concentration in mycelium, culture filtrate and in different flask conditions such as 500 mL Erlenmeyer flasks, 1 L, 2 L flasks and Rox bottles was also estimated. The crude extracts were dissolved in methanol and then diluted in sample diluting buffer (0.25 % BSA, PBS). The taxol concentration in crude extracts was estimated using the immunoassay described above.

4.5. Cultural and morphological characters of the fungus

For studying the cultural and morphological characters, the fungus was grown on PDA. Cultural characters such as color and nature of the growth of the colony were determined by visual observation. Morphological characteristics of the fungus like mycelia, conidiophores and conidia were microscopically studied (Carl Ziess Axiovert 25 Inverted microscope and Nikon Eclipse E200). Mycelia, conidiophores and conidia produced by the fungus in the culture were examined under the microscope.

4.6. Nutritional studies and factors affecting the growth and sporulation of the fungus

The fungus was grown on the following natural and semisynthetic media, Potato Dextrose Agar (PDA), Oat Meal Agar (OMA), Corn Meal Agar (CMA) and V-8 Juice Agar prepared as described by the manufacturer (Himedia). For studying the growth of the fungus on solid media, petriplates (10 cm dia) poured with 25 mL of each medium were used. Each Petriplate was inoculated in the centre with a mycelial disc (8 mm) cut from a sporulating 20 days old culture growing on PDA. The Petriplates were incubated at 25-27 ^{0}C in a B.O.D incubator. Observations on growth pattern and sporulation were made after 5 days. Sporulation of the fungus in solid media (PDA, CMA, OMA, and V-8 Juice) was determined on the basis of number of spores present per field under uniform magnification and categorized in the following grades as: No sporulation, Good and Excellent. Data set comprising of the morphological characters based on previously published description is in TABLE I. Information regarding shape, temperature, conidiophore, morphological characters of the colony, average diameters of the colony are also listed in TABLE I.

4.7. Genomic DNA isolation

Genomic DNA of the fungal culture was extracted by using the Salting out method (Neumann et al, 1992). 5 g fungal mycelia was ground into a powder using liquid nitrogen and suspended in 5 mL SET buffer (75 mM NaCl, 25 mM EDTA (pH 8.0) and 20 mM Tris (pH 7.5)). 100 µL lysozyme (final conc 1 mg/ mL) was added to the above solution and incubated at 37 ^{0}C for 60 min. 140 µL of proteinase K (final conc. 0.5 mg/ mL) and 600 µL of 10 % SDS were added and incubated for 2 h at 55 ^{0}C with occasional mixing. 2 mL of 5 M NaCl (final conc. 1.25 M) was added and the mixture

was cooled to 37 ^{0}C. 5 mL chloroform was added and mixed for about 30 min at room temperature and then the mixture was centrifuged for 20 min at 4,500 g. The supernatant was transferred into a fresh tube and to it 0.6 vol Isopropanol was added to precipitate the DNA. The DNA was pelleted and washed twice with 70 % ethanol, air dried and dissolved in 100-200 µL of TE buffer (10 mM Tris, 1 mM EDTA, pH 8.0) at 55 ^{0}C. The quality of the DNA isolated was checked on a 0.7 % agarose gel stained with ethidium bromide.

4.8. PCR amplification of ITS regions & 18S rDNA

18S rRNA and ITS regions from the fungal strain were amplified using PCR with a Robocycler GRADIENT 96, Stratagene, USA with a final reaction mixture volume of 15 µL containing 0.4 µL fungal DNA solution (40 ng), 1.5 µL 10X buffer (Bangalore Genei, India), 4 µL (0.2 mM) dNTPs (Sigma), 1 µL (1 µM) each of the universal eukaryotic primers (forward primer) ITS1-TCCGTAGGTGAACCTGCGG, (reverse) ITS2- GCTGCGTTCTTCATCGATGC and (forward primer) ITS3- GCATCGATGAAGAACGCAGC and (reverse) ITS4- TCCTCCGCTTATTGATATGC (White et al, 1990), (forward primer) NS1- GTAGTCATATGCTTGTCTC and (reverse) NS4- CTTCCGTCAATTCCTTTAAG (Gardes and Bruns, 1993) and 0.5 U/µL Taq polymerase (Bangalore Genei, India). Thermocycling parameters were: for ITS region, initial denaturation at 95 ^{0}C for 3 min, 36 cycles: 95 ^{0}C for 30 sec, 52 ^{0}C for 30 sec, 72 ^{0}C for 30 sec; final extension was at 72 ^{0}C for 3 min; for 18S rDNA: initial denaturation at 95 ^{0}C for 3 min, 36 cycles: 95 ^{0}C for 30 sec, 52 ^{0}C for 30 sec, 72 ^{0}C for 1.30 min; final extension was at 72 ^{0}C for 10 min. The resulting PCR products were analyzed on 1 % agarose gel containing ethidium bromide. PCR fragments were eluted from gel with the help of gel elution kit according to the suggested protocol. The pure PCR products were ligated with pGEM-T vector and transformed into competent cell (Sambrooks et al, 1989). Plasmid containing the insert was isolated using alkali lysis method (Sambrooks et al, 1989). The amplified bands were visualized on a 1.2 % agarose gel containing ethidium bromide.

4.9. Extraction and purification of DNA from agarose gels

Extraction of the fragment DNA was carried out by the protocol described in Axygen^{TM} GEL elution kit, Biosciences, USA. The fragment of interest was excised from the gel

and weighed. A 100 µg gel slice was transferred to a 1.5 mL microcentrifuge tube and 300 µL Buffer DE-A added. The tube was incubated at 70 ^{0}C for 5 to 10 min with intermittent mixing until the gel slice was completely dissolved. The gel mixture was cooled down to room temperature and 150 µL Buffer DE-B was added. The solubilized gel was transferred into Axyprep column and centrifuged at 12,000 rpm for 1 min. Supernatant was discarded and the column was washed with 500 µL of wash buffer 1 (provided by Axygen) and centrifuged at 12,000 rpm for 30 s. The supernatant was discarded, 700 µL of wash buffer 2 was added and spun at 12,000 rpm for 30 s. This step was repeated again, to ensure the complete removal of salt. Axyprep column was then transferred into a fresh 1.5 mL microfuge tube and DNA was eluted by adding 25-30 µL of elution buffer. After adding the eluent the tube was left at room temperature for 1 min and centrifuged at 12,000 rpm for 1 min. The filterate containing the DNA was stored at -20 ^{0}C.

4.10. Ligation

The gel-eluted PCR amplified fragment was ligated into pGEM-T vector (Promega, USA.) as given in the protocol below.

pGEM -T® vector (50 ng/ µL)	0.5 µL
Amplicon DNA fragment (10 ng/ µL)	4.0 µL
Ligase buffer (2 X)	5.0 µL
T_4 DNA ligase	0.5 µL

The ligation mixture was kept at 16 ^{0}C overnight and was used for transformation.

4.11. Bacterial transformation and selection

LB medium (50 mL) was inoculated with 1 % of the overnight grown *E. coli* culture and allowed to grow till 0.5 O.D. at 600 nm. The cells were harvested by centrifugation at 5,000 g for 10 min at 4 ^{0}C, suspended in 100 mM ice-cold $CaCl_2$ and kept on ice for 30 min. Cells were centrifuged, the pellet suspended in 1 mL of 100 mM ice-cold $CaCl_2$ and stored as aliquots of 200 µL at 4 ^{0}C. The competent *E. coli* cells, thus formed, were transformed according to Sambrook et al (1989). Briefly DNA (~50 ng in 10 µL or less) was added to the competent *E. coli* cells, mixed and kept on ice for 30 min. The cells were then incubated at 42 ^{0}C for 2 min. To each tube 800 µL of LB broth was added and

further incubated at 37 ^{0}C for 1 h. About 100 µL of the transformed competent cells were spread onto LB plates containing appropriate antibiotic, IPTG and X-gal (Sambrook et al, 1989).

Solutions	*Stock*	*Final conc.*
1) IPTG stock solution	200 mg mL^{-1} in sterile distilled water	40 µg mL^{-1}
2) X-gal stock solution	20 mg mL^{-1} in dimethylformamide	40 µg mL^{-1}

4.12. Isolation of plasmid DNA from *E. coli* cells by the alkaline lysis method

Solution I : 25 mM Tris-HCl (pH 8.0), 10 mM EDTA (pH 8.0), 50 mM Glucose.

Solution II: 0.2 N NaOH, 1 % SDS (freshly prepared).

Solution III: 3.0 M Potassium acetate (pH 4.8).

The alkaline lysis method of Sambrook et al (1989) was improvised upon so that 12-24 samples could be processed conveniently for plasmid DNA extraction within 3 h, with yields of 5-30 µg per 1.5 mL culture depending on the host strain and the plasmid vector. An important feature of this protocol was the use of PEG for purification, which resulted in precipitation of high quality super-coiled plasmid DNA free of contamination. The bacterial cultures were grown overnight (O/N) with shaking (200 rpm) at 37 ^{0}C in LB broth containing the appropriate antibiotic. About 1.5 to 3 mL culture was centrifuged for 1 min at 4,000 g to pellet the bacterial cells. The pellet was resuspended in 100 µL of TEG buffer by vigorous pipetting. 200 µL of Soln. II was added & mixed by inversion till the solution becomes clear and incubated on ice for 5 min. The cell lysate was neutralized by addition of 150 µL of Soln. III, mixed well and incubated on ice for 5 min. The cell debris was removed by centrifuging for 5 min at 12,000 x g at 4 ^{0}C. The supernatant was transferred to a clean tube. RNase A to a final concentration of 20 µg mL^{-1} (Sambrook et al, 1989) was added to this and incubated at 37 ^{0}C for 20 min. To the above solution 400 µL of chloroform was added, mixed for 30 s and centrifuged for 5 min at 12,000 g at 4 ^{0}C. The upper aqueous layer was transferred to a clean tube, 1/10th volume sodium acetate and 1 mL of absolute ethanol was added with mixing and kept at -20 ^{0}C for 1-2 h. The sample was centrifuged at 12,000 g for 10 min at room temperature. The pellet was washed thrice with 70 % ethanol and dried under vacuum. The dried pellet was dissolved in 40 µL of deionized

water and 40 µL of PEG-NaCl solution (20 % PEG 8000 in 2.5 M NaCl) was added. The mixture was incubated on ice for 20 min and the plasmid DNA pelleted out by centrifugation at 12,000 x g for 15 min at 4 ^{0}C. The supernatant was aspirated carefully, the pellet washed with 70 % ethanol and air-dried. The dried pellet was resuspended in 20 µL of deionized water and stored at -70 ^{0}C.

4.13. Restriction digestion of DNA

Insert in the plasmid was identified after the restriction digestion of DNA with EcoR1

SMQ	14.0 µL
Plasmid DNA	3.0 µL (2 µg)
Buffer *Eco* RI	2.0 µL
EcoR1 (NEB, England)	1.0 µL (10 U/ µL)

The mixture was kept at 37 ^{0}C for 3 h and checked on 1 % Agarose gel.

4.14. DNA sequencing and sequence analysis

The cloned fragments were sequenced using Sanger's dideoxy method (Sanger et al, 1977) using ABI Prism Big Dye Terminator Cycle sequencing kit from ABI systems. The most identical sequences of the strain AAT-TS-4$_1$ were identified from NR database of Genbank using BLAST algorithm (Altusch et al, 1997). Sequences showing high sequence identity were manually picked for further analysis. Multiple sequence alignment was performed for the sequences obtained from BLAST search using ClustalW algorithm (Higgins et al, 1994). Phylogenetic analysis was carried out using PHYLIP v3.62 suite of programs (Felsenstein, 1985). Since the sequences obtained from the BLAST search were the ones showing maximum homology, DNAPARS program was used for further analysis. The bootstrap values for the parsimony tree were obtained by analysis of 100 replicates with input order jumbled 10 times using SeqBoot program. A consensus tree was constructed from the output generated using the program CONSENSUS. DNAML, a program based on maximum-likelihood method was also used for comparison. Both the methods were used to analyze all the three sequences (two ITS region sequences and one 18S rRNA sequence) of the fungus AAT-TS-4$_1$. The data generated was converted into trees using DRAWGRAM.

.

5. Results

5.1. Endophytic fungi from *Taxus baccata*

Forty fungal endophytes were recovered from most of the analyzed tissue and almost equal numbers of endophytes were isolated from each of them. Other microbes like bacteria and actinomycetes were also seen but they were not considered for the study. Presence of same genera of fungi in different analyzed tissue was seen. Most of the fungi isolated were unusual and very slow growing. All the endophytic fungi isolated were brought to pure culture form. Out of forty endophytic fungal cultures screened for taxol production, one culture assigned as AAT-TS-4_1 (an endophyte isolated from the stem) was seen to produce taxol. None of the other fungal cultures produced considerable concentrations of taxol. The exact concentrations of the taxol could not be detected as the crude chloroform extracts did not dissolve completely in methanol.

5.2. Cultural and morphological characters of the fungus

The fungus AAT-TS-4_1 isolated and grown on PDA medium produced slow growing colonies. Colonies on PDA showed following characters: white, flocculose, circular, compact, reverse cream, margin smooth, hyphae branched septate, smooth and hyaline (Merritt et al, 2003). Conidiophores were non stromatic, produced from superficial hyphae, erect, branched to unbranched, septate and hyaline. Phialides were solitary or produced in a group of 2-5, straight, smooth, verticillate, hyaline (FIG 1). Conidia were produced singly or in small moist clusters apically, smooth, oval to cylindrical to curved, hyaline, single celled, variable in shape and size (Hans et al, 1999). Based on above mentioned cultural and morphological characters the strain has been identified as *Gliocladium* sp.

5.3. Effect of various nutrient media on growth and sporulation

The fungus showed significant variation in growth rate when grown on various nutrient media. The results are presented in TABLE 1 and FIG 2. Results showed that the fungus can be grown on a variety of natural as well as semi-synthetic media. Among the four different media tested, it was found that Oat Meal Agar was the best for the growth of the fungus followed by CMA. PDA medium also gave good growth. However, poor growth was recorded in V-8 Juice media. Excellent sporulation was recorded in PDA,

OMA media, whereas good sporulation was observed in CMA medium. No sporulation was recorded in V-8 Juice medium.

Characters	**PDA**	**V-8 Juice**	**OMA**	**CMA**
Average dia. (mm) of the colonies after 5 day.	25 mm	18 mm	40 mm	30 mm
Morphological characters of the colony	Circular, smooth, flocculose and dense	Circular, smooth, flocculose and dense	Sparse, woolly with definite periphery	Circular, not so compact, cottony
Colony color	White in front and pale cream on reverse	White in front and dark cream on reverse	White in front and reverse	White in front and pale cream on reverse
Conidiophore	Erect, branched to unbranched Verticillium like, with two- five phalides	No conidiophores seen	Erect, branched to unbranched Verticillium like, with two- five phalides	Erect, branched to unbranched Verticillium like, with two- five phalides
Conidia	+++	+	+++	++
Conidia shape	Cylindrical, oval and curved	None	Curved, oval and cylindrical	Cylindrical, oval and curved
Optimum temperature for growth	25- 27 ^{0}C	25- 27 ^{0}C	25- 27 ^{0}C	25- 27 ^{0}C

TABLE 1: Growth and morphological characters of the colony of fungus, AAT-TS-4$_1$

+++: Excellent, ++: Good, +: No sporulation
Excellent : More than 100 spores
Good : More than 50 spores

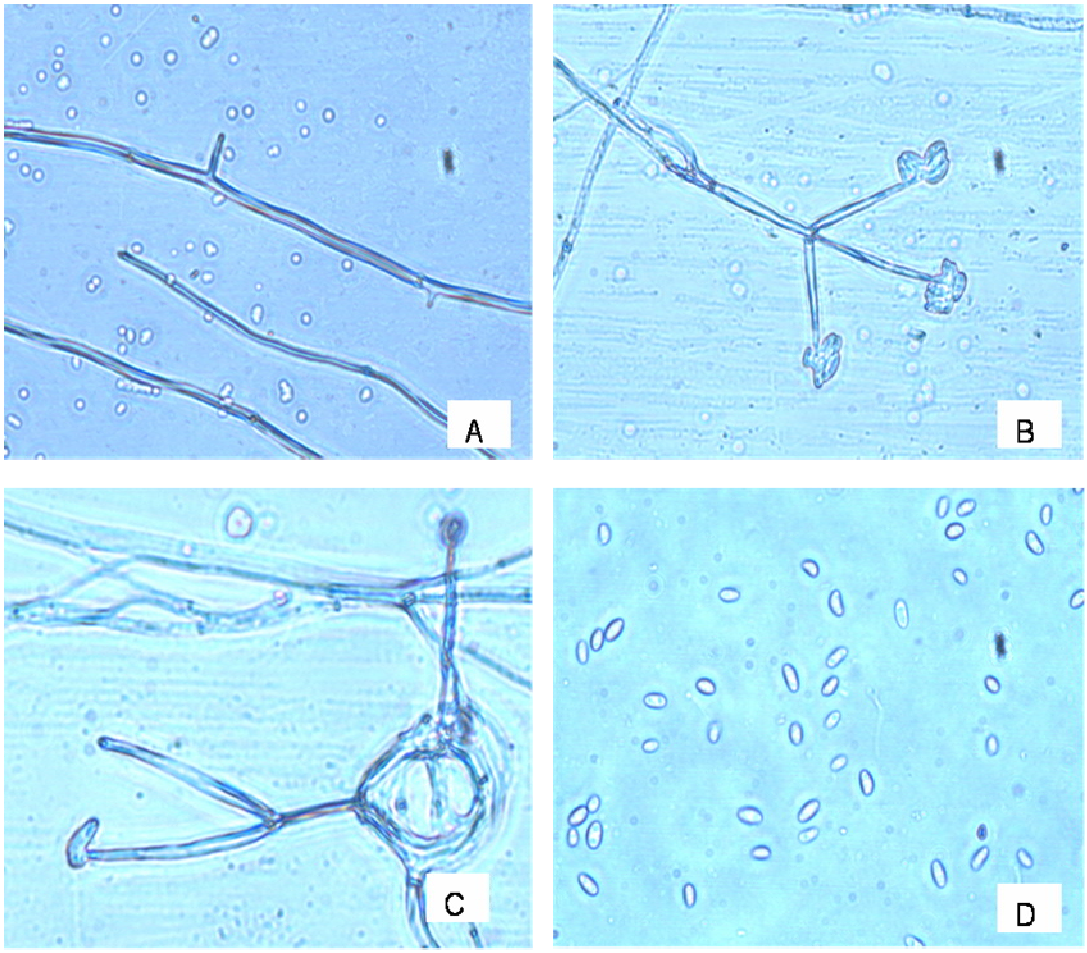

FIG 1: Micrographs of A) Mycelium, B) Conidiophores bearing conidia, C) Arrangement of conidia on phialide tip and D) Conidia.

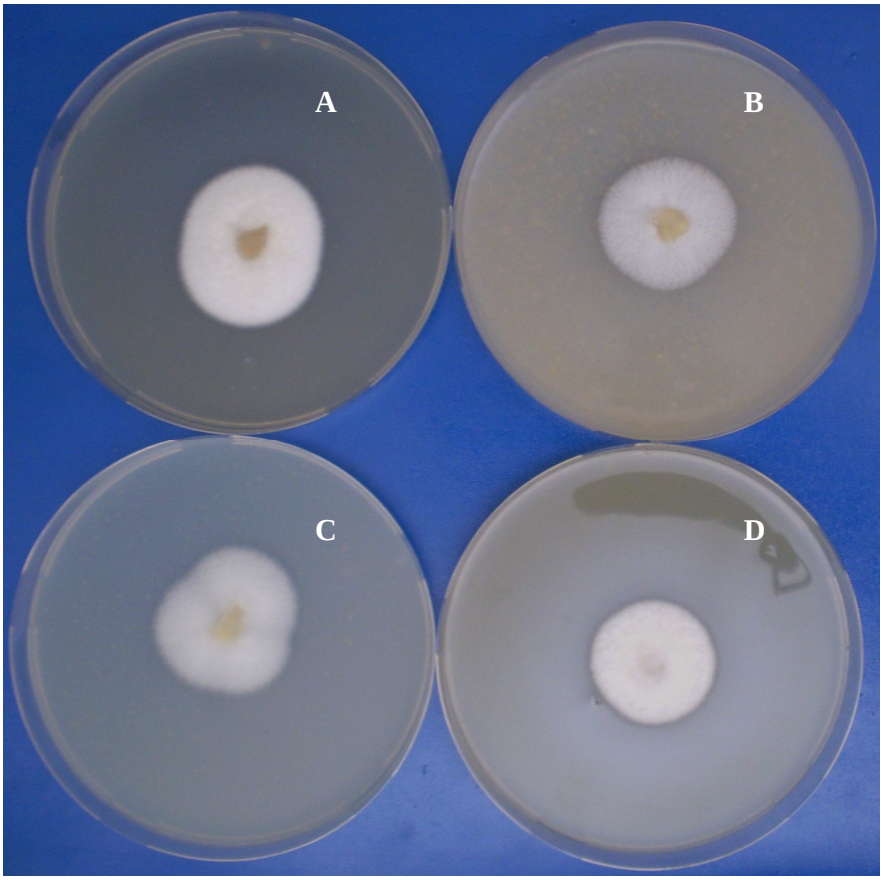

FIG 2: Picture of *Gliocladium* sp growing on A) PDA, B) OMA, C) CMA and D) V 8 Juice at different time intervals.

5.4. PCR amplification and sequence analysis

The method employed for the genomic DNA isolation resulted in obtaining high quality DNA (FIG 3). Universal eukaryotic primers (ITS 1 & 2, ITS 3 & 4 and NS1 & 4) used for the amplification of ITS regions and 18S rRNA successfully amplified fungal genomic DNA producing fragments of 0.2 kb, 0.3 kb (FIG 4) and 1.1 kb (FIG 5) respectively. All the clones obtained showed the respective inserts when subjected to restriction digestion and analyzed on agarose gel (FIG 6). Sequence analysis was done using Chromos V 2.0 program and the sequence profile was obtained in FASTA format. BLAST analysis of the sequences determined the identical sequences from the database. Majority of the hits from the BLAST search were from a group of fungus belonging to Ascomycetes which include *Gliocladium* sp., *Bionectria* sp., *Nectria* sp. and *Clonostachys* sp. All three sequences (ITS 1&2, ITS 3 & 4 and NS1 & NS4) showed similarity in the range of 95-98%. However 18S rRNA sequence showed hits from diverse genera with major hits being from *Bionectria* sp. showing more than 95% sequence similarity. The sequence analysis determined that the 0.2kb fragment is a partial ITS region at 5' end and partial 5.8S rRNA gene at 3', the 0.3 kb fragment is a partial 5.8S rRNA gene at 5' and partial ITS region at 3' and 1.2 kb fragment is 18S rRNA gene at 5' and partial 28S at 3'. All the sequences were aligned with ClustalW and the relatedness between the sequences was determined. All the sequences were submitted in NCBI gene bank and are retrievable with accession numbers: EU528675, EU581866 and EU581865.

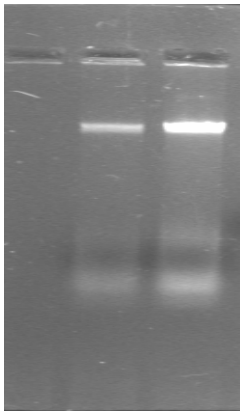

FIG 3: Fungal Genomic DNA on 0.8% Agarose Gel.

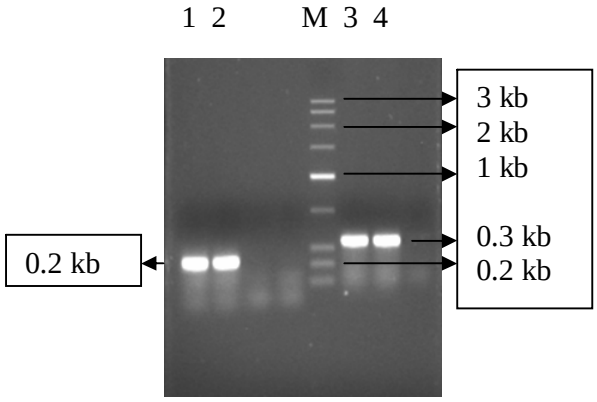

FIG 4: Lane 1 and 2: 0.2 kb PCR amplicon obtained using ITS1 & 2. Lane M: Low range ruler and Lane 3 and 4: 0.3 kb amplicon obtained using ITS3 & 4 primers.

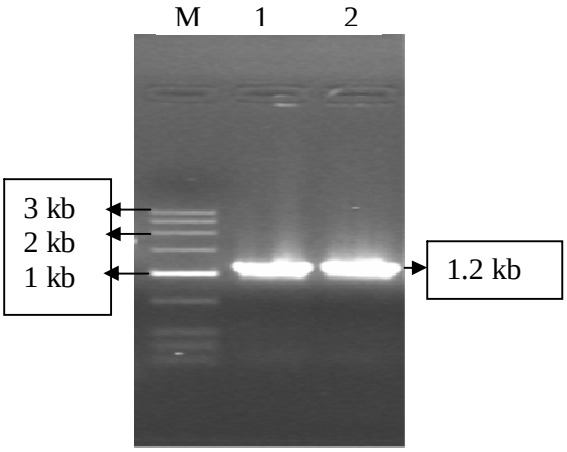

FIG 5: PCR amplification of 18S rRNA gene using primer NS 1& 2. Lane M: low range DNA marker. Lane 1 and 2: 1.2 kb PCR product.

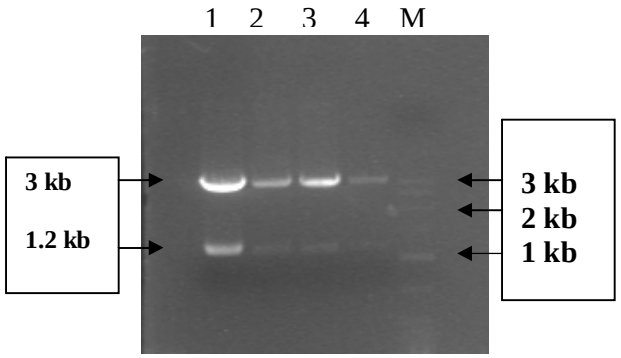

FIG 6: Agarose gel showing Plasmid DNA with 1.2 kb insert in lane 1, 2, 3 and 4 after restriction digestion with EcoRI. Lane M is DNA size marker.

5.5. Phylogenetic analysis

Sequences obtained of ITS region and 18S rRNA are accessible from genebank with accession numbers: EU528675, EU581866 and EU581865 (FIG 7). FIG 8 (A and B) shows the results of the phylogenetic analysis done using ITS 1 and ITS 3 sequences of the ITS region. The overall grouping of the fungi was same for both the methods (DNAPARS & DNAML) of analysis, however the precise ordering of the fungi was different. Sequence comparison confirmed that most sequences from database showed more than 95-98 % sequence identity, but only *Gliocladium* sp. and *Clonostachys* sp. were grouped together with the ITS region sequence of AAT-TS-4_1. To be more specific *Gliocladium* sp. showed an outstanding closeness with AAT-TS-4_1, which is evident in the phylogenetic trees. In ITS analysis, all the *Nectria* sp. (teleomorph) sequences were grouped together along with *Gliocladium* and AAT-TS-4_1 sequence (FIG 8 (B)). However, the tree obtained by sequences from ITS 1 did not give any information as seen in FIG 8 (A), apart from showing our sequence closely placed with *Gliocladium* sp. In case of 18S rRNA sequence, AAT-TS-4_1 was always grouped with *Nectria* sp. in both the methods of analysis (FIG 8 (C)) which is a teleomorph of *Gliocladium* sp. Even though fungi belonging to genera *Myrothecium*, *Geosmithia* and *Stephanonectria* showed more than 95 % sequence similarity, none of them showed relatedness with AAT-TS-4_1 in phylogenetic analysis.

A)

```
  1 CAGCCACGAG TTTACAACTC CCAAACCCAT GTGAACATAC CTACTGTTGC
 51 TTCGGCGGGA TTGCCCCGGG CGCCTCGTGT GCCCCGGATC AGGCGCCCGC
101 CTAGGAAACT TAACTCTTGT TTTATTTTGG AATCTTCTGA GTAGTTTTTA
151 CAAATAAATA AAAACTTTCA ACAACGGATC CCTTGAAAAA CGCAGCTCAA
```

B)

```
  1 TCCTTTTAAT AAGGGAAATG CAGATTCAGT GATCATCGAA TCTTTGAACG
 51 CACATTGCGC CCGCCAGTAT TCTGGCGGGC ATGCCTGTCT GAGCGTCATT
101 TCAACCCTCA TGCCCCTAGG GCGTGGTGTT GGGGATCGGC CAAAGCCCGC
151 GAGGGACGGC CGGCCCCTAA ATCTAGTGGC GGACCCGTCG TGGCCTCCTC
201 TGCGAAGTAG TGATATTCCG CATCGGAGAG CGACGAGCCC CTGCCGTTAA
251 ACCCCCAACT TTCCAAGGTT GACCTCAGAT CAGGTAGGAA TACCCGCTGA
301 ACTTAAGCAT ATCAATAAGC GGAGGAA
```

C)

```
   1 AAGGAATTTC CACCGCGGTT TGGGGAGCTC TCCCATATGG TCGACCTGCA
  51 GGCGGCCGCG AATTCACTAG TGATTGTAGT CATATGCTTG TCTCAAAGAT
 101 TAAGCCATGC ATGTCTAAGT ATAAGCAATT ATACGGCGAA ACTGCGAATG
 151 GCTCATTATA TAAGTTATCG TTTATTTGAT AGTACCTTAC TACTTGGATA
 201 ACCGTGGTAA TTCTAGAGCT AATACATGCT TAAAATCCCG ACTTCGGAAG
 251 GGATGTATTT ATTAGATTAA AAACCAATGC CCTTCGGGGC TCTCTGGTGA
 301 TTCATGATAA CTTCTCGAAT CGCATGGCCT TGCGCCGGCG ATGGTTCATT
 351 CAAATTTCTT CCCTATCAAC TTTCGATGTT TGGGTATTGG CCAAACATGG
 401 TTGCAACGGG TAACGGAGGG TTAGGGCTCG ACCCCGGAGA AGGAGCCTGA
 451 GAAACGGCTA CTACATCCAA GGAAGGCAGC AGGCGCGCAA ATTACCCAAT
 501 CCCGACTCGG GGAGGTAGTG ACAATAAATA CTGATACAGG GTTCTTTTGG
 551 ATCTTGTAAT TGGAATGAGT ACAATTTAAA TCCCTTAACG AGGAACAATT
 601 GGAGGGCAAG TCTGGTGCCA GCAGCCGCGG TAATTCCAGC TCCAATAGCG
 651 TATATTAAAG TTGTTGTGGT TAAAAAGCTC GTAGTTGAAC CTTGGGCCTG
 701 GCTGGCCGGT CCGCCTCACC GCGTGTACTG GTCCGGCCGG GCCTTTCCCT
 751 CTGTGGAACC CTATGCCCTT CACTGGGTGT AGCGGGGAAA CAGGACTTTT
 801 ACTTTGAAAA AATTAGAGTG CTCCAGGCAG GCCTTTGCTC GAATACATTA
 851 GCATGGAAAT AATAAAATAG GACGTGTGGT TCTATTTTGT TGTTTCTAGG
 901 ACCGCCGTAA TGATTAATAG GGACAGTCGG GGGCATCAGT ATTCAATTTG
 951 TCAGAGTGAA ATTCTTGGAT TTATTGAAGA CTAACTACTG CGAAAGCATT
1001 GCAAGATGTT TTTCAATAAT CAAGACGAAG TAGGGATCGA AGACGATCAG
1051 ATACGTCGTA GTCTACATAA ACCTATGGCG ACTAGATCGC AGATGTAAAA
1101 TTGACTCGTC GACTTACGGA AATTCCAAGT GTCTTGTACT
```

FIG 7: Sequences 0.2 kb, 0.3 kb and 1.2 kb fragment from ITS 1 & 2, ITS 3 & 4 and NS 1 & 4 Accession numbers EU528675, EU581866 and EU581865

(A)

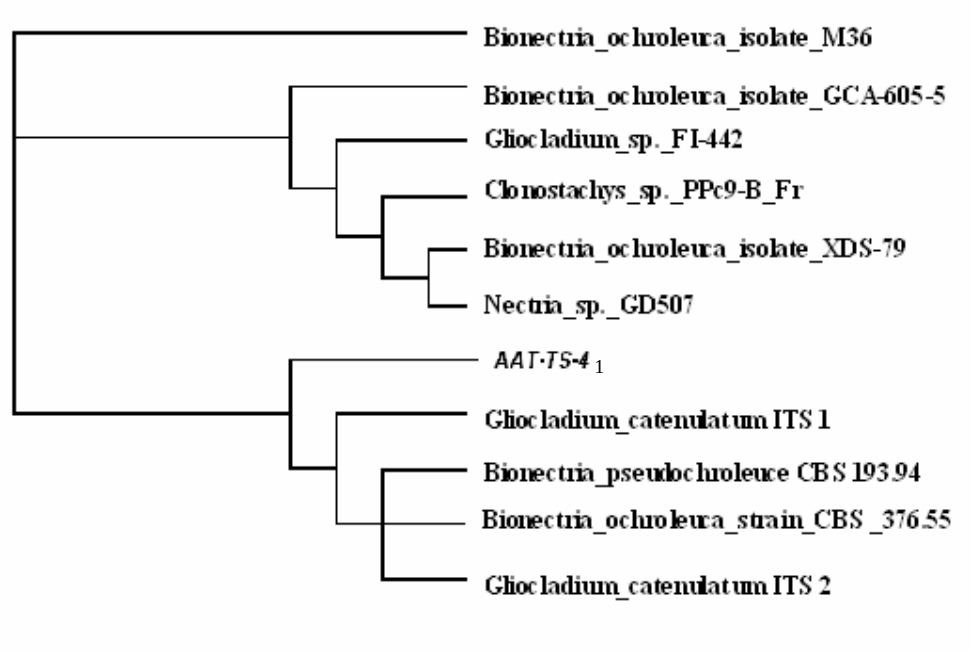
Bionectria_ochroleuca_isolate_M36
Bionectria_ochroleuca_isolate_GCA-605-5
Gliocladium_sp._FI-442
Clonostachys_sp._PPc9-B_Fr
Bionectria_ochroleuca_isolate_XDS-79
Nectria_sp._GD507
AAT-TS-4 1
Gliocladium_catenulatum ITS 1
Bionectria_pseudochroleuce CBS 193.94
Bionectria_ochroleuca_strain_CBS _376.55
Gliocladium_catenulatum ITS 2

(B)

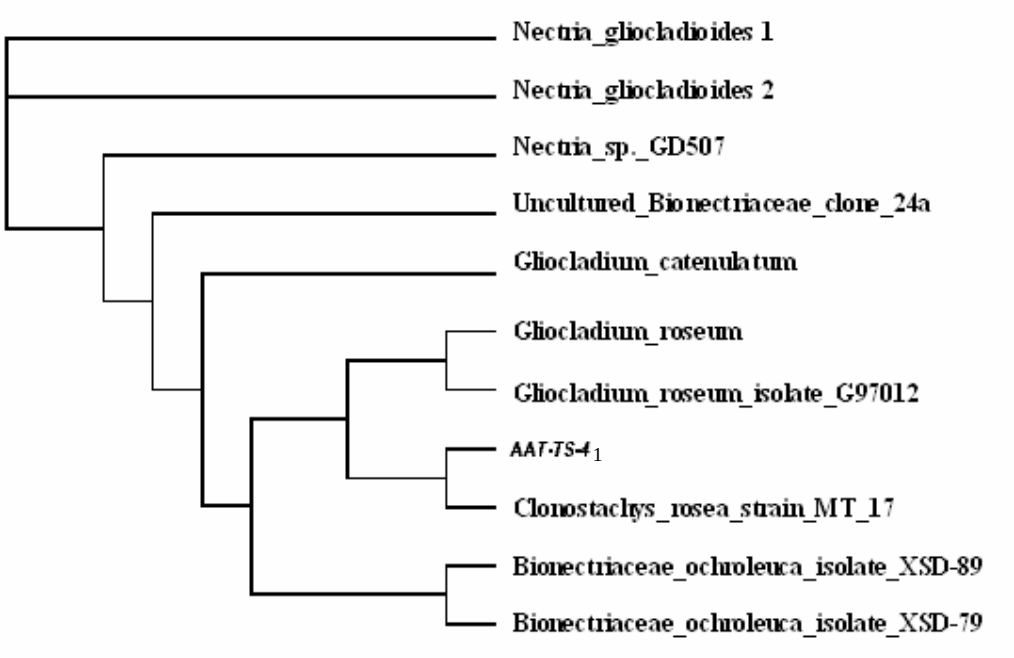
Nectria_gliocladioides 1
Nectria_gliocladioides 2
Nectria_sp._GD507
Uncultured_Bionectriaceae_clone_24a
Gliocladium_catenulatum
Gliocladium_roseum
Gliocladium_roseum_isolate_G97012
AAT-TS-4 1
Clonostachys_rosea_strain_MT_17
Bionectriaceae_ochroleuca_isolate_XSD-89
Bionectriaceae_ochroleuca_isolate_XSD-79

(C)

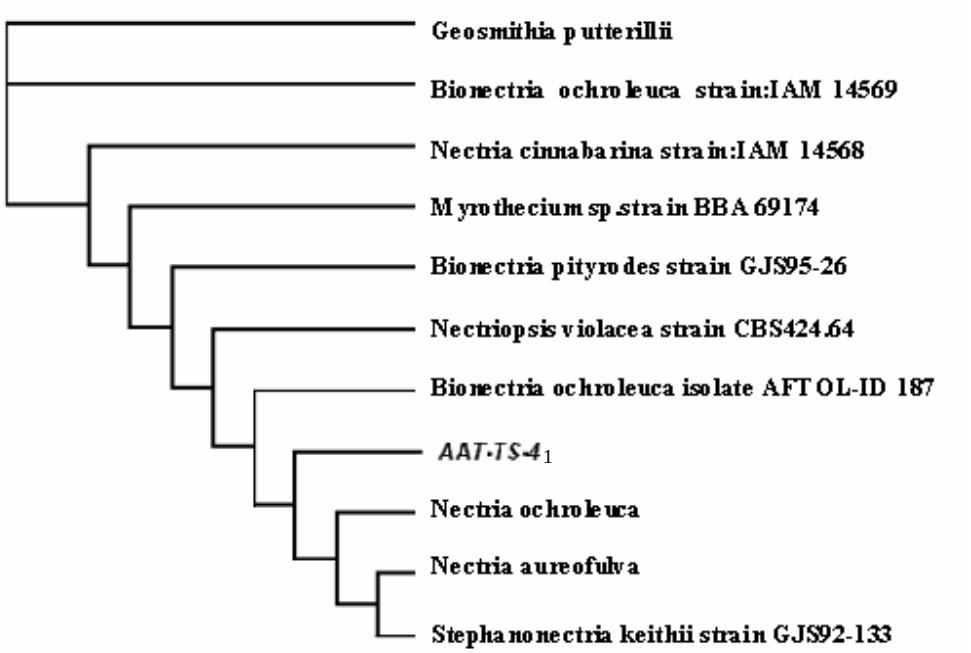

FIG 8: Phylogenetic relationships of selected members with fungi AAT-TS-4_1. The trees were generated by using parsimony algorithm (DNAPARS). A), B): The rooted tree showing relatedness of the AAT-TS-4_1 ITS region sequences with the genera *Gliocladium* and *Clonostachys.* C) Phylogenetic tree showing relatedness of 18S rRNA gene with genera *Nectria* and *Bionectria*.

5.6. Production of taxol

Taxol concentrations increased with increase in culture incubation time. Low concentration of taxol was detected in the culture as early as after two days of incubation. Approximately 118, 338, 434, 486 and 1076 ng/ 200 mL of taxol was estimated in the culture after 2, 5, 10, 15 and 21 days of incubation respectively (FIG 9 A). Taxol in the mycelium and culture broth was estimated to be 481 and 1670 ng / 200 mL respectively ((FIG 9 B) and taxol produced in 500 ml Erlenmeyer flask, 1 L, 2 L flasks and 2 L Roux bottle were 966.6, 1780, 1880 and 2130 ng/ 200 mL respectively (FIG 9 C). Exact concentrations of the taxol in the extracts were not determined as the solubility of the chloroform extracts was very poor in methanol.

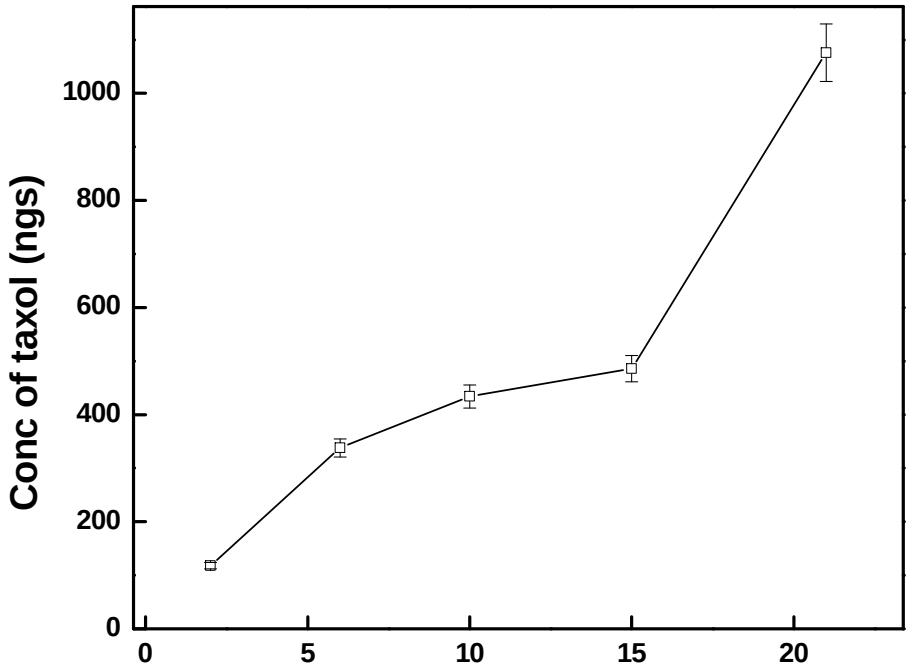

FIG 9 A: Production kinetics of taxol at different time intervals. Bar shows standard error ± 5%.

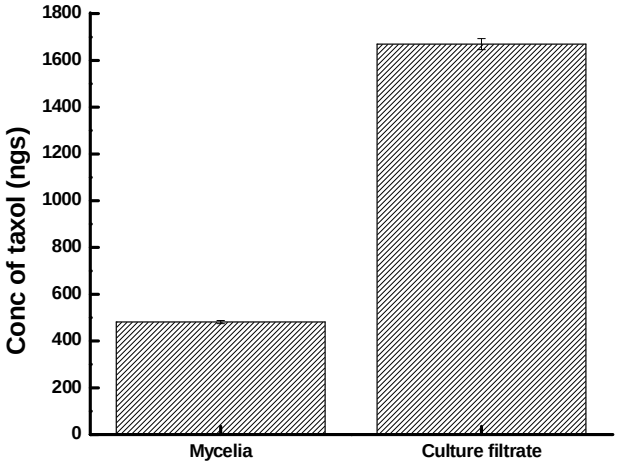

FIG 9 B: Localization of taxol with respect to mycelium and culture filtrate. The bar indicates standard error ± 1.45%.

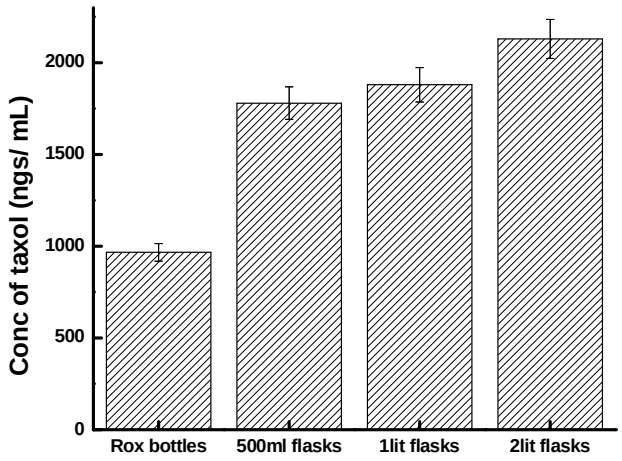

FIG 9 C: Production kinetics of taxol in different flask conditions. The bar indicates standard error ± 5%.

6. Discussion

In the present study, slow growing and unusual endophytic fungal cultures were isolated from different tissues (stem, bark and needles) of *Taxus baccata*. The endophyte population explored from the *Taxus* sp. represents different genera of fungi. Forty endophytic fungal strains were screened for taxol production using immunoassay. Among the fungal cultures, one strain designated as AAT-TS-4_1 is detected to be taxol producing. Taxol production increased exponentially with an increase in growth of the fungal culture (21 days), indicating that taxol is produced in maximum quantities at later log phase or early stationary phase of the fungal growth. However, taxol is estimated in culture after as early as two days but considerably in low concentrations. But these concentrations are much high in comparison with other fungal strains reported to produce ng quantities of taxol after 21 days (Stierle et al, 1993). Taxol production is estimated to be high in culture broth as compared to fungal mycelium indicating that the metabolite is secreted into the medium. The culture on solid media takes more than a week for its optimum growth, which is quite evident, it being an endophyte (Petrini, 1996). Microscopic analyses show the mycelia to be hyaline, septate bearing conidiophores which are verticillium-like which is a characteristic feature of *Gliocladium* sp.; however we did not observe any secondary penicilliate conidiophores. Phialides are solitary or are produced in a group of 2-5, straight, smooth and are

verticillium-like. Conidia are produced singly or in a small moist cluster apically and are smooth, oval to cylindrical to curved, hyaline, single celled and variable in shape and size which is typically seen in *Gliocladium* sp. All the mentioned characters are identical to those described for the fungus *Gliocladium* sp. (Barnett and Lilly, 1962; Merritt et al, 2003), hence fungus AAT-TS-4_1 can be referred to as *Gliocladium* sp.

In sequence analyses using BLAST and ClustalW, both ITS sequences (0.2 kb and 0.3 kb sequences) and 18S rRNA sequence (1.1 kb) show highest similarity with genera-*Gliocladium*, *Bionectria*, and *Clonostachys*. The phylogenetic studies indicate that the nearest relative of the fungus AAT-TS-4_1 is either from genus *Gliocladium* or *Clonostachys.* Considering the morphological characters we identified the fungus as *Gliocladium* sp. as the fungus does not show any asci formation which is very often seen in *Bionectria* and also does not produce conidia in columns as reported in *Clonostachys (*Barron, 1968*)*. 18S rRNA phylogenetic analysis shows that the fungus is placed closely to genus *Nectria* sp which is a teleomorph (perfect state) of *Gliocladium* sp. The sequence analyses and phylogenetic analyses do support the identification. However in recent reports, many species from genus *Gliocladium* are classified under *Clonostachys* and *Bionectria* based on morphological and molecular similarities (Hans et al, 1999). To the best of our knowledge, this is the first report of isolation of taxol from *Gliocladium* sp.

This is the first report of isolation of taxol from *Gliocladium* sp. Strobel et al (1996) and others have, however, isolated taxanes from different endophytic fungal species (*Taxomyces andreanae, Pestalotiopsis, Pestalotia, Fusarium, Alternaria* and others) obtained from *Taxus* sp. that are common in Europe, Asia and North America. The isolation of taxol from the culture of *Gliocladium* sp. is the first demonstration of its occurrence in fungi isolated from Indian Yew tree, *Taxus baccata.* This suggests that the ability to synthesize taxol, resides not only in the fungal strain isolated from *Taxus* sp. of above mentioned countries, but also from endophytic fungi of *Taxus baccata* growing in India. In conclusion, we have isolated an endophytic fungus *Gliocladium* sp. producing taxol extra /intracellularly.

7. References

1. Ahmad. A. 1991. Investigations on the grassy-shoot disease of lemongrass (*Cymbopogon flexuosus*) and characterization of toxic metabolites produced by the causal agent *Balansia sclerotica*. PhD Thesis, Univ. of Lucknow.
2. Altusch SF, Madden TL, Schaffer AA, Zhang J, Zhang Z, Miller W, Lipman DJ. 1997. Gapped BLAST and PSI-BLAST: a new generation of protein database search programs. Nucleic Acids Res 25: 3389-3402.
3. Barnett HL, Lilly VG. 1962. A destructive mycoparasite, *Gliocladium roseum.* Mycologia 54: 72-77.
4. Barron GL. 1968. The genera of Hyphomycetes from soil. Pp 177-178. The Williams and Wilkins Company, Baltimore.
5. Bills GF. 1996. Isolation and analysis of endophytic fungal communities from woody plants. In: S.C. Redlin and L.M. Carris, Editors, *Endophytic Fungi in Grasses and Woody Plants: systematics, ecology, and evolution*, American Phytopathological Society Press, St Paul, MN. 31–65.
6. Caruso M, Colombo AL, Crespi-perellino N, Fedeli L, Malyszko J, Pavesi A, Quaroni S, Saracchi M, Ventrella G. 2000. Studies on a strain *Kitasatospora* sp. paclitaxel producer 50: 89-102.
7. Croom EM. 1995. *Taxus* for taxol and taxoids. In Taxol: Sciences, Applications. Boca Raton, FL: CRC. 37-70.
8. Felsenstein J. 1985. Confidence limits on phylogenies: an approach using the bootstrap. Evolution 39: 783- 791.
9. Gardes M, Bruns TD. 1993. ITS primers with enhanced specificity for basidiomycetes – application to the identification of mycorrhizae and rusts. *Molecular Ecology*. 2: 113–118.
10. Gebetta B, Orsini P, Peterlongo F, Appendino G. 1998. Paclitaxel analogues from *Taxus baccata*. Phytochemisrty 47 (7): 1325-1329.
11. Grothus PG, Bigmnami GS, O'Malley S, Harada KE, Byrnes JB, Waller DF, Raybould TJG. 1995. Taxane-specific monoclonal antibodies: measurement of paclitaxel, baccatin III, and "total taxanes" in *Taxus brevifolia* extracts by enzyme immunoassay. Journal of natural products 58 (7): 1003-1014.

12. Hans JS, Gary JS, Keith AS, Walter G. 1999. Classification of the mycoparasite *Gliocladium roseum* in *Clonostachys* as *C. Rosea*, its relationship to *Bionectria ochroleuca*, and notes on other *Gliocladium*- like fungi. Mycologia 91(2): 365-385.
13. Higgins D, Thompson J, Gibson T, Thompson JD, Higgins DG, Gibson TJ. 1994. CLUSTAL W: improving the sensitivity of progressive multiple sequence alignment through sequence weighting, position-specific gap penalties and weight matrix choice. Nucleic Acids Research 22: 4673-4680.
14. Janardhanan KK, Ahmad A, Gupta ML, Husain A. 1991. Grassy- shoot, a new disease of lemongrass caused by *Balansia sclerotica* (Pat) Hohnel. J. Phytopath. 133: 163-168.
15. Merritt S, David E, Wilford MH, Joe S, Gary S. 2003. An endophytic *Gliocladium* sp. from *Eucryphia cordifolia* producing selective volatile antimicrobial compounds. Plant Sciences. 165: 913-922.
16. Moutia M and Dookuna A. 1999. Evaluation of surface sterilization and hot water treatments on bacterial contaminants in bud culture of sugarcane. Expl Agric. 35: 265-274.
17. Neumann B, Pospiech A, Schairer HU. 1992. Rapid isolation of genomic DNA from Gram-negative bacteria. TIGS 8: 332 - 333.
18. Page M, Landry N, Boissinot M, Halie MC, Harvey H, Gagne M. 1999. Bacterial mass production of taxanes and paclitaxel. WO 99/ 32651.
19. Petrini O. 1996. Ecological and physiological aspects of host-specificity in endophytic fungi. In: redline S. C., Carris L. M., eds, Endophytic fungi in grasses and woody plants, APS Press, St. Paul (USA), pp. 87-100.
20. Robert SC, Shuler ML. 1997. Large-scale plant cell culture. Current Opinion in Biotechnology 8: 154-159.
21. Sambrooks J, Fritsch EF, Maniatis T. 1989. *Molecular Cloning* Cold Spring Harbor Laboratory Press, Cold Spring Harbor.
22. Sanger F, Nicklen S, Coulson AR. 1977. DNA sequencing with chain-terminating inhibitors. Biotechnology 24: 104- 108.
23. Stierle A, Strobel G, Stierle D. 1993. Taxol and taxane production by *Taxomyces andreanae*, and endophytic fungus of pacific yew. *Science* 260: 214-216.

24. Strobel GA, Hess WM, Ford E, Sidhu RS, Yang X. 1996. Taxol from fungal endophytes and the issue of biodiversity. *J. Industrial microbiol* 17: 417-423.
25. Wani MC, Taylor HL, Wall ME, Coggon P, McPhail AT. 1971. Plant antitumor agents VI. The isolation and structure of taxol, a novel antileukemic and antitumor agent from *Taxus brevifolia*. J Am Chem Soc 93: 2325-2327.
26. White TJ, Bruns T, Lee S, Taylor J. 1990. Amplification and direct sequencing of fungal ribosomal RNA genes for phylogenetics. Chapter 38. In: PCR Protocols: a Guide to Methods and Applications (M. Innis, D. Gelfand, J. Sninsky and T. White, eds.). Academic Press, Orlando, Florida.
27. Witherup KM, Look SA, Stasko MW, Ghiorzi TJ, Muschik GM. 1990. *Taxus* sp needles contain amounts of taxol comparable to the bark of *Taxus brevifolia*: analysis and isolation. Journal of natural products 53 (5): 1249-1255.

Chapter 3

Production, purification, characterization and bioassays of taxol and its precursor 10 DAB III.

1. Summary

We have isolated endophytic fungi from Indian yew tree, *Taxus baccata* and then screened for taxol production. Out of the forty fungal cultures screened, one fungus *Gliocladium* sp. was found to produce taxol and 10DAB III (10 Deacetyl baccatin III). These compounds were purified by TLC, HPLC and characterized using UV-Spectroscopy, ESI-MS, MS/MS and proton NMR. One liter of *Gliocladium* sp. culture yielded 10 µg of taxol and 65 µg of 10 DAB III. The purified taxol from the fungus showed cytotoxicity towards cancer lines HL-60 (leukemia), A431 (epidermal carcinoma) and MCF-7 (breast cancer).

2. Introduction

Paclitaxel (Taxol^{R}), a tubulin binding diterpenoid was first isolated from the pacific yew tree *Taxus brevifolia* (Wani et al, 1971). Because of its ability to bind specifically to β-tubulin and its cytotoxicity at lower concentrations, it is being used for the treatment of several classical tumors (Amos and Lowe, 1999; Haldar et al, 1995; Haldar et al, 1996; Haldar et al, 1997). In comparison with other antineoplastic agents such as Vinca alkaloids and colchicine, its binding dynamics with tubulin are peculiar, the former enhance microtubule disassembly where as taxol promotes assembly and stabilization (Roberts and Hyams, 1979). Due to the complex structure and limited supply of Taxol, scientists have been posed with the difficulty of finding an alternative potential source of this compound (Gordon et al, 1993). A number of methods for the production of taxol including tissue culture of *Taxus* sp (Jaziri et al, 1996), extraction from endophytic fungi (Strobel et al, 1996) and chemical synthesis (Nicolaou et al, 1994) have been reported. But these procedures are either low yielding or very complex and tedious.

India has a large wealth of medicinal plants with abundance of *Taxus baccata*, hence a screening programme was initiated to isolate endophytic fungi from *Taxus baccata* that

produce taxol. Forty slow growing, few non-sporulating and uncommon endophytic fungi were isolated from *Taxus* bark, stem, leaves (needles) and brought to pure culture state. In this study, the production, purification and characterization of Taxol and its useful precursor 10 DAB III by an endophytic fungus identified as *Gliocladium* sp. is reported.

3. Materials

Taxol immunoassay kit was purchased from Hawaii Biotech, Hawaii, USA. Standard taxol, 10 DAB III and Baccatin III were purchased from M. P. BioMedicals, USA. TLC precoated plates, Silica G for TLC, Silica G for column chromatography and HPLC grade solvents from Merck. NMR grade solvents and tubes from Cambridge Isotope Lab. Inc USA. A431, MCF-7 and HL-60 cell lines from National Center for Cell Sciences (NCCS), Pune, India. Standard 25 cm^2 tissue culture flasks and 96 well microtiter plates from Nunc. 3-(4,5-dimethylthiazol-2-yl)-2,5-diphenyltetrazolium bromide from Sigma chemicals. All other analytical grade chemicals and solvents were from Qualigens, Merck, Himedia and Sigma.

4. Methods

A Novel endophytic fungus *Gliocladium* sp. having optimum growth at pH 7 and 25 ^{0}C was isolated from *Taxus baccata* tree growing in West Bengal, India (Sreekanth et al, 2008). This fungus was maintained on Potato Dextrose Agar (PDA) slants. Stock cultures were maintained by subculturing at monthly intervals. After growing the fungus at pH 7.0 and 25 ^{0}C for 7 days, the slants were preserved at 15 ^{0}C. From an actively growing stock culture, subcultures were made on fresh slants. After 7 days of incubation at pH 7.0 and 25 ^{0}C they were used as the starting materials for fermentation experiments.

4.1. Production and isolation of taxol from *Gliocladium* sp.

Production of taxol by the fungus was studied by a two stage fermentation procedure as describe by Stierle et al (1993). In brief, in first stage fungal culture was stabilized in modified mycological medium for 5 days at 25 ^{0}C at 120 rpm. After the culture stabilization, the biomass was pelleted out by centrifugation (6,000 rpm for 20 min) and washed twice with sterile distilled water. The final biomass obtained was used as

inoculum for the second stage fermentation. Culture was incubated at 25 ^{0}C for 21 days, under stationary condition, after which it was harvested and preceded for the further processing.

4.2. Lyopillization and extraction

The culture harvested was freeze dried and powdered using pestle motor. The grounded biomass was weighed and extracted using a mixture of polar and non polar solvents. For maximum compound extraction, chloroform and methanol (9:1) ratio solvent system was used. The organic layer was separated from the aqueous layer using separating funnel. The procedure was repeated thrice and the solvent was dried using anhydrous sodium sulphate and concentrated under vacuum using rotavapor at 40 ^{0}C. The crude compound thus obtained was analyzed on TLC for taxol content.

4.3. Thin layer chromatography (TLC)

The crude extract thus obtained was analyzed on TLC on silica gel G (0.25 mm thickness) using chloroform: acetonitrile (7:3) solvent system. The TLC plates were developed with anisaldehyde-sulphuric acid reagent or vanillin sulphuric acid reagent (Wang et al, 2000). Taxanes produced a dark blue spot that later turned gray with use of these reagents. Purity of the isolated compound was checked on TLC in different solvent systems such as (A) chloroform: acetonitrile (7:3); (B) chloroform: methanol (7:1) and (C) ethlyacetate: 2-propanol (95:5).

4.4. Silica Gel Column chromatography and preparative TLC

Purification of the fungal taxol was done by silica gel column chromatography. The crude extract was loaded on silica gel column (60-120 mesh size, 30 cm x 3 cm length/ width) pre-equilibrated with chloroform, and eluted with a gradient of chloroform: acetonitrile (chloroform 100, 75:25, 50:50, 25:75, 100% acetonitrile). Fractions containing compounds with R_f value similar to that of the standard taxol were pooled and subjected to preparative TLC on a 0.5mm thick (20 cm x 20 cm) silica plate and developed in solvent system chloroform: acetonitrile (7:3). The putative taxol was scraped and eluted out with chloroform: methanol (9:1).

4.5. HPLC and Spectroscopic analysis

Purity and characteristics of putative taxol were determined by HPLC using C18 Symmetry column (Waters). Sample was taken in 10 µL chloroform, injected in HPLC column and gradient elution was performed using 25 % to 95 % acetonitrile at a flow rate of 0.5 mL / min. A dual wavelength recorder set at 227 and 254 nm was used to detect the compounds eluting from the column (Martin et al, 1998). The absorption maximum of the purified compound was determined by Shimadzu PC 101 Spectrophotometer. Sample was dissolved in HPLC grade methanol and spectral data was collected over 200 to 450 nm range.

4.6. Immunoassay and Quantification of Taxol

Taxol in the crude extracts was qualitatively and quantitatively determined by competitive inhibition enzyme immunoassay (CIEIA) using immunoassay kit (TA01) purchased from Hawaii Biotechnology, Hawaii. The crude extracts were dissolved in methanol and centrifuged to remove the insoluble materials. In brief, this assay was performed in a 96-well microtitre plate coated with Taxol –protein coating antigen. The plate was blocked with 1 % (w/v) BSA in PBS. After washing, the solid phase bound taxol was incubated with samples and taxol standard and a specific antitaxol monoclonal antibody. The taxol in the sample competes with solid phase bound taxol for binding to the monoclonal antibody. The monoclonal antibody bound to the solid phase bound taxol was detected by an alkaline phosphatase conjugated second antibody and alkaline phosphatase substrate, p-nitro phenyl phosphate the inhibition of color development was proportional to the concentration of free taxol present in the samples. The amount of taxol in each sample was calculated from an inhibition curve made using different concentrations of standard taxol supplied with the kit. This technique was used to screen for taxol in each of the fungal extracts. The assay is sensitive to about 1 ng/ mL.

4.7. ESI-MS and MS/MS

Molecular mass of the purified compound was determined by M/S Applied Biosystems API QSTAR pulsar (ESI-MS) mass spectrometer. Samples for the analysis were dissolved in HPLC grade methanol, water, acetic acid in the ratio of 50:50:0.1. Samples were then analyzed by infusion method / (injected into MS) at a flow rate of

5 µL/ min and at a IS voltage of 3800 V in TOF mode. Spectrum from a range of m/z 500 to 900 Daltons was obtained. Fragmentation of the desired molecule was obtained by acquiring the product ion spectrum using MS/MS with similar parameters as used for ESI-MS. Molecular ions of the standard taxol were also obtained for comparison.

4.8. ^{1}H-NMR (Proton NMR)

^{1}H-NMR analysis was carried out on a Bruker AV 400 Spectrophotometer at 400 MHz. NMR spectrum was measured with a spectral width of 8223.68 and data was acquired into 32 K data points. An acquisition time of 1.9 s and a relaxation delay of 1.0 s were used. Samples were then dissolved in $CDCl_3$ (deuterochlorofrom) and scanned overnight. NMR of the standard Taxol was also obtained, however the number of scans acquired for obtaining signals were less in comparison with that of the test.

4.9. Cytotoxicity of fungal taxol on different cancerous cell lines

In general the protocol is as described: Cells were kept frozen (0.5 mL) stock at 2-5 X 10^6 cells/ mL in 70 % FBS containing 30 % DMSO. Frozen stocks were thawed at 37 ^{0}C, then 5 mL fresh animal cell culture medium (all supplements) and 10 % Fetal Calf Serum (FBS) was added into 25 cm^2 Tissue culture flask. The approximate seeding ratio from frozen stock is one ampoule to two flasks. Cells were grown to 90 % confluency, replacing medium every 48-72 h as required. Subculture cells at 90 % confluence every 48-72 h at a ratio of 1:3 (or 4) for cells. Cells were suspended in medium to a concentration of 1 x 10^4/ mL. 100 µL cell suspension was aliquoted into each well of a 96 well microtiter plate (i.e. 1 x 10^4 cells/ well). Plates were incubated overnight at 37 ^{0}C. Complete medium containing test compound in 5 % v/v was serially diluted in 8 wells. All the samples were taken in triplicates.

To each well 10 µL of MTT reagent (5 mg/ mL) was added. Then cells were stained for 20 h at 37 ^{0}C. At the end of this period, 200 µL acidified isopropanol was added to solubilize the purple formazan crystals produced. Absorbance was measured at 490 nm with a Titertek Multiskan. For each test compound the highest "no effect" concentration was determined, i.e. the highest concentration of test compound to which the cells were exposed and which did not result in a decrease in absorbance, compared to the control situation.

Cytotoxicity of the compound against cell lines HL-60 (leukemia), A431 (epidermal carcinoma) and MCF-7 (breast cancer) was determined by MTT assay (Twentyman and Luscombe, 1987). The cell suspension at a concentration of 1 x 10^4 cells / mL was added in 96 well microtiter plates. Culture media used for HL-60, MCF-7 and A431 were RPMI 1640, MEM and DMEM respectively. Plates containing culture media and test compound were incubated overnight for HL-60, 7-8 days for MCF-7 and 4 days for A431 at 37 ^{0}C, 5 % v/v CO_2 and 95 % humidity. All the samples were taken in triplicates. 10 µL of MTT reagent (5 mg/ml) was added to each well and cells were incubated for 1 h at 37 ^{0}C. At the end of this period, 200 µL of acidified isopropanol was added and plates were incubated for 4 h to solubilize the purple formazan crystals produced. Absorbance was measured at 490 nm with a Beckman coulter spectrophotometer.

4.10. Antibacterial activity

Eight pathogenic bacteria were tested for the bacterial growth inhibition studies of Taxol, 10DAB III and Baccatin (commercially available). Briefly, bacteria (*Staphylococcus aureus , Proteus vulgaris, Streptococci group D, Bacillus, Escherichia coli, Klebsiella pneumoniae, Pseudomonas aeruginosa, Serratia morganii*) grown to mid-logarithmic phase were harvested by centrifugation, washed with 10 mM sodium phosphate buffer (SPB) at pH 7.4, and diluted to 2×10^5 colony-forming units (CFU)/ mL in SPB containing 0.03 % Luria–Bertani (LB) broth. Taxol, 10DAB III and Baccatin 10 µL of 1 mg/ mL concentration was added in 50 µL of LB medium in 96-well microtitre plates. Each well was inoculated with 50 µL of 5×10^4 CFU of bacteria. All the tests were done in triplicates. O.D at 660 nm of the plates was taken at 0, 1, 6, 8, 16 and 21 h time interval. Growth inhibition was calculated accordingly with respect to control.

4.11. Production and Isolation of 10DAB III from *Gliocladium* sp.

Production of 10 DAB III by the fungus was studied by a two stage of fermentation procedure as described above for taxol production. For 10 DAB III production, the flasks were incubated at 25-27 ^{0}C for 14 days as stationary culture (Second stage). Culture filtrate and mycelia obtained were lyophilized, extracted thrice with chloroform: methanol (9:1) and solvent dried at 40 ^{0}C in vacuo. The crude extract was then subjected

to silica gel chromatography and eluted with gradient of chloroform: acetonitrile as described earlier. Fractions showing 10 DAB III on TLC were pooled and subjected to further fractionation on preparative TLC using Chloroform: acetonitrile (7:3) as solvent phase. Homogeneity of 10 DAB III was checked using HPLC and molecular mass was determined by ESI-MS as described earlier. 10 DAB III from one liter of culture was estimated by immunoassay kit TA 04 as described for taxol estimation.

5. Results

5.1. Taxol from culture of fungus *Gliocladium* sp

Extraction of fungal culture yielded dark brown crude compound, which was fractionated on silica gel column with 100 % chloroform and chloroform: acetonitrile (75:25). Partially purified compound with chromatographic properties similar to that of the standard taxol (FIG 1) was obtained. The partially purified taxol on preparative TLC yielded considerably pure compound. Partially purified taxol obtained from preparative TLC showed single dark blue spot that later turned to gray (with R_f value 0.5) when sprayed with the anisaldehyde sulfuric acid reagent / vanillin sulfuric acid reagent on TLC as shown in FIG 2 (Chan et al, 1994). The purity of the putative taxol showed similar chromatographic properties as that of the standard taxol in three different solvent systems A, B and C on TLC (FIG 2).

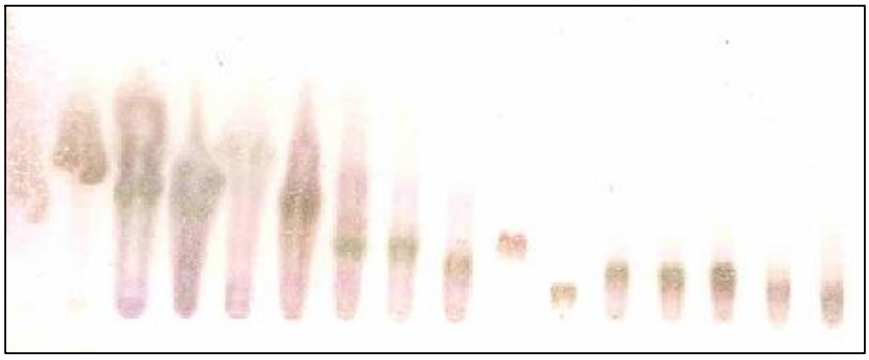

A B C D E F G H I J K L M N O P

FIG 1: Thin layer chromatography compounds obtained after Silica Gel column chromatography. Lane A- I and L- P fractions obtained from the gradient of chloroform, acetonitrile. Lane J standard taxol and Lane K standard 10 DAB III. Fractions in lane F and G show putative fungal taxol.

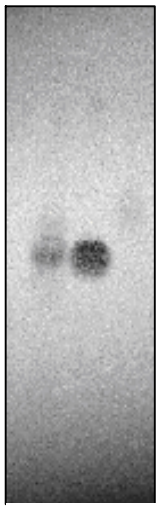

A B

FIG 2: The TLC of fungal taxol purified from culture broth along with standard taxol on silica gel G using chloroform: acetonitrile (7:3) solvent system. Lane A: purified fungal taxol, Lane B: Standard taxol. Detection: Vanillin sulphuric acid.

5.2. HPLC and Spectroscopic analysis

The homogeneity of the purified compound was confirmed by HPLC analysis, which showed a single, symmetrical peak with retention time 25.5 min on C18 symmetry column (FIG 3). Absorbance of the eluting compound showed high intensity at 227 nm and relatively low at 254 nm. The UV absorption analysis showed a peak showing absorption maxima at 227 nm. An absorbance maximum of standard taxol was also obtained for comparison (FIG 4).

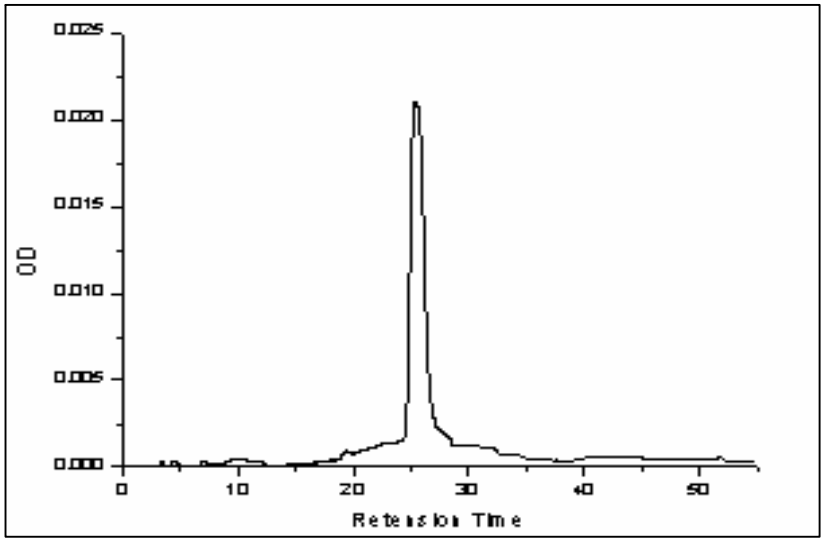

FIG 3: HPLC profile of pure fungal taxol with retention time of 25.5 min.

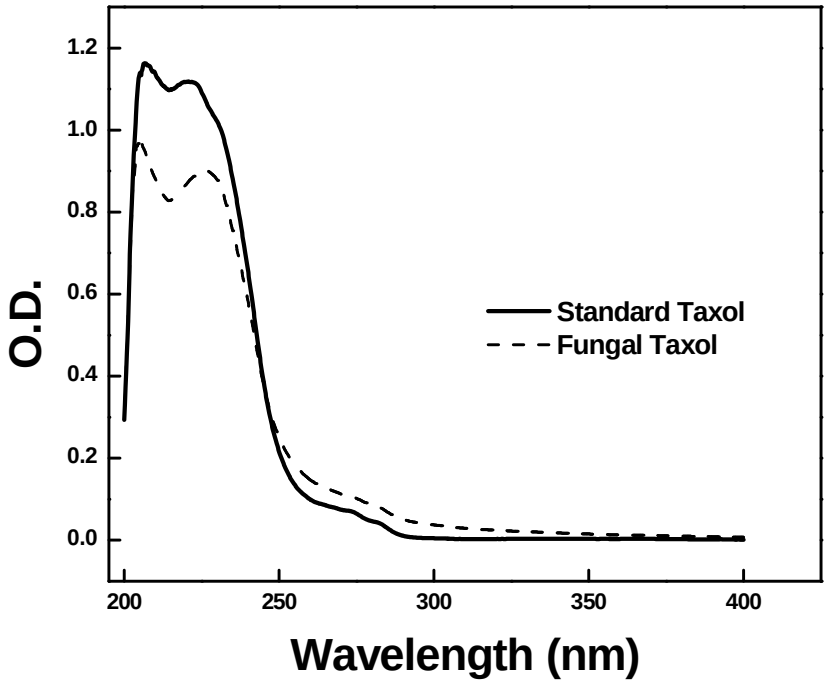

FIG 4: UV absorption spectrum of standard taxol and fungal taxol.

5.3. ESI-MS and MS/ MS

Electrospray ionization mass spectrometry yielded a major ion at 854 *m/z* and at 876 *m/z*. Apart from the major ions, fragment ion at 569 *m/z* is also seen (FIG 5). In MS/MS fragment ions at *m/z* 286 and at *m/z* 570 were seen, but the relative abundance of the same was very low (FIG 6).

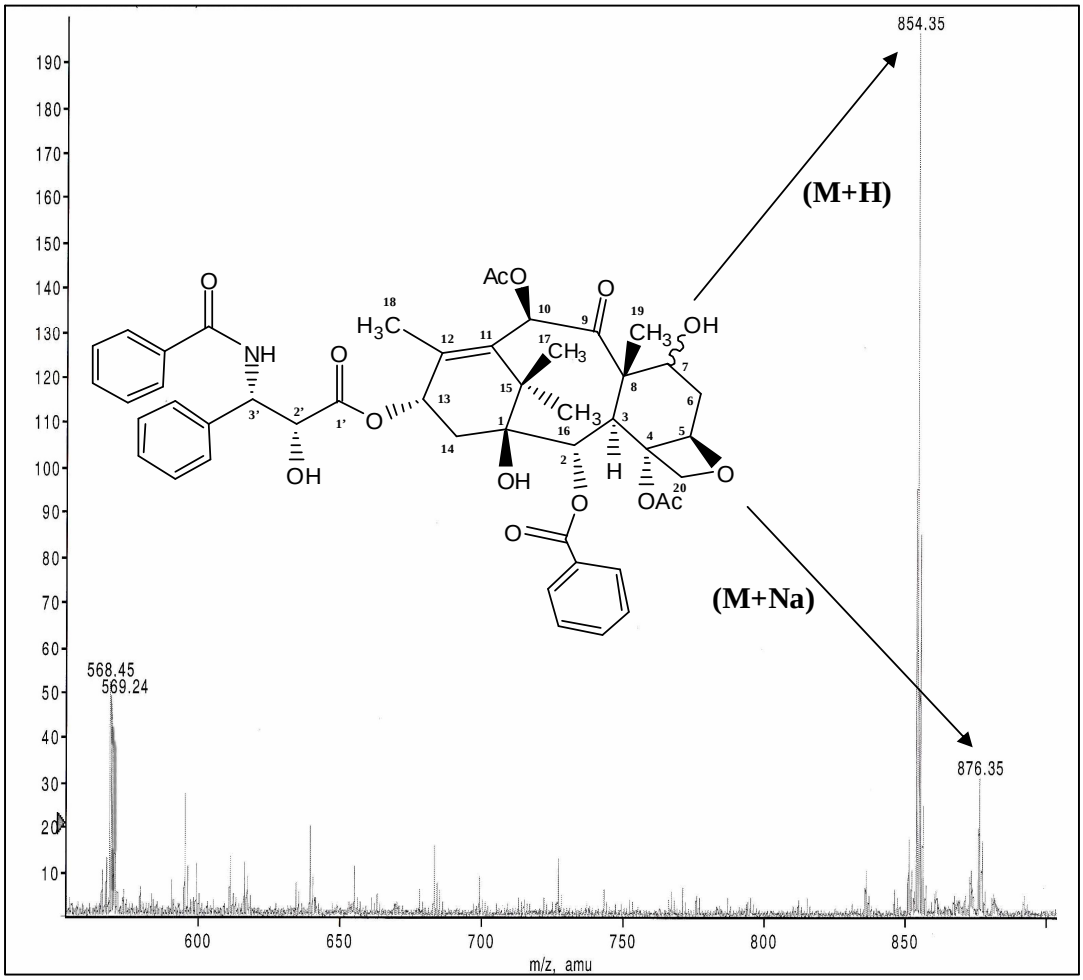

FIG 5: ESI-MS spectrum of the *m/z* 854 (M+H) and *m/z* 876 (M+Na) ion of fungal taxol.

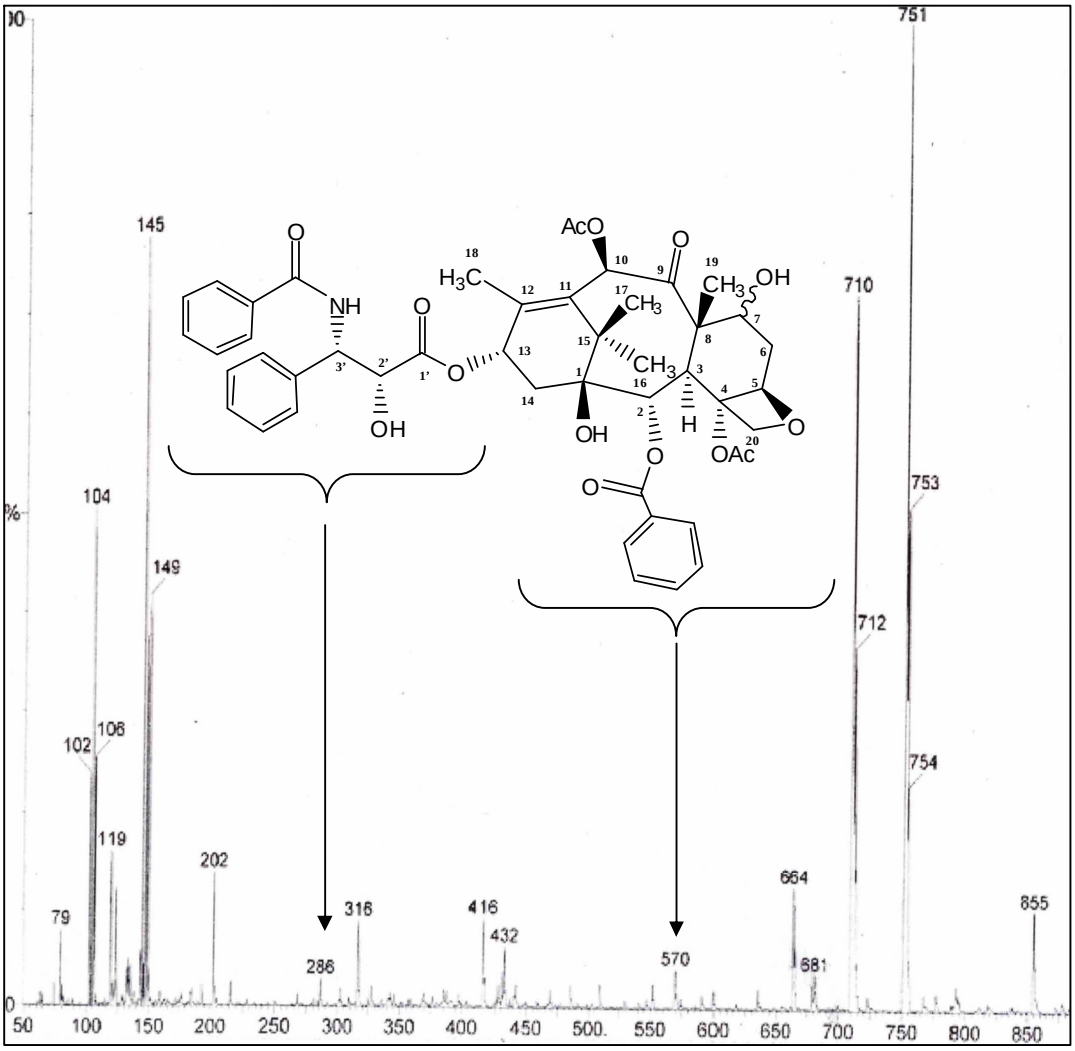

FIG 6: MS-MS spectrum of fungal taxol showing product ions 570 *m/z* and 286 *m/z* attributing to taxane substructure and side chain substructure.

5.4. Proton NMR

^{1}H NMR spectrum showed well resolved signals which were distributed in the region from 1.0 to 8.5 ppm. The three proton signals caused by methyl group and acetate groups were seen in the range of 1.0 to 2.5 ppm which include H16, H17, H18, H19, 10-OAc, 4-OAc, H14α, H14β, 1-OH, 7-OH, H6α and H6β. Multiplets caused by certain methylene groups were also seen in this range. Protons in the taxane skeleton and the side chain such as H10, H13, H3', H2, H5, H2', H7, H20α, H20β and H3 including NH

and 2'-OH were observed in the region between 2.5 and 7.0 ppm and the aromatic proton signals caused by the C2 benzoate, C3' phenyl and C3' benzamide groups such as *o*, *m*, *p*-Ph1, *o*, *m*, *p*-Ph2, and *o*, *m*, *p*-Ph3 appeared in the region between 7.0 and 8.5 ppm (FIG 7).

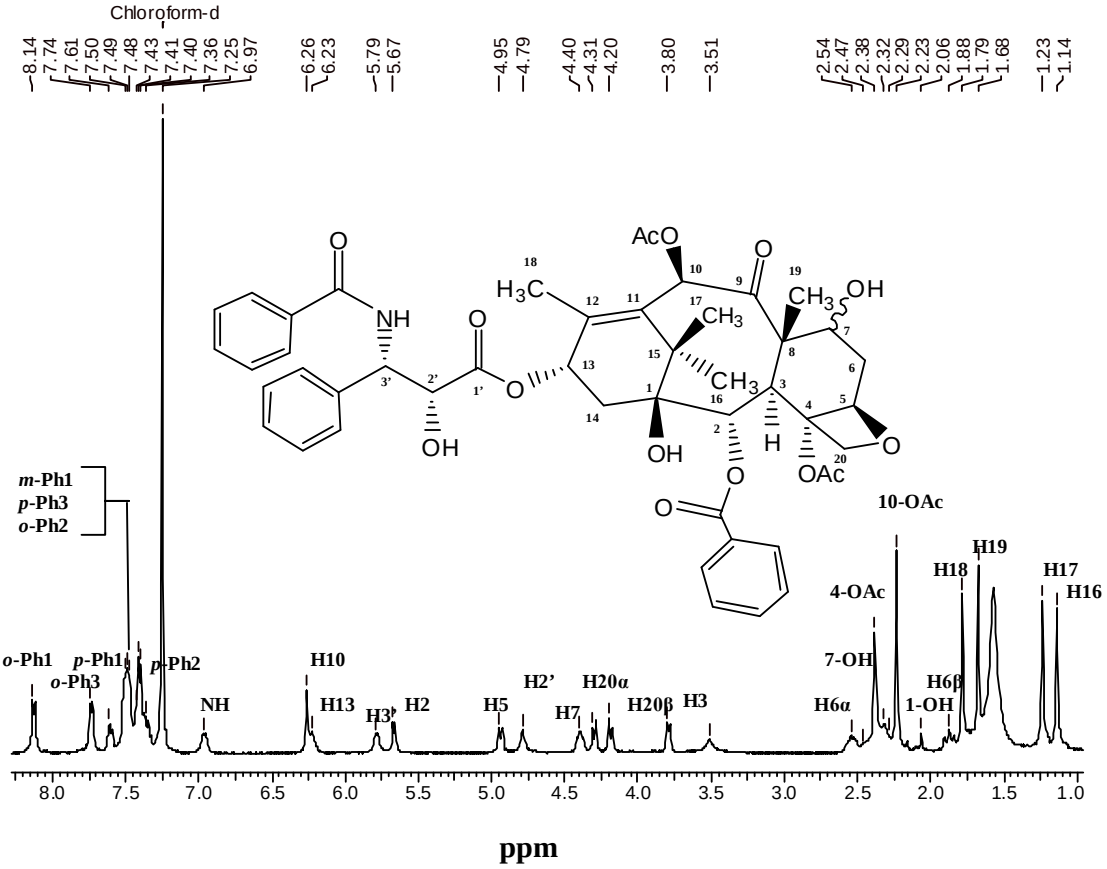

FIG 7: ^{1}H NMR spectrum of fungal taxol. Proton signals were resolved in the region 1 to 8.5 ppm. The methyl group (H17, H16, H18, and H19) and acetate group (10-OAc, 4-OAc, 1-OH, and 7-OH) protons along with methylene group multiplets were seen in the region 1- 2.5 ppm. Other taxane and side chain protons such as H3, H20α, H20β, H7, H2', H5, H2, H3', H13, H10 and NH are seen in the region of 2.5 to 7 ppm. protons from the aromatic groups such as C2 benzoate, C3' phenyl and C3' benzamide are see in the range of 7 to 8.5 ppm. Measured in $CDCl_3$, (400 MHz).

5.5. Quantification and cytotoxicity

Calculations for quantifying taxol in the sample are as follows:

Mean absorbance of the background wells was calculated and subtracted from all the wells. Mean absorbance of test and standard samples taken in duplicates were also calculated. Absorbance of well #8 is considered as uninhibited reference well. This absorbance is proportional to the concentration of anti-taxol or anti-taxane antibody bound by Taxol–protein coating the well, in the absence of inhibitor Taxol standard (B_0). The absorbance of each of wells #1- #7 is proportional to the concentration of anti Taxol antibody bound by Taxol-protein coating the well, in the presence of that particular concentration of inhibitor Taxol (B). The ratio of the absorbance for each concentration of inhibitor Taxol standard in wells #1- #7 (B) to the absorbance of well #8 (B_0) will provide a B/B_0 value for each standard concentration of Taxol. Using this data a standard curve of B/B_0 (on Y-axis) is constructed against the inhibitor concentrations (on X axis). The ratio of the absorbance for each dilution of all unknown samples to the absorbance of well #8 is B/B_0. Using the B/B_0 values that fall on the linear portion of the standard curve, extrapolate the concentration. Calculate the concentration of the analyte in the sample by multiplying the extrapolated concentration by the dilution factor. Using the above method concentrations of taxol produced by the fungal culture *Gliocladium* sp is 10 µg/lit taxol (FIG 8).

Sample/2lit	Sample dilution	Mean absorbance (B)	B/B_0	Extrapolated taxol Conc from Std Curve	Mean Taxol Conc(x dilution) (µg/ml)
Pure fungal Taxol	1/1000	0.075	0.330	10.2 ng/ mL	10.2 µg/ L

Table summarizing the values obtained

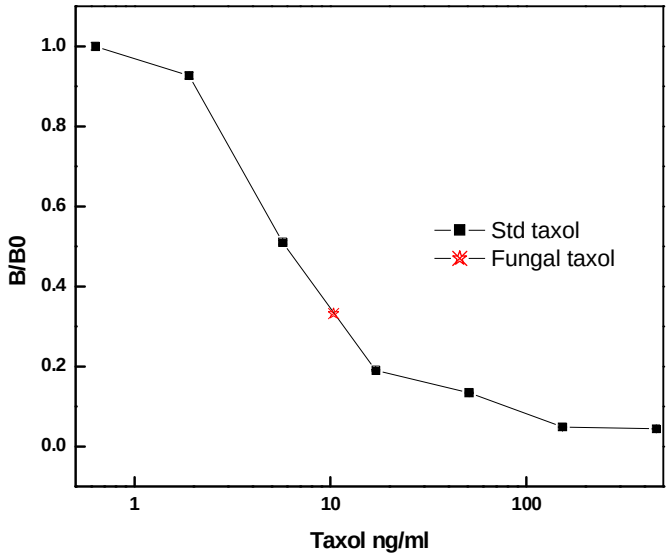

FIG 8: Standard plot obtained using different concentrations of standard taxol and with extrapolated test sample concentration.

Approximately 58 % inhibition of cell proliferation was observed with 30 µM fungal taxol against HL-60 leukemia cell line, 46 % with 3.65 µM fungal taxol against MCF-7 breast cancer cell line and 53 % with 3.65 µM fungal taxol against A431 epidermal carcinoma cell line (FIG 9).

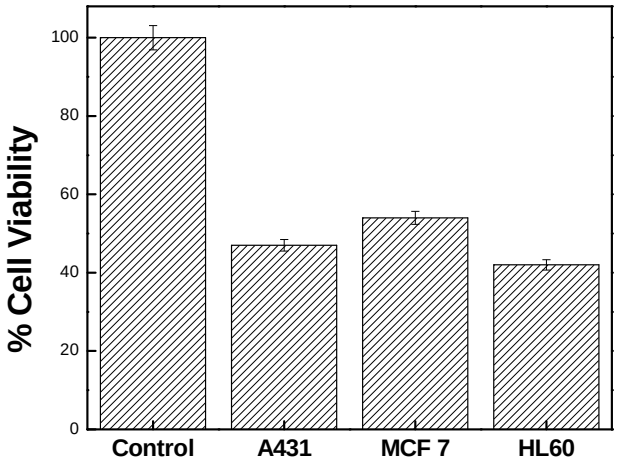

FIG 9: Cytotoxicity of fungal taxol in terms of % cell viability, HL-60 showing 58 % cell inhibition with 30 µM of fungal taxol treatment, MCF-7 showing 46 % with 3.6 µM and A431 showing 53 % cell inhibition with 3.6 µM. Bar shows standard error 3.1 %.

5.6. Antibacterial activity

Out of eight pathogenic bacteria, five of them were susceptible for taxol, 10 DAB III and Baccatin III treatment. Highly susceptible being *E coli and Proteus vulgaris* (FIG 10). 10 DAB III showed high activity against all the five susceptible bacteria, the next potent molecule being baccatin III and then taxol. The probable difference in the activity of these molecules may be because of difference in the hydrophobicity. As the hydrophobicity is inversely proportional to antibacterial activity, 10 DAB III being less hydrophobic shows higher activity than taxol and baccatin III.

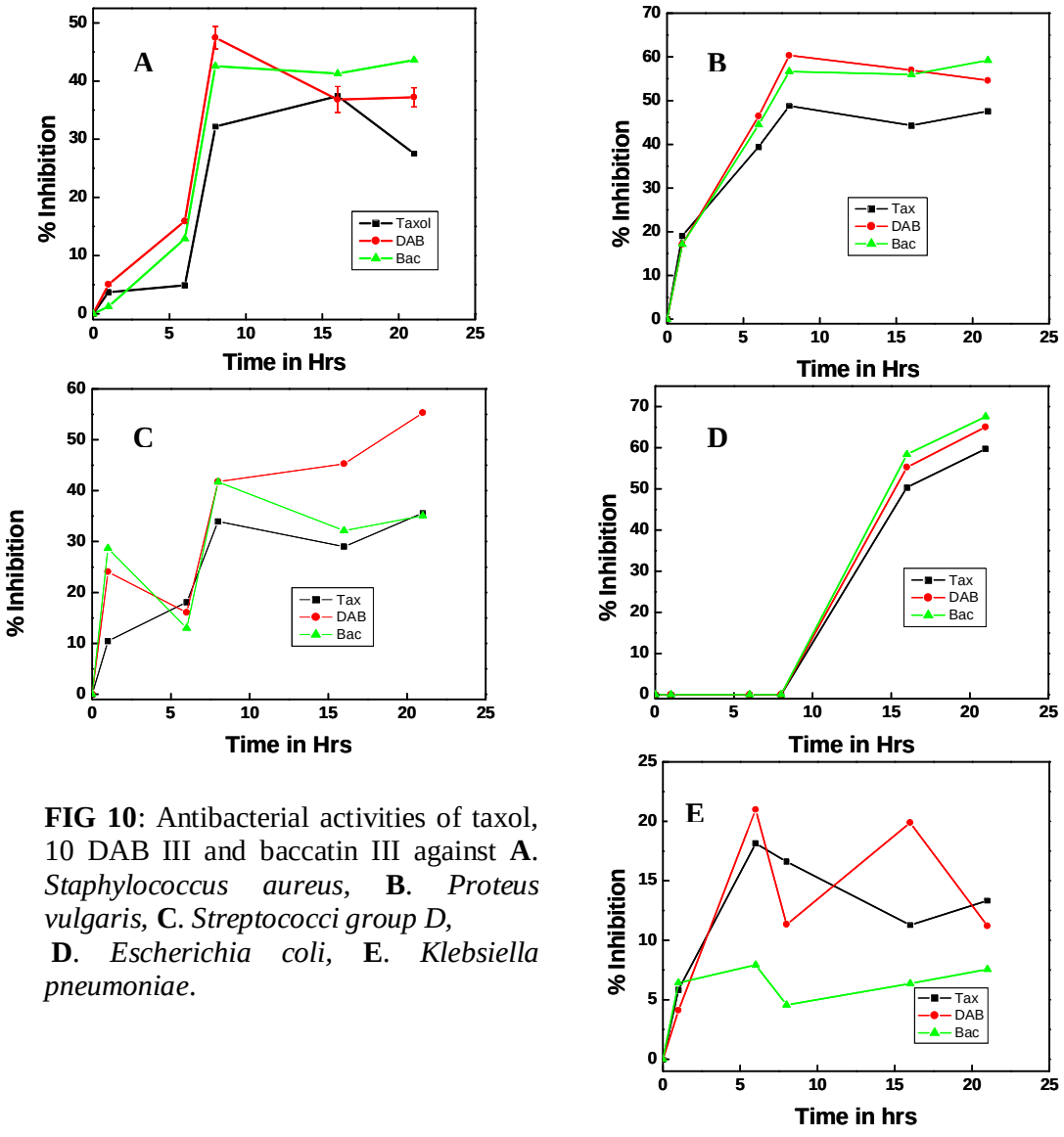

FIG 10: Antibacterial activities of taxol, 10 DAB III and baccatin III against **A**. *Staphylococcus aureus*, **B**. *Proteus vulgaris*, **C**. *Streptococci group D*, **D**. *Escherichia coli*, **E**. *Klebsiella pneumoniae*.

5.7. 10 DAB III from culture of *Gliocladium* sp

Fungal 10 DAB III was isolated from a 14 day old culture. The crude fractions eluted with chloroform: acetonitrile (50:50 and 75:25) showed compounds similar to the standard 10 DAB III. Purified compound showed a single bluish violet spot when sprayed with vanillin sulphuric acid and had R_f value 0.2 (FIG 11). ESI-MS analysis showed molecular ions at *m/z* 545 and at *m/z* 567 (FIG 12) (Edward et al, 1994) and the yield was 65 µg / L culture (FIG 13).

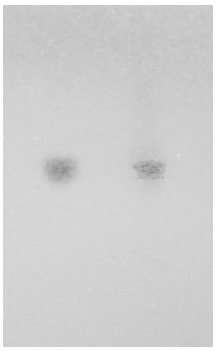

A B

FIG 11: TLC showing purified fungal 10 DAB III in comparison with standard on silica gel G using chloroform: acetonitrile (7:3) solvent system A: fungal purified 10 DAB III, B: Standard 10 DAB III. Detection: Vanillin sulphuric reagent.

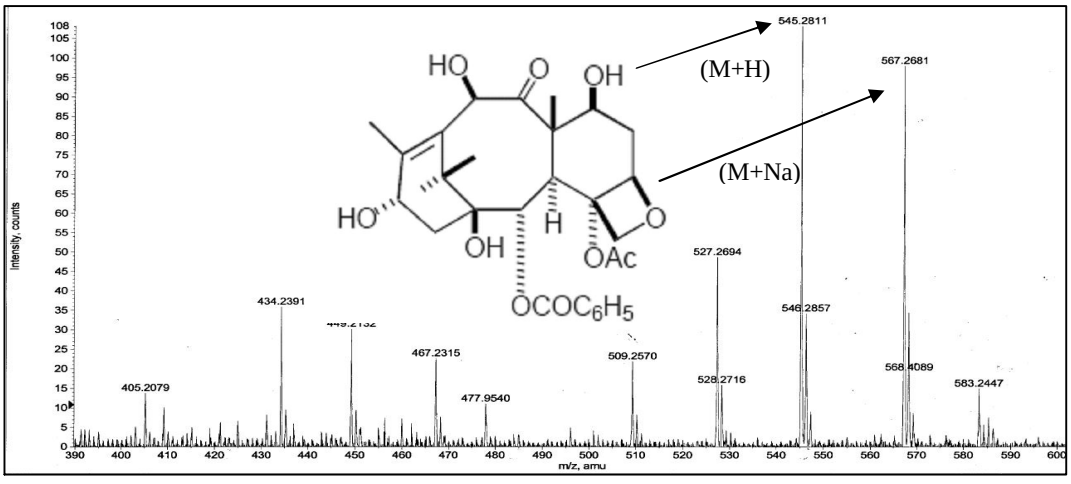

FIG 12: ESI-MS spectrum showing ions at *m/z* 545 and *m/z* 567 of 10 DAB III attributing to M+H and M+Na.

Sample dilution	Mean absorbance (B)	B/B0	Extrapolated taxol Conc from Std Curve	Mean calc Taxane Conc(x dilution) (µM/ L)
1/1000	0.221	0.184	13.0 nM	13.0 µM

Table summarizing the values obtained

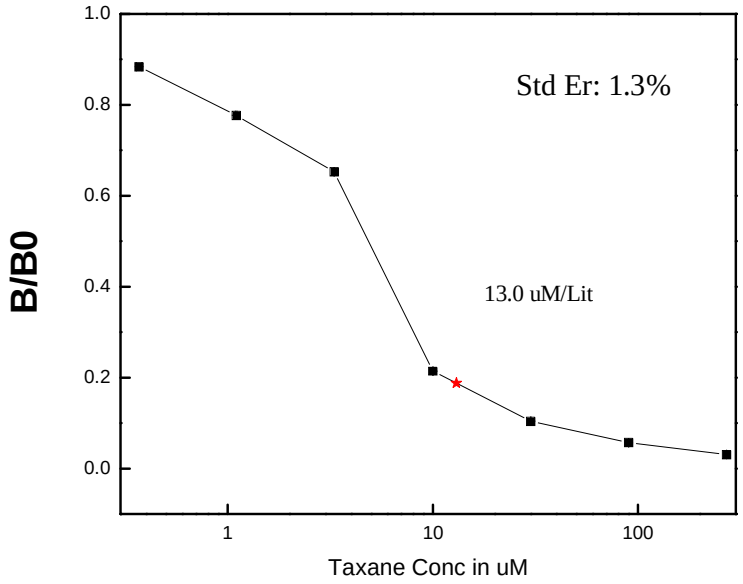

FIG 13: Standard plot obtained using different concentrations of standard taxane and with extrapolated test sample concentration.

6. Discussion

Studies on the isolation of the taxanes produced by *Gliocladium* spp. indicate that the fungus produces taxanes 10 DAB III and taxol in the culture broth *in vitro*. TLC, HPLC and other analyses of the extracts from culture broth confirm this conclusion. In addition to 10 DAB III and taxol, this fungus also produces few unidentified taxanes, although in trace amounts. To the best of our knowledge, this is the first report of isolation of 10 DAB III and taxol from *Gliocladium* sp. isolated from Indian Yew tree *Taxus baccata*.

However, Wang et al, 2000 and others (Strobel et al, 1996) have isolated taxanes from different endophytic fungal species (*Taxomyces andreanae, Pestalotiopsis, Pestalotia,*

Fusarium, Alternaria and others) obtained from *Taxus* sp. that are common to Europe, Asia and North America. The necessary precursor molecules such as sodium benzoate, sodium acetate, biotin, pyridoxal required for the formation of the taxane ring and L-phenylalanine required for the formation of side chain were provided in the growth medium, as they are essential for taxol production as reported earlier (Stierle et al, 1993). Endophytic fungi producing taxol and baccatin III in 3 weeks have been reported earlier (Noh et al, 1999), but the fungus *Gliocladium* sp. produces taxol in 21 days. However, it does produce 10 DAB III after 14 days.

The ability of *Gliocladium* sp. to make taxol was confirmed by isolation of a compound having chromatographic properties similar to those of standard taxol in three solvent systems A, B and C which showed a single dark bluish violet spot on TLC when sprayed with anisaldehyde reagent or vanillin sulfuric acid reagent. Putative taxol on HPLC C18 symmetry column showed a single symmetrical peak at retention time of 25.5 min that confirmed its homogeneity. Absorption maximum of the purified fungal taxol was found to be at 227 nm as reported earlier (Chan et al, 1994). In ESI-MS, molecular ions at *m/z* 854 attributing to the $(M+H)^+$ and at *m/z* 876 attributable to $(M+Na)^+$ confirmed its molecular weight to be 853 (Edward et al, 1994). MS/MS showed fragment ions at *m/z* 570 attributable to taxane ring substructure and at *m/z* 286 for the side chain substructure which are usually seen as taxol fragment ions (Thomas, 1992). ^{1}H NMR spectrum was identical with that of the standard taxol spectrum (Chmurny et al, 1992). Taxol obtained per liter of culture was estimated to be approximately 10 μg. The concentration of taxol produced is neither low nor high when compared with the other reports (Guo et al, 2006; Strobel et al, 1996). However, this is the first report on taxol from an endophyte of yew tree growing in India. Anti-tumor activity of taxol was checked against HL-60 leukemia cell line, A431 epidermal carcinoma cell line, and MCF-7 breast cancer cell line, showing 58 %, 53 % & 46 % inhibition with 30 μM, 3.65 μM & 3.65 μM, fungal taxol respectively. Taxol showed less cytotoxicity on HL-60 cell line. However, in case of MCF7 and A431, the cell-growth inhibition was significantly high even at low taxol concentration. A number of *Taxus* sp. has been reported to produce 10 DAB III (Xueli et al, 1998) and we have also isolated this compound from a 14-day old fungal culture. ESI-MS showed a molecular

ion at *m/z* 545 and at *m/z* 567 attributable to $(M+H)^+$ and $(M+Na)^+$, inferring its mass to be 544 (Edward et al, 1994). 10 DAB III produced was 65 µg / L culture.

7. References

1. Amos L, Lowe J. 1999. How Taxol® stabilizes microtubule structure. *Chem. Biol*. 6 R65-R69.
2. Barnett HL, Hunter BB. 1998. Illustrated genera of imperfect fungi (Fourth edition). APS Press, USA.
3. Chan KC, Alvarado AB, McGuire MT, Muschik GM, Issaq HJ, Snader KM. 1994. High-performance liquid chromatography and micellar electrokinetic chromatography of taxol and related taxanes from bark and needle extracts of *Taxus* species. J. Chrom. B. 657: 301-306.
4. Chmurny GN, Hilton BD, Brobst S, Look SA, Witherup KM, Beutler JA. 1992. ^{1}H- and ^{13}C-NMR assignment for taxol, 7-epi-taxol and cephalomannine. J. Nat Prod. 55: 414-423.
5. Edward KH, Kevin JV, Susan EH. 1994. Profiling taxanes in Taxus extracts using LC/MS and LC/MS/MS techniques. J. Nat Prod. 57: 1391-1403.
6. Gordon MC, Saul SA, Matthew S, Michael RG. 1993. The taxol supply crisis: New NCI policies for handling the large-scale production of novel natural product anticancer and anti-HIV agents. J. Natl. Pro. 56: 1657-1668.
7. Guo BH, Wang YC, Zhou XW, Hu K, Tan F, Miao ZQ, Tang KX. 2006. An endophytic taxol-producing fungus BT2 isolated from *Taxus chinensis* var. *mairei,* Afr. J. Biotec. 5: 875-877.
8. Haldar S, Basu A, Croce CM. 1997. Bcl2 is the guardian of microtubule integrity. Cancer. Res. 57: 229-233.
9. Haldar S, Chintapalli J, Croce CM. 1996. Taxol induces bcl-2 phosphorylation and death of prostate cancer cells. Cancer. Res. 56: 1253-1255.
10. Haldar S, Jena N, Croce CM. 1995. Inactivation of Bcl-2 by phosphorylation. Prod. Natl. Acad. Sci. USA 92: 4507-4511.

11. Jaziri M, Zhiri A, Guo YW, Dupon JP, Shimonura K, Hamada H, Vanhaelen M, Homes J. 1996. *Taxus* sp. Cell, tissue and organ cultures as alternative source for taxoids production: a literature survey. Plant Cell Tiss Org Cult. 46: 59-75.
12. Malerba I, Gribaldo L, Diodovich C, Carloni M, Meschini R, Bowe G, Collotta A. 2005. Induction of apoptosis and inhibition of telomerase activity in human bone marrow and HL-60 p53 null cells treated with anti-cancer drugs. Toxicol in vit. 19: 523-532.
13. Martin N, Catalin J, Blachon MF, Durand A. 1998. Assay of paclitaxel (Taxol) in plasma and urine by high performance liquid chromatography. J. Chrom B. 709: 281-288.
14. Nicolaou KC, Yang Z, Liu JJ, Ueno H, Nantermet PG, Guy RK, Claiborne CF, Renaud J, Couladours EA, Paulvannan K, Sorensen EJ. 1994. Total synthesis of taxol. Nat. 367: 630-634.
15. Noh MJ, Yang JG, Kim KS, Yoon YM, Kang KA, Han HY, Shim SB, Park HJ. 1999. Isolation of novel microorganism, *Pestalotia heterocornis*, producing paclitaxel. Biotech and Bioeng. 64: 620-623.
16. Roberts K, Hyams JS. Microtubules. 1979. Chapter 2, p. 65, Academic press, New York.
17. Scatena CD, Stewart ZA, Mays D, Tang LJ, Keefer JC, Leach DS, Pietenpol AJ. 1998. Mitotic Phosphorylation of Bcl-2 during Normal Cell Cycle Progression and taxol-induced Growth Arrest. J. Biol. Chem. 273: 30777-30784.
18. Sreekanth D, Sushim GK, Syed A, Khan BM, Khan IM, Absar A. 2008. Molecular and morphological characterization of a taxol producing endophytic fungus, *Gliocladium* sp. from *Taxus baccata*. Communicated.
19. Stierle A, Strobel G, Stierle D. 1993. Taxol and taxane production by *Taxomyces andreanae*, and endophytic fungus of pacific yew. Science. 260: 214-216.
20. Strobel GA, Hess WM, Ford E, Sidhu RS, Yang X. 1996. Taxol from fungal endophytes and the issue of biodiversity. J. Industrial microbiol. 17: 417-423.
21. Strobel G, Yang X, Sears J, Kramer R, Sidhu RS, Hess WM. 1996. Taxol from *Pestalotiopsis microspora*, an endophytic fungus of *Taxus wallachiana*. Microbiology. 142: 435-440.
22. Thomas D, Clure Mc, Karl HS. 1992. The mass spectrometry of taxol. J Am Soc Mass Spectrom. 3: 672-679.

23. Twentyman PR, Luscombe M. 1987. A study of some variables in a tetrazolium dye (MTT) based assay for cell growth and chemosensitivity. Br. J. Cancer. 56: 279-285.
24. Wang J, Li G, Lu H, Zheng Z, Huang Y, Su W. 2000. Taxol from *Tubercularia* sp. strain TF5, an endophytic fungus of *Taxus mairei*. FEMS Microbiol. Let. 193: 249-253.
25. Wani MC, Taylor HL, Wall ME, Coggon P, Mc Phail AT. 1971. Plant antitumor agents. VI. Isolation and structure of taxol, a novel antileukemic and antitumor agent from *Taxus brevifolia*. J. Am. Chem. Soc. 93: 2325-2327.
26. Xueli C, Yu T, Tian ZY, Yoichiro I. 1998. Separation and purification of 10-deacetylbaccatin III by high-speed counter-current chromatography. J. Chrom A. 813: 397-401.

Chapter 4

Microbial transformation of 10 DAB III and side chain to biologically active taxanes.

1. Summary

A microbial transformation method for synthesis of biologically active taxanes using 10 Deacetyl baccatin III (10 DAB III) and N-benzoyl-(2R, 3S)-3-phenylisoserine (Side chain) with the help of a taxol producing fungus *Gliocladium* sp. is described in this study. The purified compound has identical chromatographic and spectroscopic properties as that of standard taxol. However further characterization with the help of MALDI-TOF and LC-MS lead to the conclusion that the compound obtained is 10 Deacetyl paclitaxel. Further confirmation of the structure was done by proton NMR. 10 Deacetyl paclitaxel showed affinity to tubulin, the prime target of many taxanes and was immunologically detected using taxane antibodies. It showed cytotoxicity against A431 and THP1 cancer cell lines.

2. Introduction

Taxol, a structurally complex diterpenoid is now called “wonder drug” as it is used for the treatment of an array of cancers including Breast and Ovarian cancer (Gordon et al, 1993). The essential structure of taxol has two parts: a taxane nucleus and a side chain moiety linked to it at C13 position (Wani et al, 1971). Any structural modifications in taxane nucleus or/ and in side chain would lead to the formation of a new taxane molecule. These structural similarities leading to similar chemical properties have imparted difficulties in purification of these taxanes from each other (Cardellina, 1991). Very little has been done to purify and identify these taxanes obtained by many *Taxus* sp. using chromatographic techniques. Difficulty in taxol purification from that of the contaminant taxanes such as Cephalomanine and 7-epi-10 Deacetyl paclitaxel can be an example. Most of the taxanes illustrate similar mechanism of action, which includes stabilization and enhanced polymerization of microtubules, leading to mitotic arrest (Amos and Lowe, 1999). Since many taxol analogs show antitumor activity, research has been focused on synthesis of such analogs chemically (Jordan and Wilson, 1998). This approach might ultimately provide a long term solution for the availability of taxol

and its related taxanes. Another taxane which has gained importance as a potent candidate for cancer treatment is Docetaxel (Cortes and Pazdur, 1995).

Semi-synthesis of taxol using 10 Deacetyl baccatin III (10 DAB III) and N-benzoyl-(2R, 3S)-3-phenylisoserine (Side chain) is in practice, which did not prove to be more promising because of the multi step reaction procedures and low yield of desired product (Gueritte et al, 1986). Our research describes a procedure for synthesis of biologically active taxanes, synthesized using 10 DAB III which is abundantly present in *Taxus* sp. and the side chain which can be easily synthesized with the help of taxol producing endophytic fungus *Gliocladium* sp.

3. Materials

Taxane immunoassay kit was purchased from Hawaii Biotech, Hawaii, USA. TLC precoated plates were purchased from Merck, Germany**.** Standard taxol and 10 DAB III were purchased from M. P. BioMedicals, USA. Side chain (N-benzoyl-(2R, 3S)-3-phenylisoserine) was purchased from Aldrich. NMR grade solvents and tubes from Cambridge Isotope Lab. Inc USA. A431 and THP 1 cell lines from National Center for Cell Sciences (NCCS), Pune, India. Standard 25 cm^2 tissue culture flasks and 96 well microtiter plates from Nunc. 3-(4,5-dimethylthiazol-2-yl)-2,5-diphenyltetrazolium bromide from Sigma chemicals. All other analytical grade chemicals and solvents were from Qualigens, Merck, Himedia and Sigma.

3.1. Depolymerization Buffer

MES	50 mM
$CaCl_2$	1 mM
pH was adjusted to 6.6 with HCl	

3.2. PIPES Buffer

PIPES	1 M
$MgCl_2$	10 mM
EGTA	20 mM
pH was adjusted to 6.9 with KOH	

50 mM GTP	pH was adjusted to 7.5 with NaOH
50 mM ATP	pH was adjusted to 7.5 with NaOH

3.3. BRB80 Buffer

PIPES	80 mM
$MgCl_2$	1 mM
EGTA	1 mM
pH was adjusted to 6.8 with KOH	

3.4. SDS PAGE Buffers

Acrylamide 30%	29.2 % Acrylamide	0.8 % Bis acrylamide
Gel Buffer	3 M Tris	pH was adjusted to 8.8 with Conc. HCL
Electrode Buffer 20 X	Tris	pH was adjusted to 8.9 with Conc. HCL
	Glycine	

4. Methods:

4.1. Culture conditions

Fungus *Gliocladium* sp. maintained on PDA slants was transferred into 100 mL MM medium pH 7 in a 500 mL Erlenmeyer flask and incubated for 5 days at 27 ^{0}C on rotor shaker (200 rpm). After 5 days of fermentation, mycelium was separated from the culture broth by centrifugation (5,000 rpm) at 20 ^{0}C for 20 min and then the mycelium was washed thrice with sterile distilled water under sterile conditions. The harvested mycelia mass (20 gm wet weight of mycelia) along with 10 DAB III and side chain at a concentration of 1 mg/ mL and 10 mg/ mL respectively were transferred into 100 mL sterile distilled water and left on shaker at 27 ^{0}C (200 rpm) and the reaction was carried

out for five days. After 5 days, the culture was harvested and mycelium was separated from the culture filtrate.

4.2. Taxane isolation and purification

The culture filtrate obtained is lyophilized and extracted with chloroform: methanol 10:1. The organic layer was separated using separating funnel. This procedure was repeated thrice to for maximum recovery of the compounds. The solvent layer is then dried using anhydrous sodium sulphate and evaporated with the help of rotavapour in vacuum. The crude extract obtained was subjected to preparative thin layer chromatography (TLC) on 0.5 mm thickness TLC glass plates. Chloroform, acetonitrile 7:3 was used as mobile phase, the resolved compounds were scraped and eluted using chloroform, methanol (10:1).

4.3. TLC, HPLC and spectroscopic analysis

The purity of the compound is analyzed on TLC using three different mobile phases: chloroform, acetonitrile (7:3); chloroform, methanol (7:1); and ethlyacetate, 2-propanol (95:5) and visualized by vanillin sulphuric acid or anisaldehyde reagents. All the analysis was done in comparison with taxol and 10 DAB III standards (MP Biomedicals). C18 Symmetry column (Waters) was used to analyze the behavior of the putative taxane compounds using acetonitrile gradient 5 % to 95 % as mobile phase. A dual wave length detector set at 227 nm and 254 nm was used to detect the compounds eluting from the column. Spectroscopic analysis of the putative taxane was done on Shimadzu PC 1601 spectrophotometer. Compound was dissolved in 100 % HPLC grade methanol and spectral data were collected over the range of 200 to 400 nm.

4.4. Standardization of taxane production

Two different concentrations of 10 DAB III and side chain were added to the culture to optimize the transformation. 10 DAB III at concentrations of 1 mg and 2 mg, side chain at 5 mg and 10 mg concentrations were added. The fungal culture with different concentrations was incubated for 5 days at 25 ^{0}C stationary. Further, taxane production was estimated with HPLC using Chloroform: Acetonitrile gradient 70:30 gradient on a C18 symmetry column.

4.5. Immunoassay

Taxane content in the sample was qualitatively and quantitatively determined using taxane immunoassay kit (TA 04) manufactured by Hawaii Biotech, Hawaii. In brief the protocol is as described as follows (Grothaus et al, 1993): the putative taxane was dissolved in methanol and centrifuged to remove the insoluble materials. Baccatin - protein conjugate as antigen was coated in 96 well microtitre plate and incubated at 37 ^{0}C for one hour. Non-specific sites were blocked using 1 % BSA in PBS by incubated for 1 h. After washing, the solid phase bound taxane was incubated with samples and taxane standard and a specific anti-taxane polyclonal antibody. The taxane in the sample competes with solid phase bound taxane for binding to the polyclonal antibody. The primary antibody was detected using secondary antibody–alkaline phosphotase conjugate, where in the enzyme use p-nitro phenyl phosphate as substrate leading to a colorimetric reaction. Inhibition of color development was proportional to the concentration of free taxane present in the samples. The amount of taxane in each sample was calculated from an inhibition curve made by using different concentrations of standard taxane supplied with the kit.

4.6. Tubulin isolation and *in vitro* microtubule assembly

To determine the affinity of the putative taxane for tubulin, turbidity assay was done (Chun et al, 1995). Tubulin was isolated from goat brain through two cycles of temperature dependent assembly/ disassembly by method described by Shelansky et al, 1973. In brief, the procedure is as follows: Fresh goat brain (150 gm) was homogenized in depolymerization buffer (approximately 100 mL) and was extracted in the same buffer for 20 min at 4 ^{0}C. The homogenate was centrifuged at 10,000 rpm for 30 min at 4 ^{0}C. This step of extraction and centrifugation was repeated. The supernatant obtained was supplemented with equal volumes of prewarmed (37 ^{0}C) high molarity PIPES buffer, ATP (1.5 mM final conc.), GTP (0.5 mM final conc.) and 1/3rd volume of anhydrous prewarmed (37 ^{0}C) glycerol . The mixture was incubated at 37 ^{0}C in water bath for 1 h (Polymerization step). The polymerized tubulin in the mixture was separated by centrifuging the mixture at 40,000 rpm for 30 min at 20 ^{0}C. The resulting pellet was resuspended in 10 mL ice cold 50 mM depolymerization buffer and incubated in ice for 30 min (depolymerization step). The depolymerized tubulin was subsequently recovered by centrifuging at 30,000 rpm for 30 min at 4 ^{0}C. The supernatant obtained

was subjected to polymerization step and the resulting pellet of tubulin was suspended in BRB80 buffer and depolymerized by incubating in ice for 10 min. The suspended tubulin was centrifuged briefly to remove any unwanted particulate matter. Tubulin was snap frozen in liquid nitrogen and stored at -20 ^{0}C.

To obtain high purity of tubulin it was subjected to phosphocellulose chromatography (Weingaster et al, 1975). The purified tubulin was characterized using SDS-PAGE and concentration was estimated by Lowry's method (Lowry et al, 1951). Prior to the use, the frozen tubulin is thawed gently and centrifuged at 1,000 rpm to remove any insoluble material. Microtubule assembly was determined using tubulin concentrations 0.235 mg/ mL. Samples for the test were dissolved in DMSO, a 5 µL aliquot of sample was added into 1 mL tubulin in MES buffer pH 6.4 containing GTP 1 mM and was monitored at 350 nm after every 5 min to detect the insoluble precipitates formed (Chun et al, 1995)**.**

4.7. LC-MS and MALDI-TOF

M/S Applied Biosystems API QSTAR pulsar mass spectrometer was used for determining the molecular mass of the purified compound. Test samples were dissolved in HPLC grade methanol, water, acetic acid in the ratio of 50:50:0.1. Samples were then analyzed by infusion method / (injected into MS) at a flow rate of 5 µL/ min and at a IS voltage of 3800 V in TOF mode. Spectrum from a range of *m/z* 100 to 900 Daltons was recorded. Molecular weight of the purified compounds was determined by Allied Biosystems Voyager DE-STR (MALDI-TOF-MS) Biospectrometry equipped with 337 nm nitrogen laser. The best spectra were obtained with an accelerating voltage of 20 kV. Samples for the analysis were dissolved in HPLC grade chloroform and mixed with Cynohydroxy cinnamic acid (CHCA) which was used as matrix for ionization. Approximately 10 µL of the sample was spotted on wells on the sample loading plate. Spectrum from a range of *m/z* 400 to 1000 Daltons was obtained.

4.8. Proton NMR

^{1}H-NMR analysis was carried out on a Bruker AV 400 Spectrophotometer at 400 MHz. NMR spectrum was measured with a spectral width of 8223.68 and data were acquired into 32 K data points. An acquisition time of 1.9 s and a relaxation delay of 1.0 s were

used. Samples were then dissolved in $CDCl_3$ (deutero- chlorofrom) and scanned over night.

4.9. Cytotoxicity and MIC of taxane

Cytotoxicity and MIC (Minimum inhibitory concentration) of the compound on cell lines A431 (epidermal carcinoma) and THP1 (Human acute monocytic leukemia) was determined by MTT assay (Twentyman and Luscombe, 1987). The cell suspension at a concentration of 1 x 10^4 cells/ mL was added in 96 well microtiter plates. Culture media used for A431 and THP1 were DMEM and MEM respectively. Plates containing culture media and test compound were incubated overnight for 4 days for A431 and 72 h for THP1 at 37 ^{0}C, 5 % v/v CO_2 and 95 % humidity. For obtaining MIC of the compound on THP1 cell line, serial dilutions of the compound were used. All the samples were taken in triplicates. At the end of the incubation period 10 µL of MTT reagent (5 mg/ mL) was added to each well and cells were incubated for 1 h at 37 ^{0}C. At the end of this period, 200 µL of acidified isopropanol was added and plates were incubated for 4 h to solubilize the purple formazan crystals produced. Absorbance was measured at 490 nm with a Beckman coulter spectrophotometer.

5. Results

5.1. Production of taxanes

Minimum contaminants were obtained in the crude extracts as we adopted the reaction in sterile distilled water. Analysis of the crude extract showed dark bluish grey spots on TLC when charred with anisaldehyde, among which one has similar R_f value as that of standard 10 DAB III which confirms that the transformation of the precursor was not complete. Of the other two transformed compounds one showed identical R_f value as that of the standard taxol while other did not match with either of the standards used and have R_f value of 0.7 (FIG 1). However, the other precursor provided (side chain) was not detected on TLC. Only the two major compounds obtained during the transformation have been the focus for the study and were titled as compound A and compound B. Compound A, showed similar R_f values as that of the standard taxol i.e. 0.5, while compound B showed R_f of 0.7 on TLC. Nevertheless there are many unidentified taxane molecules which were detected.

A B C

FIG 1: TLC showing crude extract containing two biotransformed products of which one showing almost similar R_f value as that of standard taxol and other have R_f value 0.7, the crude extract also shows unconverted 10 DAB III spot in Lane B, Standard taxol Lane A, Lane C Standard 10 DAB III. Detection: Anisaldehyde reagent.

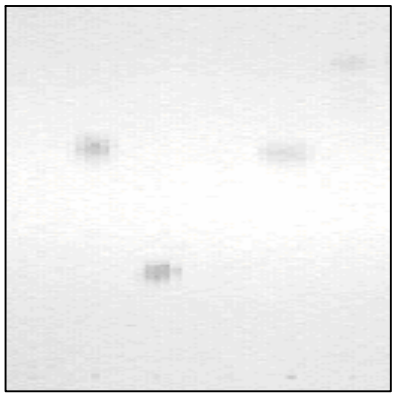

A B C D

FIG 2: TLC showing purified compound with similar R_f value as that of the standard taxol. Lane A: Standard taxol, Lane B: Standard 10 DAB III, Lane C: Purified compound A and Lane D: compound B.
Detection: Anisaldehyde reagent.

5.2. TLC, HPLC and UV

Purity of the compounds was authenticated, as the compounds showed homogeneity when run in three different solvent systems (FIG 2). Crude sample on C 18 Symmetry column showed peak having equal retention time (21 min) as that of the standard 10 DAB III and two major peaks indicating the two major compounds seen on TLC with retention times 22.5 min and 34 min (FIG 3). However compound A did not show similar retention time as that of the standard taxol on HPLC. Spectroscopic analysis showed that the pure taxanes have absorption maxima at 225 nm and 205 nm (FIG 4 [A and B]).

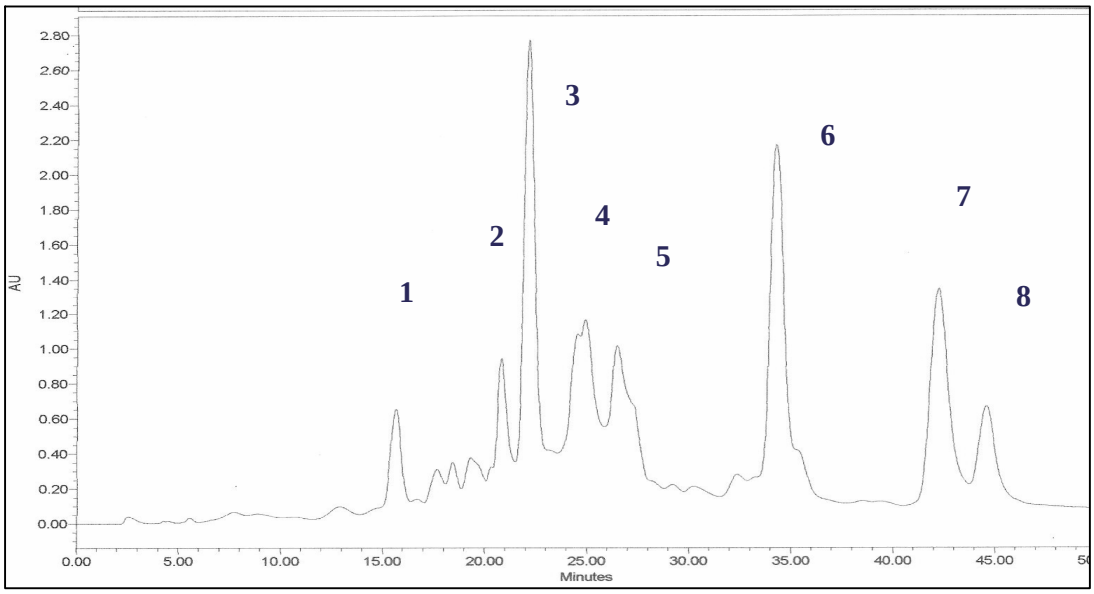

FIG 3: HPLC profile showing well resolved peaks. Peak with retention time 21 min was determined to be untransformed 10 DAB III and peak 2 with retention time 22.5 min was further focused for the study. Absorbance was recorded at wavelength 227 nm.

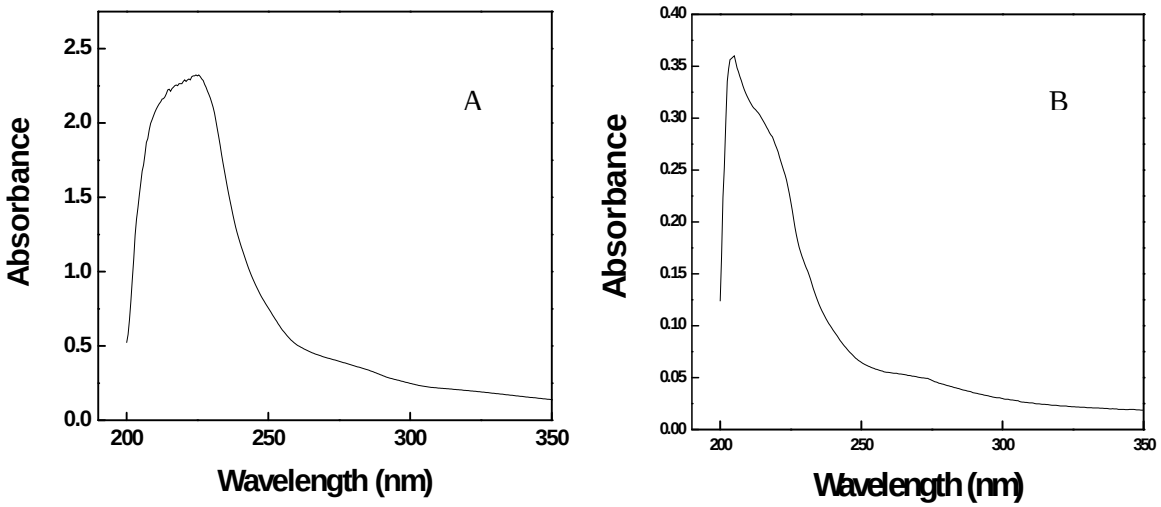

FIG 4 (A and B): U V absorbance spectrum of purified compound A and B showing λ max at 225 nm and 205 nm.

5.3. Immunoassay and turbidity assay

The taxane nature of the compounds was evaluated using anti taxane antibodies. The purified compound A showed affinity for anti taxane antibodies and was quantified to be 11.20 µM/ mL (FIG 5 and Table 1). Compound B, however, showed very low affinity for anti taxane antibodies. Assembly & Disassembly method and phosphocellulose chromatographic method yielded highly homogeneous tubulin. Tubulin obtained was characterized using SDS- PAGE which showed its molecular weight to be 55 KD (FIG 6). Increase in the insoluble precipitate formation of microtubules was quite evident with increase in O. D. at 350 nm (FIG 7). Maximum increase in the precipitates was seen in first 10 min after the addition of compound after which there was no considerable change in the O. D.

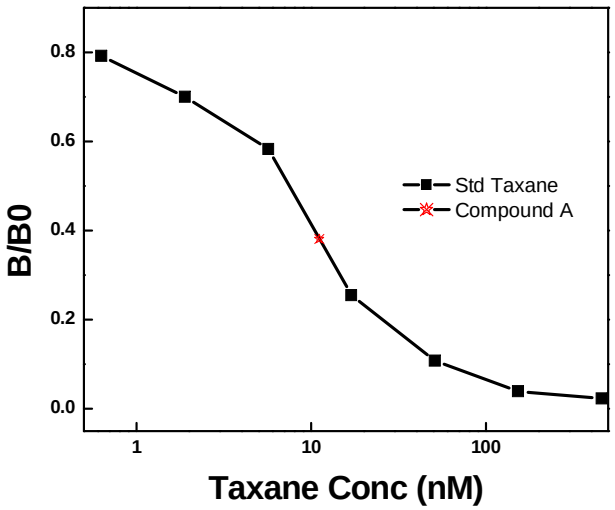

FIG 5: Standard plot obtained using different concentrations of standard taxanes with extrapolated Compound A concentrations.

Sample dilution	Mean absorbance(B)	B/B_0	Extrapolated taxane Conc from Std Curve	Mean calc Taxane Conc X (dilution) (µM/ mL)
1/1000	0.221	0.381	11.12 nM	11.12 µM/ mL

Table summarizing the values obtained.

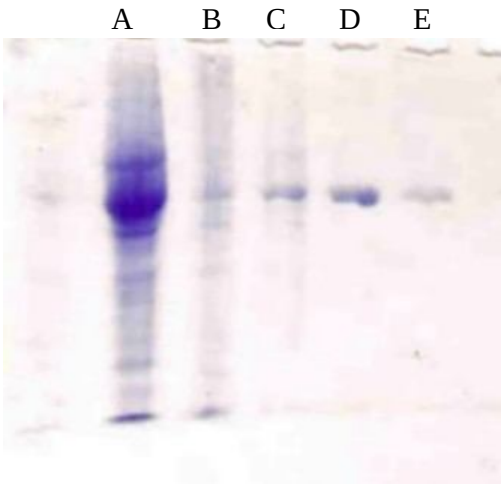

FIG 6: SDS PAGE showing 55 KD tubulin protein in a 10 % gel. Lane A: Protein in the crude extract. Lane B and C: protein obtained by assembly and disassembly cycles. Lane D and E: pure protein obtained from Phosphocellulose column chromatography.

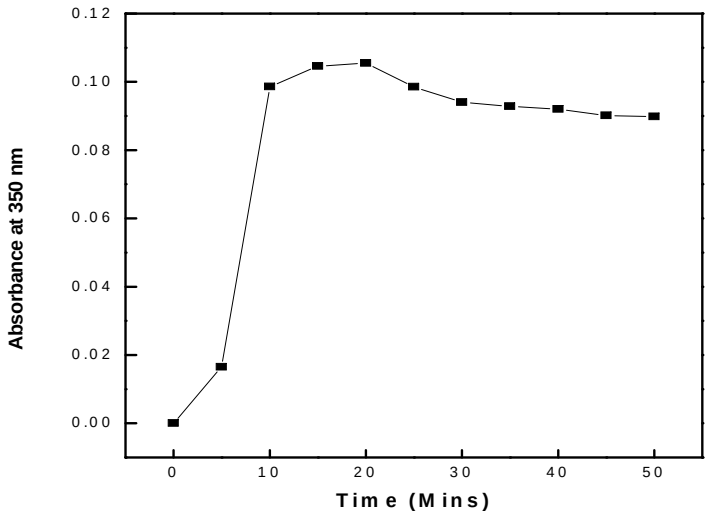

FIG 7: Absorbance spectrum showing increase in O. D. after the addition of 10 Deacetyl paclitaxel at 350 nm. The formation of insoluble precipitates was observed within 10 min after the addition of taxane.

5.4. Standardization of taxane production

Higher concentrations of 10 DAB III and side chain did not bring considerable increase in the production of compound A, but compound B concentration was increased which is shown in the HPLC profile FIG 8 (A and B).

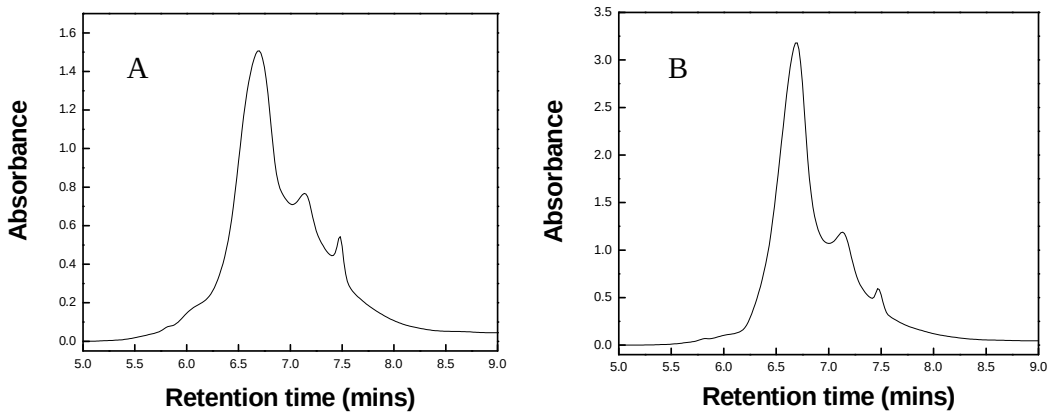

FIG 8: HPLC profiles showing increase in the yield of Compound B with increase in the precursor's concentration (FIG 8 B); while no considerable change in the yield of Compound A.

5.5. LC-MS, MALDI-TOF and ^{1}H NMR

LC-MS spectrum of compound A showed a peak at *m/z* 811 (FIG 9- A) and MALDI-TOF analysis showed major ion at *m/z* 811 attributing to the M^+ ion of 10 Deacetyl paclitaxel (FIG 9- B). Fragment ion at *m/z* 568 was also seen but relatively low in abundance. However these ions were found to be very unstable while a peak at *m/z* 870 attributing to $M+NH_4+CH_3CN$ ion of 10 Deacetyl paclitaxel (FIG 10). Paclitaxel was also seen in LC-MS analysis showing peak at *m/z* 853 attributing to M+H ion (FIG 11). Compound B did not show any prominent peak in the spectrum which can be accounted as molecular ion. Thus, further studies were focused only on compound A which was characterized as 10 Deacetyl paclitaxel. The proton spectrum of the 10 Deacetyl paclitaxel showed well resolved signals in the range of 1-8.5 ppm. The three strong signals in the aliphatic region between 1- 2.5 ppm were seen, probably because of the methyl and acetate groups. The basic protons signals caused because of the taxane skeleton and side chain were seen in the range of 2.5 to 7 ppm. The aromatic signals caused by benzamide and benzoate groups of the side chain and taxane structure are seen in the range of 7 to 8.5 ppm. The most important observation from the comparative analysis of taxol and compound was the absence of proton signal at 2.5 ppm caused by the C-10 acetate group, which is present in taxol (FIG 12 [A and B]).

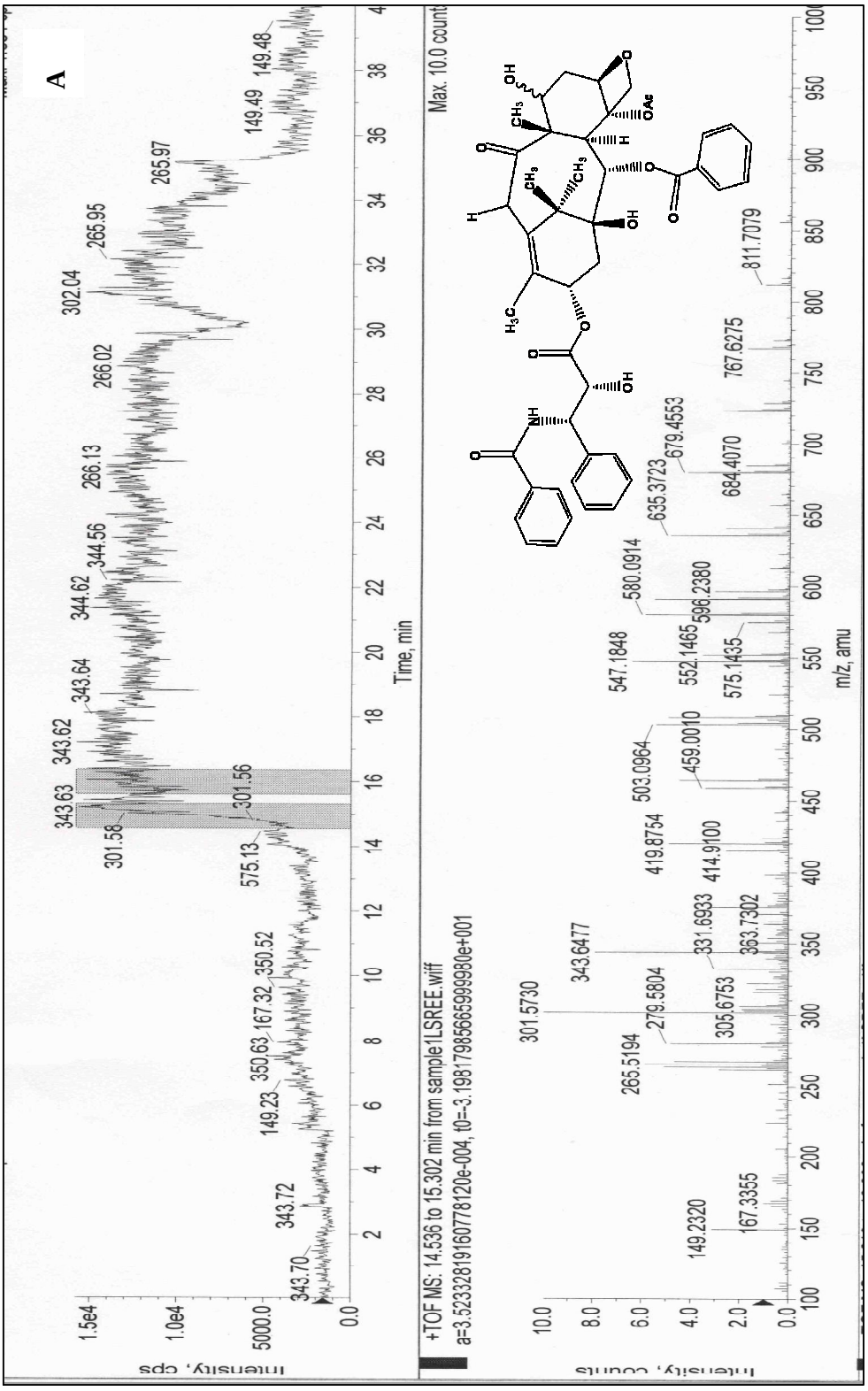
A
Intensity, cps
Time, min
+TOF MS: 14.536 to 15.302 min from sample1LSREE.wiff
a=3.52332819160778120e-004, t0=-3.19817985665999980e+001
Intensity, counts
m/z, amu
Max. 10.0 count

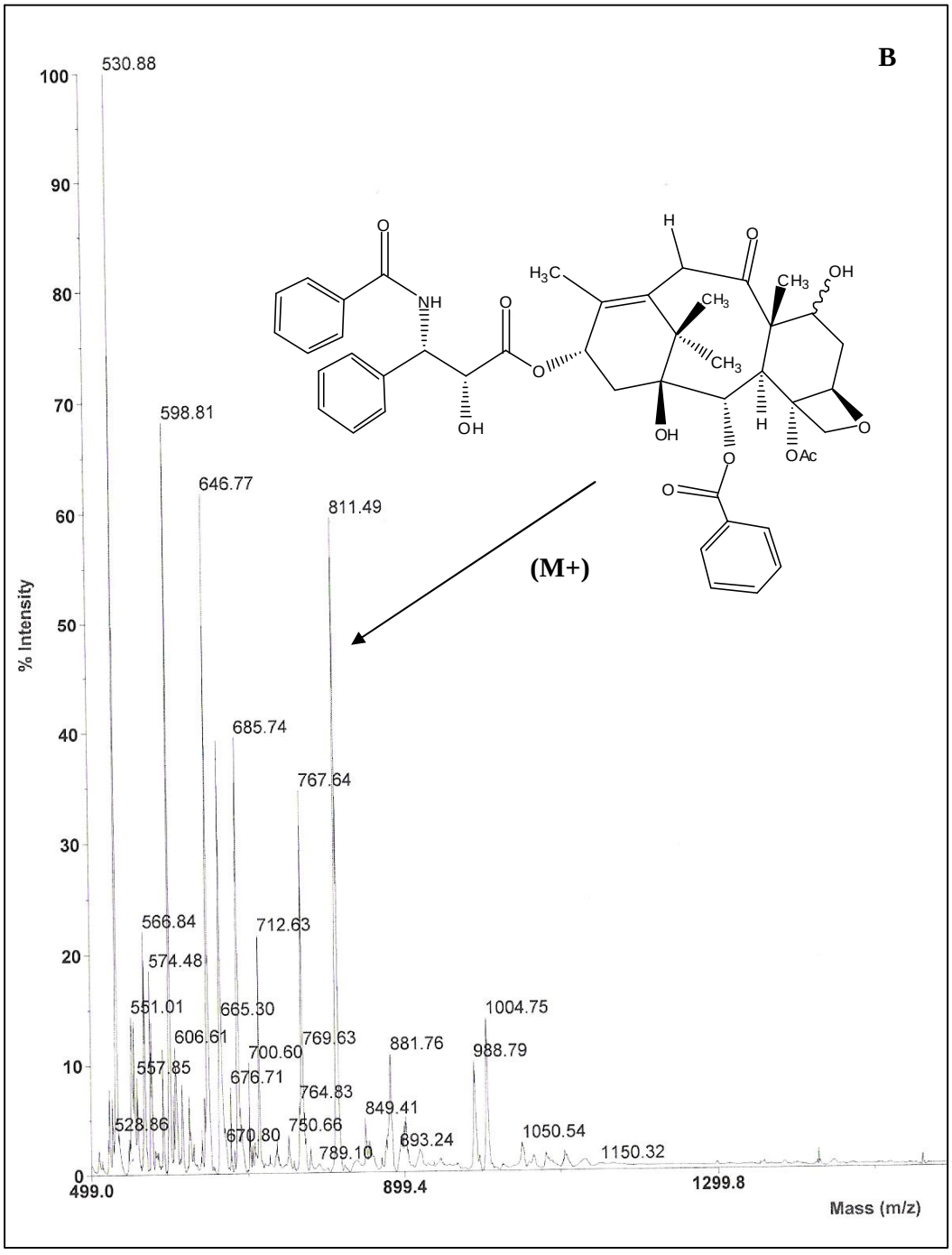

FIG 9: A) LC-MS spectrum showing peak at m/z 811 attributing to M+ ion of 10 Deacetyl paclitaxel. B) MALDI-TOF spectrum showing peak at *m/z* at 811 attributing to 10 Deacetyl paclitaxel.

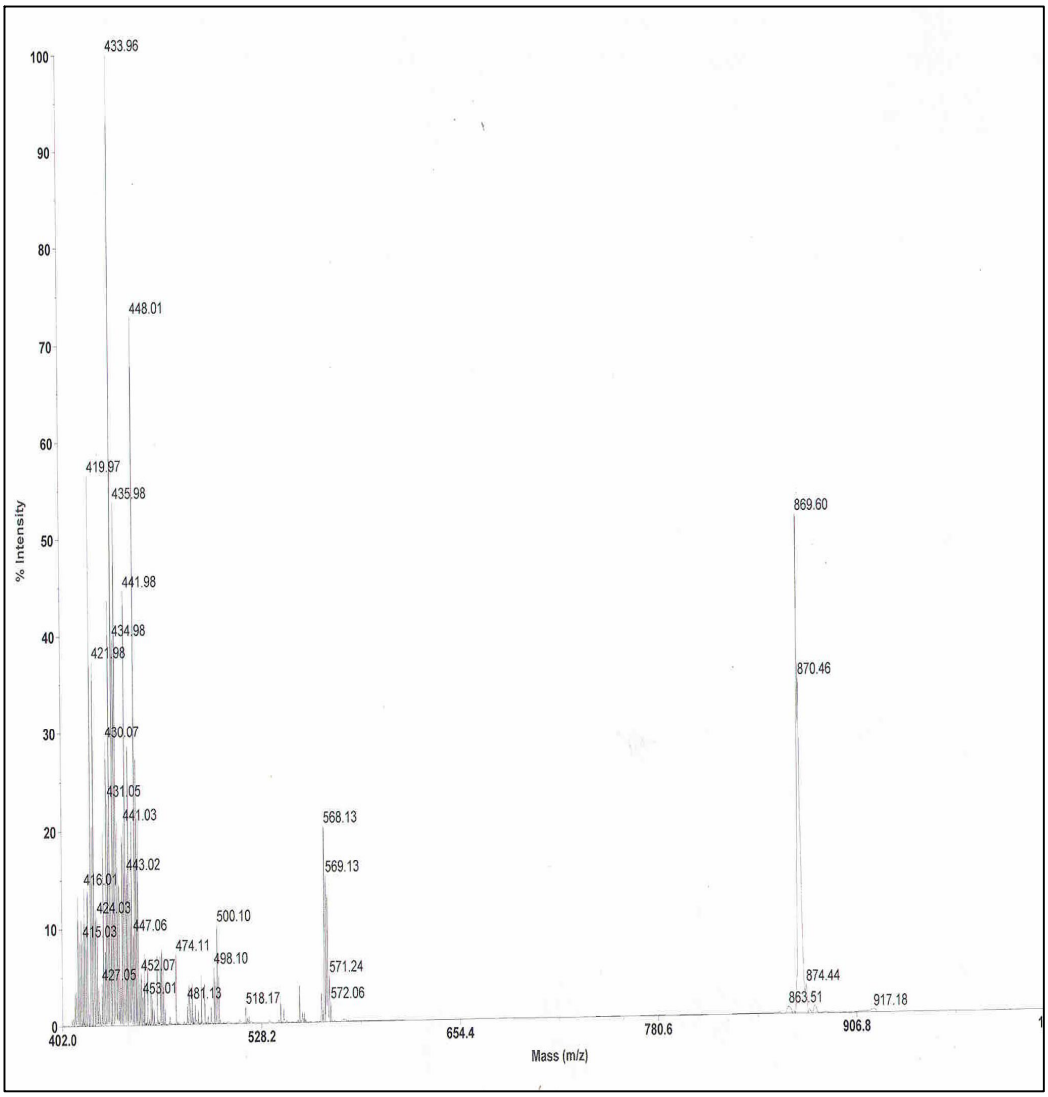

FIG 10: MALDI-TOF spectrum showing the peak at *m/z* 870 attributing to the $M+NH_4+CH_3CN$ ion of 10 Deacetyl paclitaxel (Kerns et al, 1994). This was found to be more stable than the M+ ion.

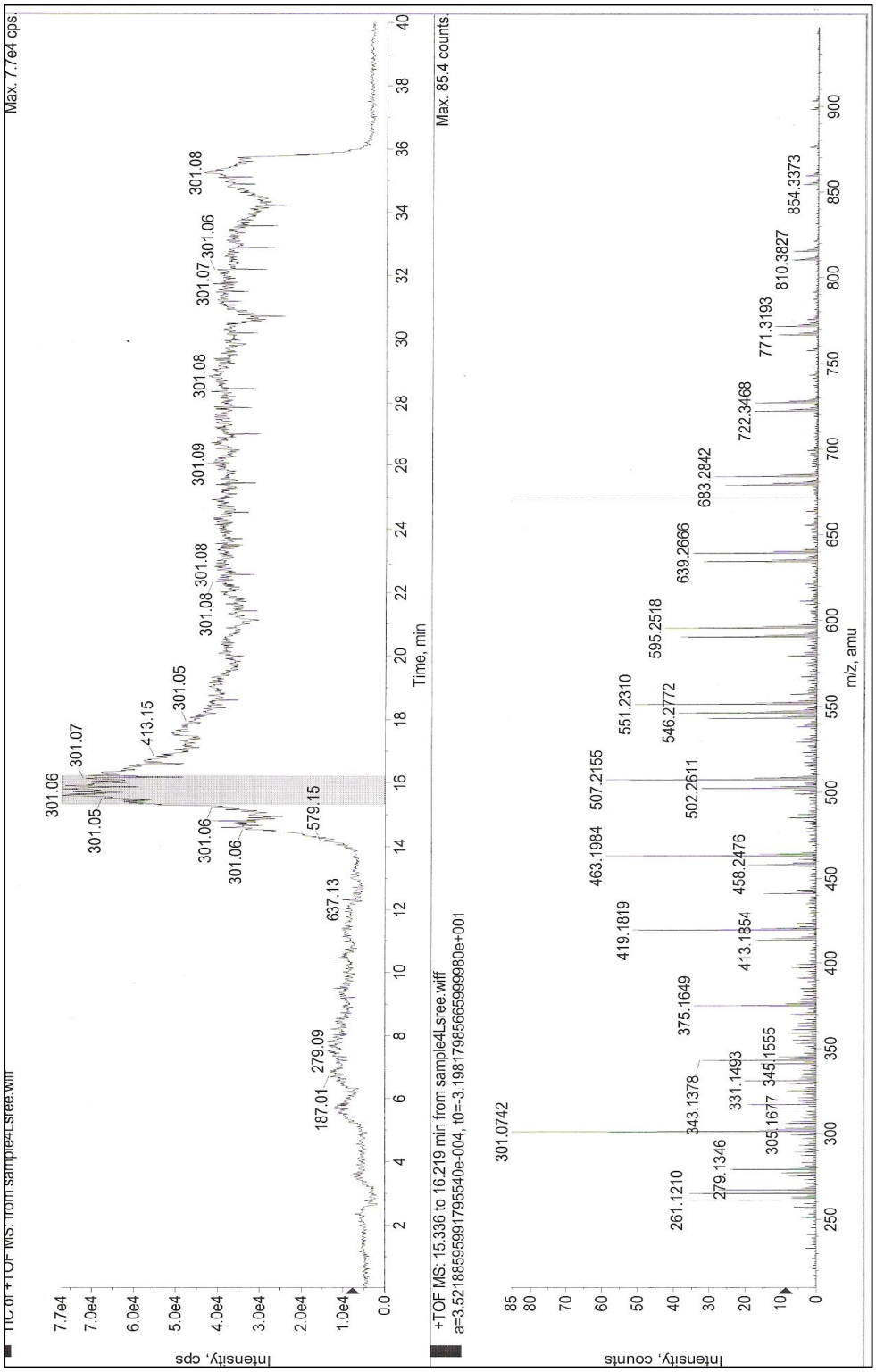

FIG 11: LC-MS spectrum of showing peak at m/z 854 attributing to the M+H ion of paclitaxel.

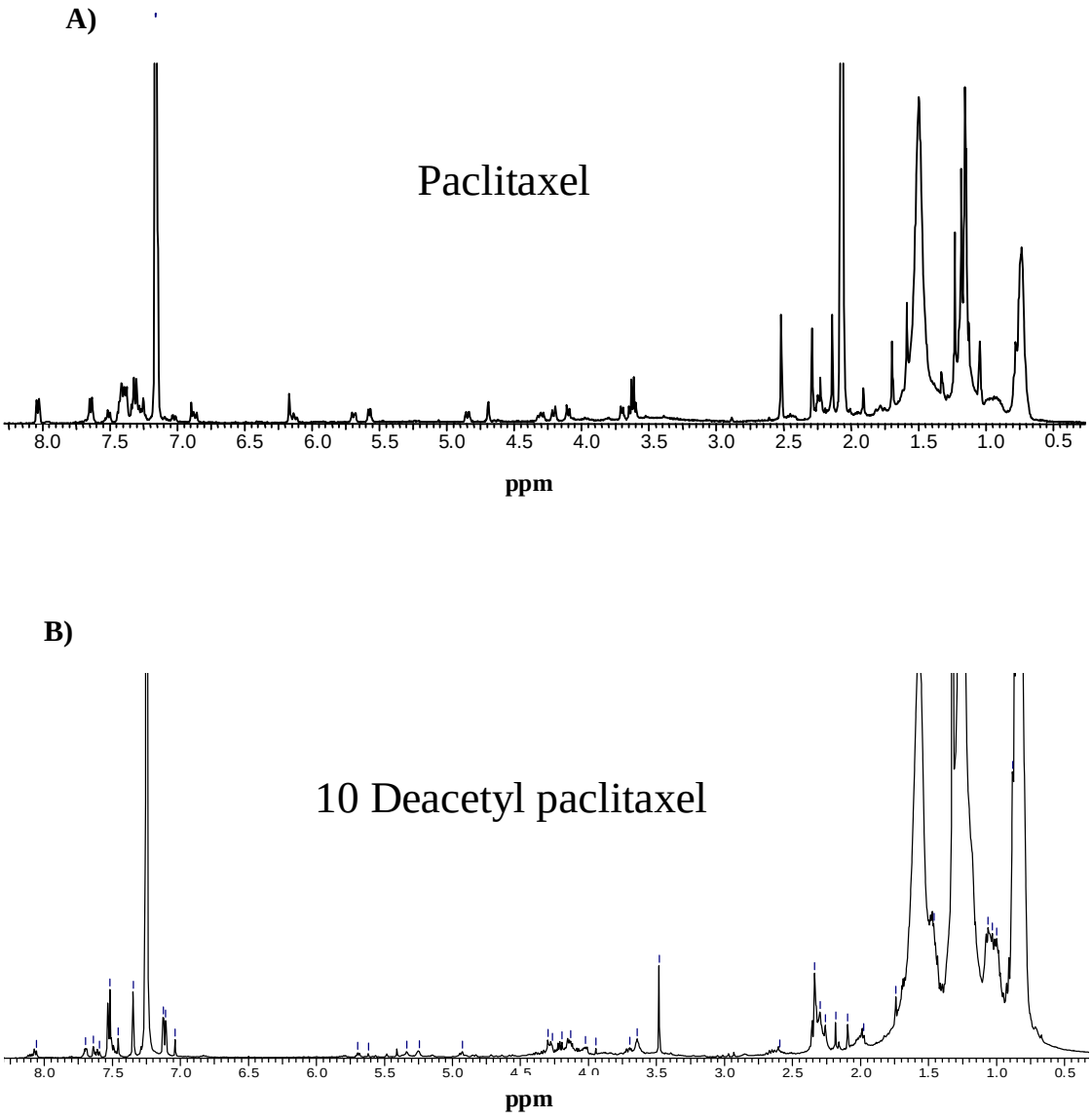

FIG 12: Proton NMR spectrums of standard taxol (A) and 10 Deacetyl paclitaxel (B). Proton signal at 2.5 ppm caused because of C10 Acetyl group which is very prominent in taxol is absent in 10 Deacetyl paclitaxel, other than that all other signals which are seen in taxol are present. This authenticates that the compound transformation into 10 Deacetyl paclitaxel.

5.6. Cytotoxicity and Minimum Inhibitory Concentration

Approximately 82 % cell growth inhibition was seen on A431 epidermal carcinoma cell line with a concentration of 125 μM (FIG 13). Minimum inhibitory concentration of the compound was found to be 6 μg, which was effective against THP1 cell line. Higher concentrations (> 30 μM) of the compound did not show greater change in the activity on THP1 cell line (FIG 14).

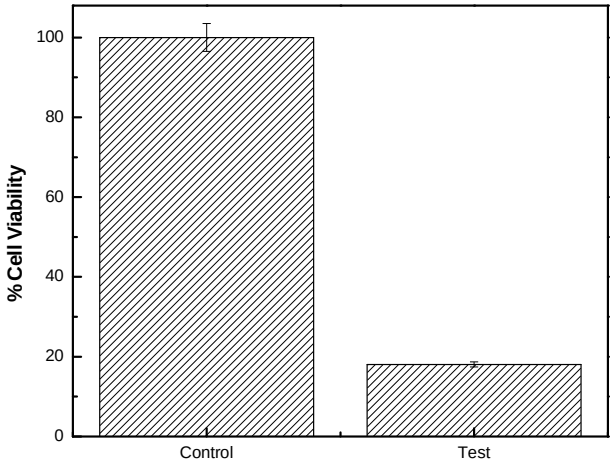

FIG 13: Cytotoxicity of 10 Deacetyl paclitaxel showing 18.05 % cell viability with respect to 100 % in control.

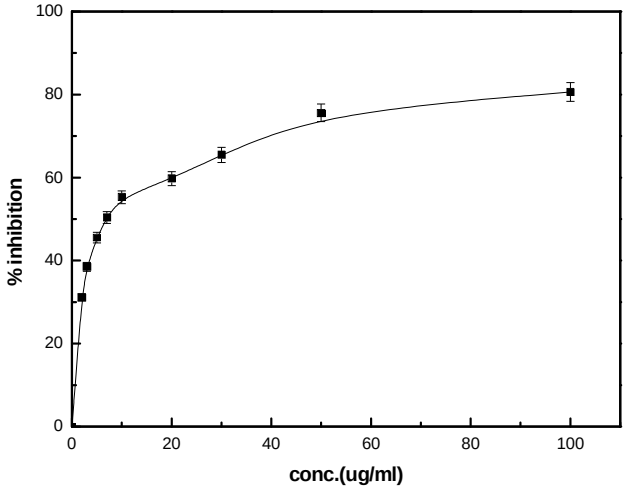

FIG 14: MIC graph showing 50 % cell growth inhibition of THP1 cell line at > 30 μM concentration of 10 Deacetyl paclitaxel.

6. Discussion

Microbial transformed compounds, using precursor molecules 10 DAB III and Side chain of taxol by *Gliocladium* sp were successfully purified by preparative TLC and HPLC. The homogeneity of the purified compound was determined by TLC using solvent systems A, B, and C. Complete transformation of the precursor molecules was not seen which was evident by presence of 10 DAB III on TLC and HPLC. However, side chain (N-benzoyl-(2R, 3S)-3-phenylisoserine) could not be detected in either of them. Maximum conversion of the precursors was seen when 10 DAB III and side chain were taken in 1:5 ratio respectively. The UV absorption analysis showed a peak showing absorption maxima at 225 nm (Theodoridis et al, 1998). Depending on the R_f values observed on TLC in different solvent systems and UV absorbance, it was postulated that the biotransformed molecule could have similar structure as that of taxol, though not exact.

The possibility of forming 10 Deacetyl paclitaxel using precursors 10 DAB III and side chain with the help of fungus *Gliocladium* sp. was authenticated when the LC-MS analysis and MALDI-TOF analysis showed peak at *m/z* 811 attributing to the M^+ ion of 10 Deacetyl paclitaxel (Kerns et al, 1994). Further fragment ion of 10 Deacetyl paclitaxel at *m/z* 568 attributing to taxane sub structure was also seen. However, the peak obtained was considerably unstable and undergoes fragmentation easily, which is quite evident in spectrum. A peak at *m/z* 871 attributing to $(M+NH_4+CH_3CN)^+$ of 10 Deacetyl paclitaxel was consistently seen constituting to its stability (Kerns et al, 1994). Further analysis of the fractions obtained showed that taxol was also formed but in low concentrations. 10 Deacetyl paclitaxel does mimic the mode of activity as that of the taxol and its derivatives in terms of it showing affinity to bind to tubulin and polymerizing them which is evident by turbidity assay. Cytotoxicity of 10 Deacetyl paclitaxel against A431 does prove the above statement. MIC of the compound was determined to be 6.7 µM against THP1 cell line.

In conclusion, we can say that the above biotransformed, purified molecule showing chromatographic and spectroscopic similarities to taxol is confirmed to be 10 Deacetly paclitaxel. This report on its own is a novel discovery of converting abundantly present

taxol precursor 10 DAB III and easily synthesized side chain into a biologically active 10 Deacetyl paclitaxel, a taxane molecule, using taxol producing fungus *Gliocladium* sp.

7. References

1. Amos LA and Lowe J. 1999. How Taxol stabilises microtubule structure. *Chem. Biol*. **6** pp. 65-69.
2. Cardellina JH II. 1991. HPLC separation of taxol and cephalomannine. J. *Liq. Chromatogr*. 14:659-65.
3. Chun IK, Yong HK, Young JY and Chan UK. 1995. New taxol assay method using tubulin assembly stimulation. Biotechnology Techniques. 9, 885-890.
4. Cortes JE, Pazdur R. Docetaxel. J Clin Oncol 1995. 13 (10), 2643–55.
5. Gordon MC, Saul SA, Matthew S, Michael RG. 1993. The taxol supply crisis: New NCI policies for handling the large-scale production of novel natural product anticancer and anti-HIV agents. J. Natl. Pro. 56: 1657-1668.
6. Grothaus PG, TJG Raybould, GS Bignami, CB Lazo and JB Byrnes. 1993. An enzyme immunoassay for the determination of taxol and taxanes in *Taxus* sp tissues and human plasma. J Immunol Meth 158: 5–15.
7. Gueritte-Voegelein F, Senilh V, David B, Guenard D, Potier P. 1986**.** Chemical Studies of 10-deacetyl baccatin III. Hemisynthesis of Taxol Derivatives, *Tetrahedron, 42*, 4451.
8. Jordan MA, Wilson L. 1998. Microtubules and actin filaments: dynamic targets for cancer chemotherapy. Curr Opin Cell Biol; 10(1), 123–30.
9. Kerns E, Volk KJ, Hili SE and Lee MS. 1994. Profiling of taxanes in *Taxus* extracts using LC/MS and LC/MS/MS techniques. J. Nat. Prod. 57, 1391-1403.
10. Lowry OH, Rosebrough NJ, Farr AL and Randall RJ. 1951. Protein measurement with the Folin- Phenol reagents. J. Biol. Chem. 193, 265-275.
11. M. C. Wani, H. L. Taylor, M. E. Wall *et al*, Plant Antitumor Agents. VI. The Isolation and Structure of Taxol, a Novel Antileukemic and Antitumor Agent from Taxus breoifolia. *Journal of the American Chemical Society* **1** (1971) pp. 2325-2327.
12. Shelansky MLF, Gaskin F and Cantor CR. 1973. Proc. Natl acad. Sci, USA. 70, 765.

13. Theodoridis G, Laskaris G, De Jomg CF, Hofte ATP and Verpoorte R. 1998. Determination of paclitaxel & related diterpeniods in plant extracts by high performance liquid chromatography with U. V detection in high performance liquid chromatography- mass spectrometry. J Chrom A. 802, 297- 305.
14. Twentyman PR, Luscombe M. 1987. A study of some variables in a tetrazolium dye (MTT) based assay for cell growth and chemosensitivity. Br. J. Cancer. 56: 279-285.
15. Weingaster MD, Lockwood AH, Hwo S and Krischnee MW. 1975. Proc. Natl. Acad. Sci, USA 72, 1858-1862.

Chapter 5

Taxol-fluorescent conjugates: Synthesis and their applications.

1. Summary

Commercially available taxol was chemically derivatized (accordingly) to couple with FITC, Rhodamine and CdS nanoparticles. Two different strategies were applied to synthesize taxol with free amino group and with free carboxyl group. All the conjugates were purified by preparative TLC and HPLC. Further characterization was carried out by spectroscopic and fluoremetric techniques. Cytotoxicity of all the intermediate compounds and conjugates was determined by MTT assay. All the purified conjugates were immunologically analyzed and used further for different *in vivo* studies. Fluorescence properties and interactions of CdS-taxol conjugate with the J779 (Murine) cell line and HL 60 (leukemia) cell lines were exploited by fluorescent microscopy.

2. Introduction

Paclitaxel, better known by its trade name Taxol, has expressed cytotoxicity against an array of cancers (Longnecker et al, 1987; Rose, 1992; Suffiness 1993; Donehower and Rowinsky, 1993; Rowinsky et al, 1990). The mode of action is by freezing the microtubule bundles, which play an important role in cell division (Kumar, 1981). Apart from taxol, many taxol derivatives have been found to be more potent as mitotic binders (Jordon et al, 1998), increasing the scope to find more competitive taxanes to use in the treatment of cancer. A majority of these derivatives are intermediates from different methods of taxol chemical synthesis. A small part of them are synthesized to facilitate taxol coupling to different fluorescent moieties, proteins and nanomaterials.

These conjugates have guided us to understand the mechanisms involved in taxol mediated cytotoxicity and in the detection of taxol and taxanes in many biological samples (Morais, 2003; Bicamumpaka, 1998). In the present study, we have synthesized taxol conjugates with FITC, CdS nanoparticles and Rhodamine to study the interactions involved in the cell membrane and taxol.

3. Materials

Rhodamine, FITC, Glutaric anhydride, N, N'-Cardonyldiimidazole, t-butyldimethylsilyl chloride, Imidazole, Dimethyl formamide, Succinic anhydride, Dimethylamino-pyridine, 3-(4, 5-dimethylthiazol-2-yl)-2, 5-diphenyltetrazolium bromide, EDC and 1-Hydroxyl benzo-triazol were purchased from Sigma. Taxol immunoassay kit was purchased from Hawaii Biotech, Hawaii, USA. Standard taxol was purchased from M. P. BioMedicals, USA. TLC precoated plates, Silica G for TLC, Silica G for column chromatography and HPLC grade solvents from Merck. J779 and HL 60 cell lines from National Center for Cell Sciences (NCCS), Pune, India. Standard 25 cm^2 tissue culture flasks and 96 well microtiter plates from Nunc.

4. Methods

4.1. Synthesis of FITC-labeled Taxol

4.1.1. 2'-Glutaryl-taxol

2'-Glutaryl-taxol was prepared by reacting 10 mg of taxol, dissolved in 1.2 mL of pyridine, with 140 mg of Glutaric anhydride (Bicamumpaka and Page, 1998). The reaction was carried out at room temperature for about 2 hrs and was monitored on TLC using a mobile phase of Chloroform: Acetonitrile (7:3). After the incubation period, the solvent was evaporated under high vacuum and the residue was washed twice with water. The product obtained was precipitated using acetone and further purified by preparative TLC using the mobile phase Chloroform: Acetonitrile (7:3).

4.1.2. 2'-Glutaryl-hexanediamine-taxol

The recovered 2'-Glutaryl-taxol from the preparative TLC was solvent dried and dissolved in 100 µL of dry acetonitrile: 5 µmol of N, N'-Carbonyldiimidazole (CDI) was added and heated at 45 ^{0}C for about 15 min. After the reaction mixture comes to room temperature, 5 µmol of 1, 6-hexanediamine.2HCl was added and left at room temperature for 1 h. the reaction was monitored on TLC and purified as described above.

4.1.3. FITC-Taxol conjugate

FITC (2.5 mg) dissolved in methanol was added to a solution of 2'-glutaryl-hexanediamine-taxol dissolved in 0.1 M carbonate buffer/ methanol (50:50, v/v) pH 9. The mixture was allowed to react for 8 h in dark and purified as described above.

Absorbance of the conjugate was measured on Shimadzu PC 1601 Spectrophotometer. Spectrum was collected in the range of 200 to 600 nm. Fluorescence measurements were carried out using a Perkin Elmer LS-50B spectrofluorimeter, with slit width of 7 nm for both the monochromators and scan speed of 100 nm/min. Concentrations of all the derivatives were estimated by taxol immunoassay kit. The antitumor activity of the FITC-taxol conjugate was tested on different cell lines in comparison with taxol to check whether the structural modifications would affect its activities. Three mammalian cell lines A431 (Epidermal carcinoma), HL-60 (leukemia), MCF 7 (Breast cancer) were used for testing the antitumor activities. The cytotoxicity of the derivatized taxol was checked by MTT-assay as described earlier.

4.2. Synthesis of CdS–Taxol conjugate

2'-glutaryl-hexanediamine-taxol was synthesized as described above and was further used to conjugate with CdS nanoparticles. Biologically synthesized nanoparticles have a natural protein coat (Capping proteins); the carboxyl group present on these proteins was targeted to couple with the free amino group present on 2'-glutaryl-hexanediamine-taxol. Carboxyl group on the nanoparticles was estimated as described by Ansary et al, 2007.

2'-glutaryl-hexanediamine-taxol (400 µg) was dissolved in anhydrous DMF (300 µL), EDC (1.2 µmol, 1.1 eq) and 1- Hydroxyl benzo-triazol (HBT) (4 µmol, 2.2 eq) were added to it (Grothaus, 1993; Ansary et al, 2007). The reaction mixture was stirred at room temperature for about 1 h and a solution of CdS nanoparticles in phosphate buffer pH 7.2 was added to it. After stirring for 12 h at room temperature, the reaction mixture was concentrated under high vacuum and further purification of the 2'-glutaryl-hexanediamine-taxol-CdS conjugate was done by HPLC.

The conjugate from other chemical contaminants was purified by HPLC using Acetonitrile 5% - 95% on a C18 Symmetry column. The compounds eluted from the columns were detected at 227 nm and 348 nm using a dual wavelength detector. Fluorescence measurements were carried out using a Perkin Elmer LS-50B spectrofluorimeter, with slit width of 7 nm for both the monochromators and scan speed 100 nm/min. Concentrations of all the derivatives were estimated by taxol immunoassay kit. Cytotoxicity of the derivatized taxol and CdS-taxol conjugate was checked against THP1 (Acute monocyte leukemia) cell line by MTT assay as described elsewhere.

4.2.1. Fluorescent microscopy

To exploit the fluorescence properties of CdS nanoparticles after conjugating with taxol, *in vivo* microscopic studies were done. To 100 µL of J779 and HL 60 cell culture 10 µM CdS-taxol conjugate was added and the immediate changes occurring were observed with a Nikon ECLIPSE E200 fluorescent microscope and fluorescence optics via a 40X or a 100X magnification lens. Images were captured after every 5 minutes using Evolution VF camera.

4.3. Synthesis of Rhodamine-taxol conjugate

4.3.1. 2'-(t-Butyldimethylsilyl) Taxol

Taxol (10 mg) was treated with 50 µL (5 eq.) of a silylating solution consisting of 20.4 g t-butyldimethylsilyl chloride and 18.6 g imidazole dissolved in 18 mL of dry DMF (Magri and Kingston, 1988). After 12 h of incubation at room temperature, the reaction was worked out with the standard methods and the product was purified by preparative TLC (Chloroform: acetonitrile; 7:3).

4.3.2. 7-Succinlytaxol

To a solution of 2'-(t-butyldimethylsilyl) taxol (9.6 mg, 9.9 µ mol) in anhydrous N, N-dimethylformamide (DMF) (0.5 mL) succinic anhydride (5.9 mg, 59.0 µ mol, 6 eq) and dimethylamino-pyridine (1.2 mg, 9.9 µ mol, 1.0 eq) were added. After 18 h of stirring at 85 ^{0}C the reaction mixture was cooled and solvent dried. The dried compound obtained was dissolved in methylene chloride (CH_2Cl_2) (2 mL) and washed with 1 N HCl and brine. The CH_2Cl_2 layer was dried over anhydrous sodium sulphate and solvent was evaporated in vacuum. The residue was dissolved in THF 1 mL and treated with 2 M

triethylammonium hydrogen fluoride (5.5 µL, 11 µmol, 1.1 eq). After 6 h of stirring at room temperature, the solvent was evaporated and dissolved in CH_2Cl_2 and washed with 1 N HCl and brine. The CH_2Cl_2 layer was dried over sodium sulphate anhydrous and solvent evaporated. The product was purified by preparative TLC using chloroform: acetonitrile (7:3). Further purification was carried out using HPLC on C18 symmetry column with acetonitrile 5 %- 95 % gradient as the mobile phase (Mellado et al, 1984).

4.3.3. Rhodamine- taxol conjugate

To a 500-µL solution of 7-succinylpaclitaxel (2.5 mg, 2.6 µmol) in anhydrous methylene chloride, 2.2 mg of tetramethylrhodamine cadaverine (4.1 µ mol) and 2.1 mg of N,N'-dicyclohexylcarbodiimide (10 µmol) were added. 800 µL of distilled methlylene chloride was added and the reaction mixture was stirred for 20 h at room temperature under nitrogen stream. The reaction product was concentrated by micro rotary evaporation, redissolved in methanol and purified by HPLC using 5 to 95% gradient of acetonitrile (Morais, 2003).

Further the absorbance of the HPLC purified conjugate was measured by Shimadzu PC 1601 UV-Vis spectrophotometer. Fluorescence measurements were carried out using a Perkin Elmer LS-50B spectrofluorimeter, with slit width of 7 nm for both the monochromators and a scan speed of 100 nm/min. Concentrations of all the derivatives were estimated by taxol immunoassay kit. Cytotoxicity of the derivatized taxol and rhodamine-taxol conjugate was checked by MTT-assay as described elsewhere.

4.4. Cytotoxicity of taxol fluorescent conjugate intermediates

Cytotoxicity of the intermediates such as 2'-glutaryl taxol, 7-succinyl taxol, 1, 6-hexanediamine taxol was checked against THP1 cell line by MTT assay as described elsewhere.

5. Results

5.1. Synthesis of FITC- Taxol conjugate

All the reactions were monitored on TLC, UV and by detecting fluorescence. The purified conjugate showed absorbance at 227 nm attributing to taxol absorbance and at

488 nm attributing to FITC absorbance (FIG 1). Shift in the λ max of FITC probably indicates the coupling of it with taxol as shown in Fig 1. Coupled FITC excited at 488 nm showed an emission spectrum with λ max at 560 nm (FIG 2).

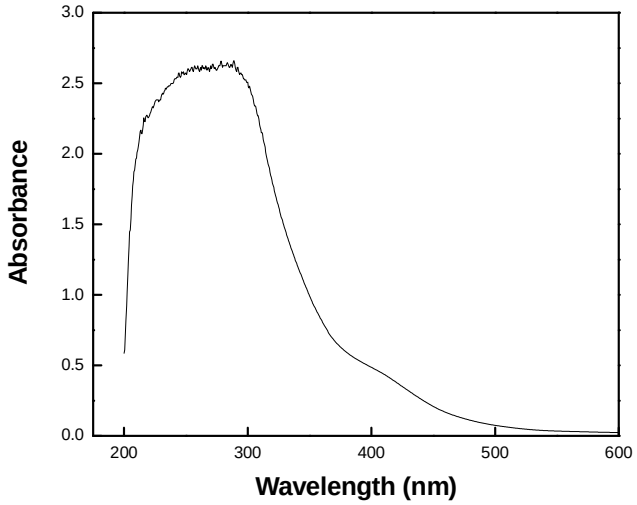

FIG 1: Absorbance spectrum of FITC-taxol conjugate showing absorbance maxima at 227 nm (taxol absorbance maxima) and a shoulder at 430 nm (FITC absorbance maxima).

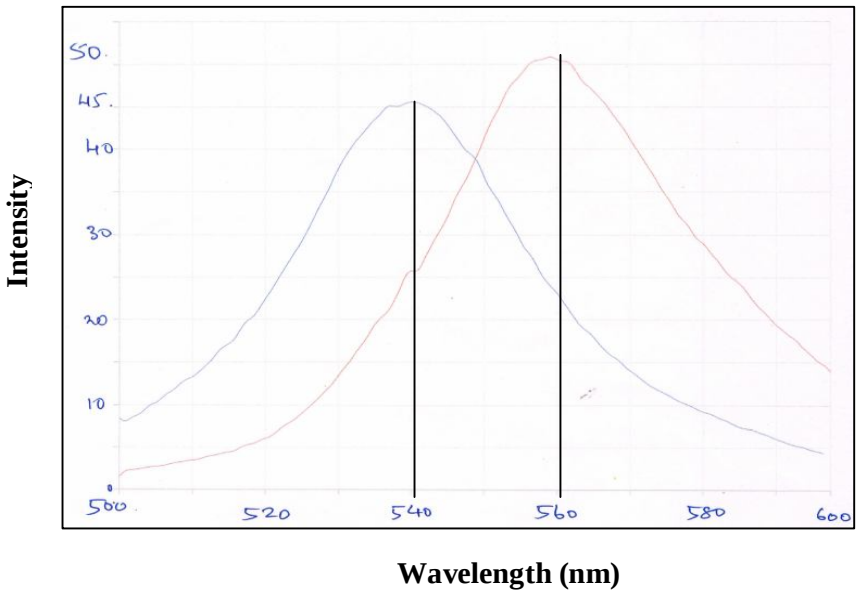

FIG 2: Fluorescence spectrum of FITC blank (Blue) and FITC coupled to taxol (Red). Shift in the λ max of FITC indicates the coupling.

Cytotoxicity of the derivatized compounds was checked by MTT assay to confirm its potential as a drug in spite of its structural modifications. The FITC-conjugate showed higher activity in all the three cell lines used for the test in comparison with standard taxol. Approximately 2 μM samples were used to test the cytotoxicity; higher concentrations could not show proper activity as the color of FITC was interfering. In A431 (epidermal carcinoma) cell line, 42.49 % inhibition was seen, in HL-60 (leukemia), 40.43 % inhibition and in MCF-7 (Breast cancer) 50.74 % inhibition was seen. In comparison to taxol, FITC-taxol conjugate showed higher cell cytotoxicity as shown in FIG 3 (A, B and C). FITC-taxol conjugate thus synthesized could not be used for further *in vivo* studies because of signal spillover seen when used along with GFP.

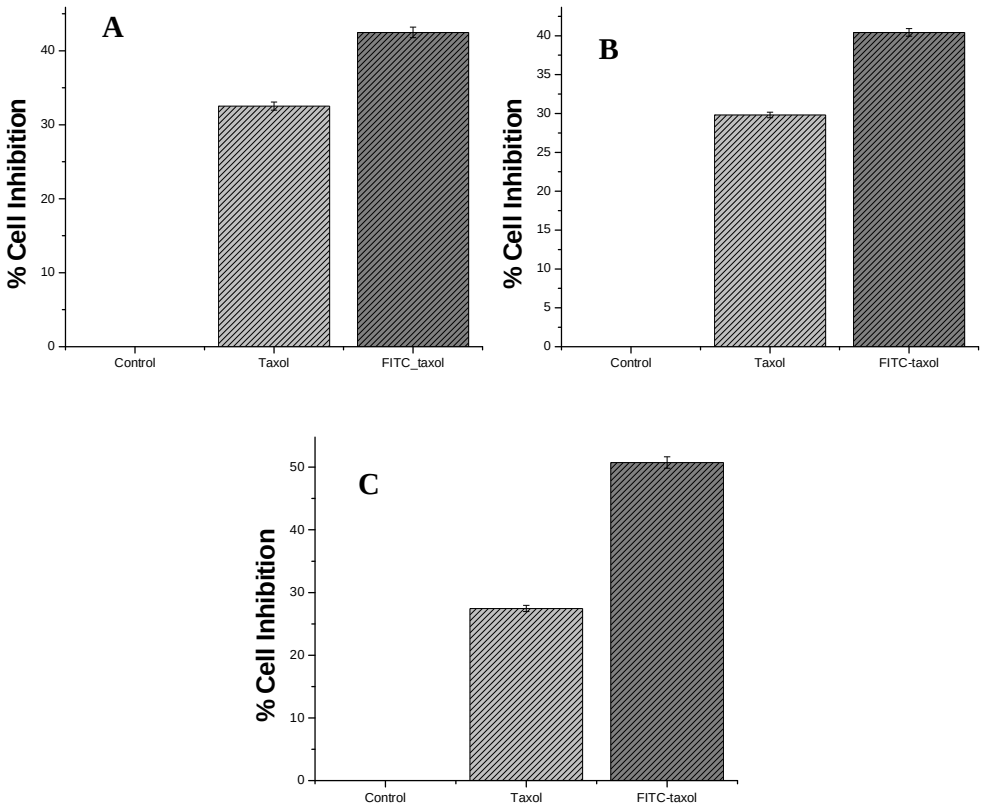

FIG 3: Cytotoxicity of FITC-Taxol in comparison to Taxol on Epidermal carcinoma cell line: A431 (A), Leukemia cell line: HL-60 (B), Breast cancer: MCF-7 (C) with Standard errors ±1.7 %, ±1.2 % and ±1.8 % respectively. On all the cell lines FITC-taxol conjugate showed higher cytotoxicity than plain taxol. The structural modifications might be attributing to the higher activity.

5.2. Synthesis of CdS-Taxol conjugate

The HPLC profile showed three distinct peaks at 227 nm and one peak at 348 nm (FIG 4). The peak having absorbance at 227 nm and 348 nm was collected and further analyzed. Fluorescence of the purified conjugate was measured by exciting at 350 nm. Emission spectra of the conjugate showed λ max at 398 nm as shown in FIG 5.

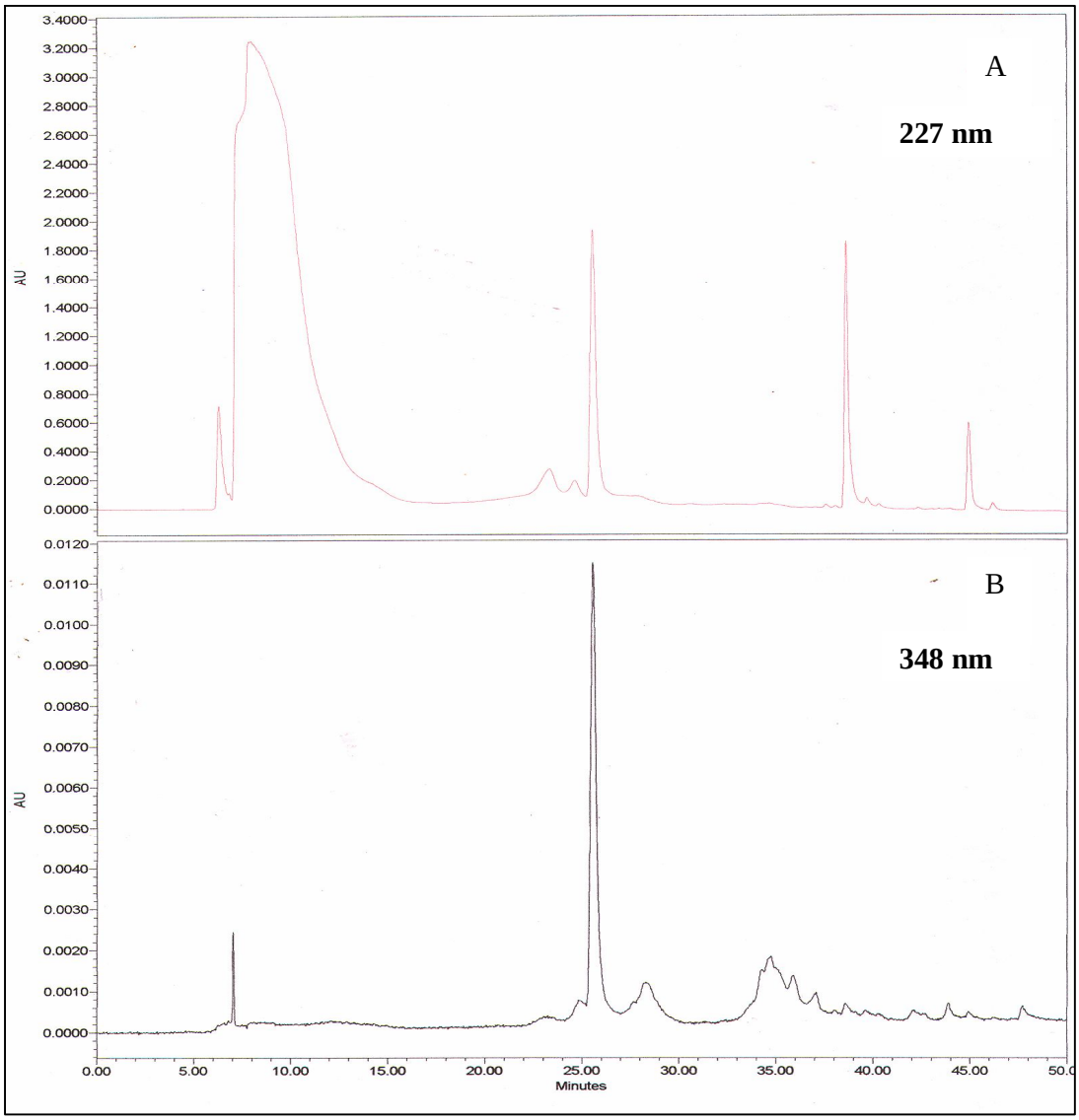

FIG 4: HPLC profile of the reaction mixture visualized at two different wavelengths A) 227nm for taxol detection and B) 348nm to detect CdS nanoparticles.

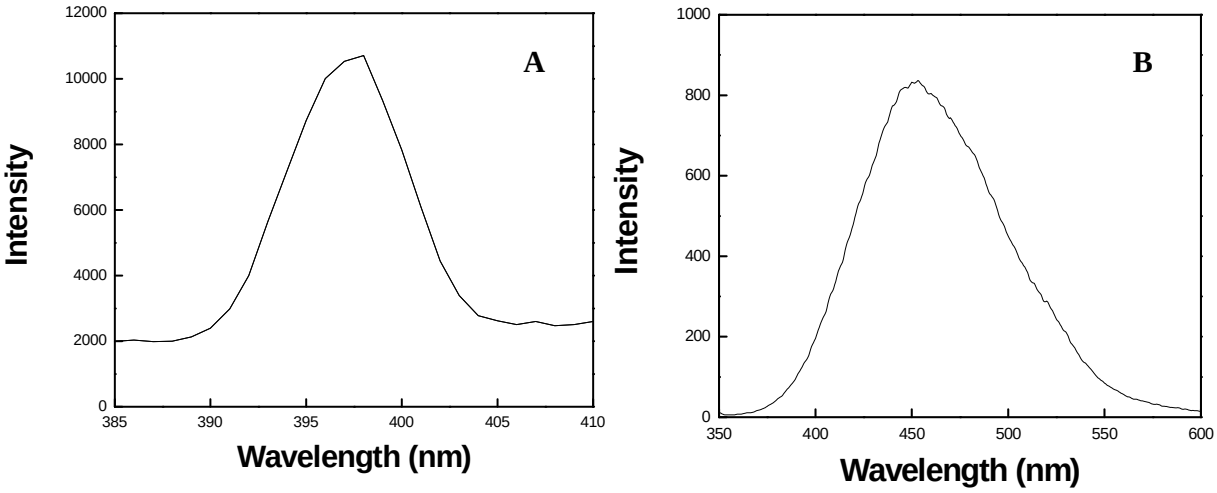

FIG 5: A) Fluorescence spectrum of purified CdS-taxol conjugate and B) emission spectrum of plain CdS.

CdS- taxol conjugate showed cytotoxicity against THP1 cell line which was higher than the plain taxol (FIG 6). This might account for CdS cytotoxicity also.

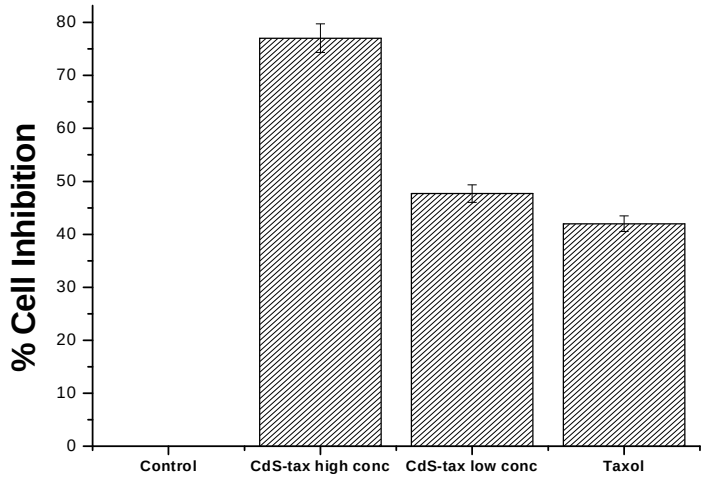

FIG 6: Bar diagram showing cytotoxicity of Taxol conjugated CdS nanoparticles against THP1 (Acute monocyte leukemia) cell line. Control cells showing no inhibition, while cells treated with high (9.6 μM) and low (3.2 μM) concentrations of CdS conjugate show up to 76 % and 48 % inhibition. Standard error ±3.5 %.

5.2.1. Fluorescence microscopy

HL-60 and J779 cells after addition of CdS-taxol conjugate did not show any immediate change on the morphology. However, rounding of cell was seen in HL-60 cells after an incubation time of 1 h. Accumulation and reasonable intensities of CdS signal started only after 15 min of incubation. Signal strength increased with increase in time; after about 30 min of incubation, saturation was observed. Fluorescence was found to be homogenous throughout the cell surface suggesting that the conjugate is interacting with some moiety on cell membrane. Fluorescence signal was diffused and did not appear as bright spots. In comparison to J779 cell line, HL-60 showed good resolution of fluorescence on the cell surface. This probably is because of smaller surface area of J779 cell line. The intensities were good enough to locate the cell under focus (FIG 7).

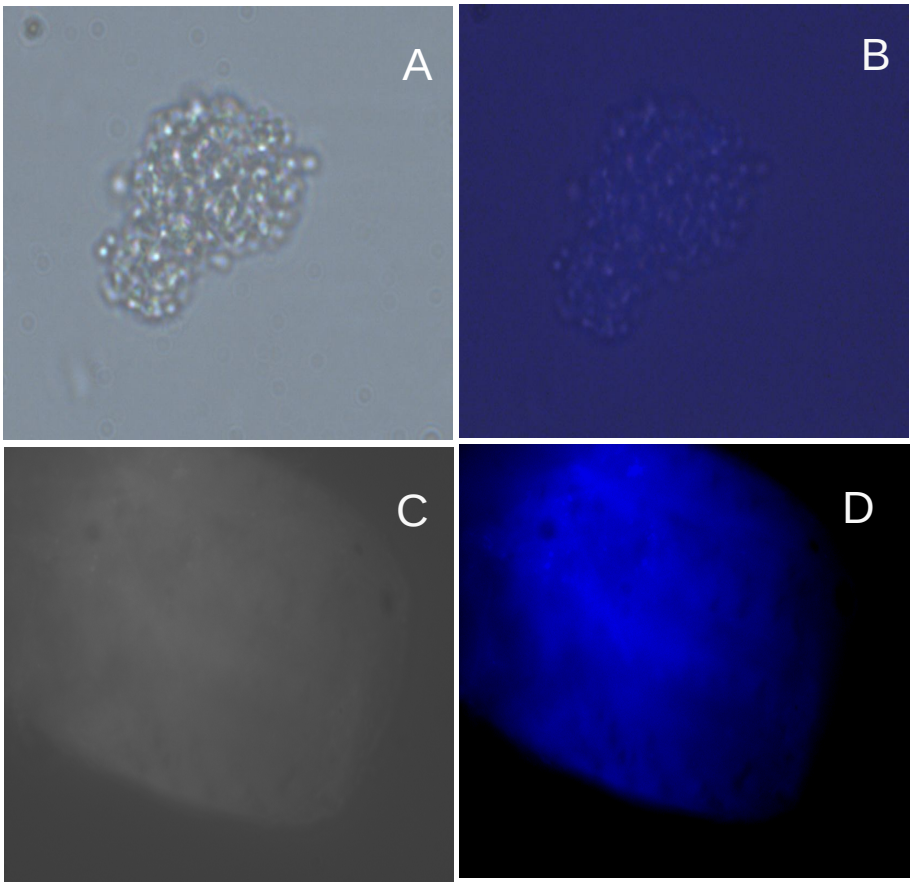

FIG 7: Fluorescence micrograph of THP1 (A and B) and HeLa cells (C and D) showing CdS- Taxol conjugates distribution on the cell membrane. A& C Phase contrast micrographs and B& D micrographs showing fluorescence of CdS-taxol conjugate on THP1 and HeLa cells.

5.3. Synthesis of Rhodamine-taxol conjugate

HPLC analysis of the crude compound showed 3 peaks at 227 nm and one major peak at 540 nm. The peak which showed intensities at both the wave lengths was collected and further used for the analysis. Absorbance spectrum of rhodamine-taxol conjugate showed absorbance maxima of both the compounds. Peak at 227 nm attributed to taxol λ max and peak at 550 nm attributed to rhodamine λ max as seen in FIG 8. Conjugate when excited at 540 nm showed an emission spectrum with λ max at 590 nm (FIG 9). Rhodamine-taxol conjugate showed similar cytotoxic activities as that of the plain taxol.

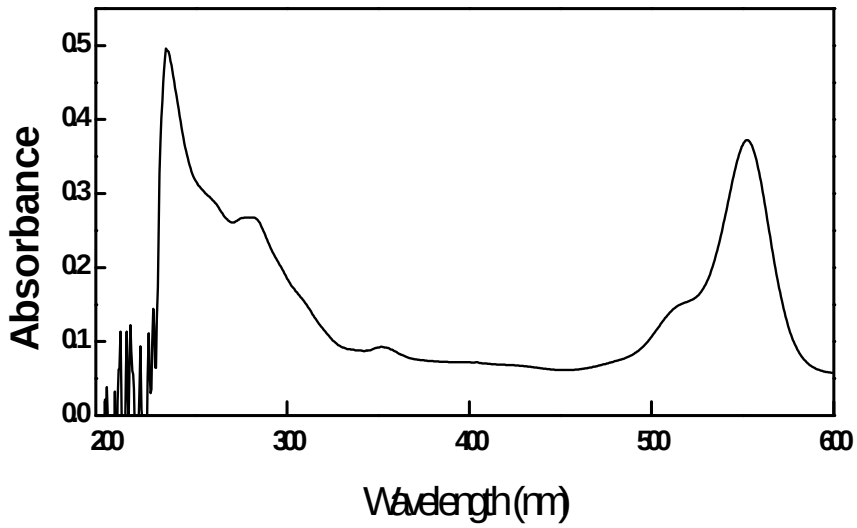

FIG 8: Absorbance spectrum of Rhodamine-taxol conjugate showing absorbance maxima at 227 nm (taxol absorbance maxima) and at 550 nm (rhodamine absorbance maxima).

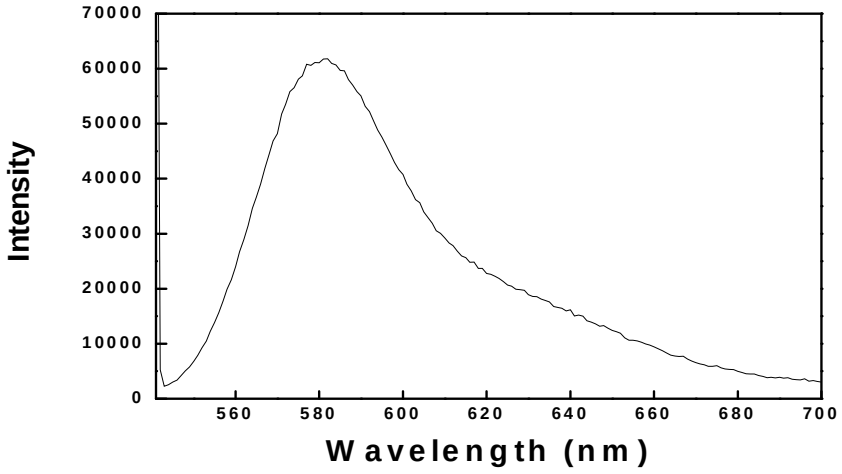

FIG 9: Fluorescence spectrum of purified Rhodamine-taxol conjugate

5.4. Cytotoxicity of taxol fluorescent conjugate intermediates

Taxol fluorescent conjugate intermediates showed cytotoxicity greater than plain taxol. Of all the derivatives 2'-glutaryl taxol showed higher cytotoxicity; 49 % and 77 % even at concentrations as less than 78 nM and 156 nM, respectively. Glutaryl hexanediamine taxol showed 50% and 77% cytotoxicity with 5.25 µM and 10.5 µM concentrations, respectively. Even 7-succinyl taxol showed higher Cytotoxicity; 54 % and 75 % with 2.25 µM and 4.5 µM concentrations, (FIG 10) respectively.

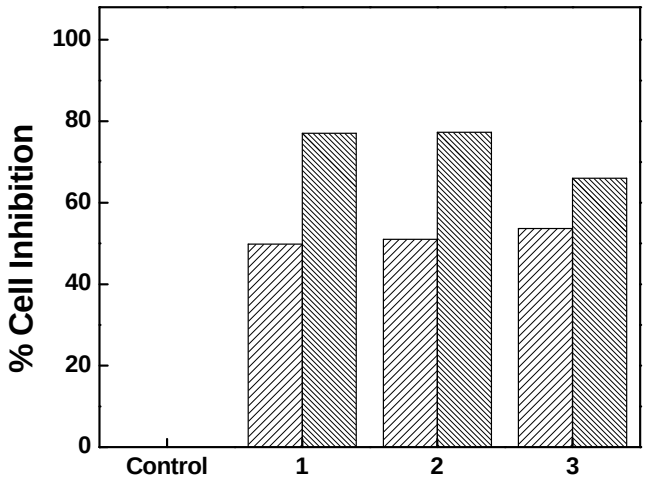

FIG 10: Cytotoxicity of taxol fluorescent intermediates against THP1 cell line 1) 2'-glutaryl taxol (78 and 156 nM), 2) glutaryl hexanediamine taxol (5.25 and 10.5 µM) and 3) 7-succinyl taxol (2.25 and 4.5 µM).

6. Discussion

The aim of the study, to synthesize fluorescent taxol conjugates using different fluorescent compounds and using CdS nanoparticles was achieved. Taxol fluorescent conjugates were synthesized to study 1) the interactions of these taxol conjugates with cell membrane moieties, 2) to explore the fluorescent properties of CdS- taxol conjugate and 3) to study the caveolin dynamics. Taxol was derivatized chemically to 2'-glutaryl hexanediamine taxol and 7-succinyl taxol with a free amino and carboxyl group respectively. These modifications have eased the mechanism of coupling fluorescent molecules to taxol.

Ideally none of the fluorescent molecules should give any toxic effect on the samples treated as they are used for many *in vitro* and *in vivo* studies. In our studies, the FITC and Rhodamine dyes used are conventionally used for many cell based studies and it has been observed that both of them do not have any toxic effect on cells.

FITC-taxol conjugate purification by HPLC method resulted in a good recovery of the conjugate by this method. Method described by Bicamumpaka, (1998) is tedious and recovery is poor. UV-Vis absorbance spectrum reveals a hump at 430 nm attributing to FITC absorbance. Nevertheless, it is not similar to that of plain FITC which shows absorbance maxima at 488 nm. The shift in the λ max might be because of coupling with the taxol moiety which is usually seen in many cases. Emission spectrum obtained when the conjugate was excited at 488 nm shows that there is a shift in the λ max, this also might be a reason as described above. However, the spectrum was broad which was same with plain FITC as well. Higher cytotoxicity shown by conjugate than plain taxol could be because of the increased hydrophilicity of the conjugate. Plain taxol is highly hydrophobic but when it is modified with glutaric anhydride, the resulting glutaryl taxol is hydrophilic because of the free carboxylic group conferred on it. Further, on treatment with hexanediamine, the product glutaryl-hexanediamine taxol gets an additional amino group which also contributes to the hydrophilic nature. These derivatives are more potent as cytotoxic molecules than the plain taxol. FITC-taxol conjugate thus synthesized could not be used for further *in vivo* studies because of its spectroscopic disadvantages to use along with GFP.

Synthesis of CdS-taxol conjugates and its fluorescence studies revealed the possible usage of CdS nanoparticles as fluorescent labels. Taxol was successfully derivatized to hexanediamine taxol and the free amino group of it was targeted to couple with the carboxyl group of capping protein present on CdS nanoparticles (Ansary et al, 2007). CdS-taxol conjugate on HPLC showed absorbance at both the wave lengths attributing to taxol and CdS absorbance maxima. The fluorescence spectrum of the conjugate showed a very sharp emission spectrum with λ max at 398 nm. CdS-taxol conjugate showed an increase in cytotoxicity in comparison with that of plain taxol. However, this could be because of toxicity of CdS nanoparticle or modifications of taxol molecule. Fluorescent microscopic studies reveal that CdS nanoparticles after conjugation with

taxol also show similar fluorescent properties as that of plain CdS. The conjugate starts accumulating on the cell surface after about 15 minutes and intensifies by 30 minutes. Fluorescence appears homogenous through out the cell surface and does not accumulate on non cellular area. This indicates the probable interaction between conjugate and some moiety on cell membrane. These results do support our studies on taxol and its interactions with caveolin (Neesar et al, 2007), a marker protein on cell membrane (Pelkmans et al, 2005). The fluorescence signals were diffused and did not appear as bright spots. This could be because of the size of nanoparticles which may not be the size of quantum dots used for imaging or due to inefficient light source used. However, our studies revealed that biologically synthesized nanoparticles can not only be used for fluorescence imaging but can also be easily coupled with drugs. These studies also infer that CdS nanoparticles indeed can be used, in addition to being used as an anticancerous drug, as anticancerous agents (Li et al, 2007).

Coupling of taxol with rhodamine was successfully carried out by derivatizing taxol to 7-succinyl taxol. Further absorbance spectrum of the conjugate shows two peaks at wave length 227 nm and 550 nm attributing to λ max of taxol and rhodamine, respectively. Fluorescence spectrum of the conjugate showed emission spectrum with a smooth and sharp peak with λ max at 580 nm (Sheikh et al, 2000). Cytotoxicity of the conjugate did not increase as was seen in case of other conjugates in comparison with plain taxol. Further, this compound was used for *in vivo* studies to understand taxol interactions with that of caveolin on cell membrane.

7. References

1. Ansary AA, Anil SK, Krishnasastry MV, Majid KA, Sulabha KK, Absar A and Khan MI. 2007. CdS quantum dots: Enzyme mediated in vitro synthesis, characterization and conjugation with plant lectins. J. Biomed Nano. 3, 406-413.
2. Bicamumpaha C, Page M. 1998. Development of a fluorescence polarization immunoassay (FPIA) for the quantitative determination of paclitaxel. J. Immun. Meth. 212, 1-7.

3. Deutsch HM, Glinski JA, Hernandez M, Haugwitz RD, Narayan VL, Suffness M, Zalkow LH, 1989. Synthesis of congeners and prodrugs. 3. Water-soluble prodrugs of taxol with potent antitumor activity. J. Med. Chem. 32, 788-792.
4. Donehower RC, Rowinsky EK. 1993. An overview of experience with taxol (Paclitaxel) in USA. Cancer Tret. Rev. 19 (Supply. C), 63-78.
5. Feldkamp CS, Smith SW. 1987. Practical guide to immunoassay method evaluation. In: Chan DW, Prelstein MT (Eds.), Immunoassay: A practical guide. Academic press, New York.
6. Grothaus GP, Raybould TJG, Bignami SG, Carolyn BL and Byrnes JB. 1993. An enzyme immunoassay for the determination of taxol and taxanes in *Taxus* sp. tissues and human plasma. J. Immun. Meth. 158, 5-15.
7. Jordan MA, Wilson L. 1998. Microtubules and actin filaments: dynamic targets for cancer chemotherapy. Curr Opin Cell Biol 10(1), 123–30.
8. Kumar N. 1981. taxol induced polymerization of purified tubulin, J. Biol. Chem. 256, 10435-10441.
9. Li J, Wu C, Dai Y, Zhang R, Wang Xuemei, Fu D, and Chen B. 2007. Doxorubicin-CdS nanoparticles: A potential anticancer agent for enhancing the drug uptake of cancer cells.
10. Longnecker SM, Donehower RC, Cater AE, Chen TL, Brundrett RB, Grochow LB, Ettinger DS, Colvin M. 1987. High-performance liquid chromatographic assay for taxol in human plasma and urine and pharmacokinetics in a phase I trial. Cancer Treat. Rep. 71, 53.
11. Magri NF and Kingston DGI. 1998. Modified taxols, 4. Synthesis and biological activity of taxols modified in the sidechain. J. Natl. Prod, 51, 298.
12. Mellado W, Magri NF, Kingston DGI, Garcia AR, Orr GA and Horwitz SB. 1984. Preparation and biological activity of taxol acetates. Biochem. Biophys. Res. Commun. 124, 329.
13. Morais S, O'Malley S, Chen W and Mulchandani A. 2003. A tubulin- based fluorescent polarization assay for paclitaxel. Analytical Biochem. 321. 44-49.
14. Neesar A, Sreekanth D, Saumya SS, Amita S, Absar A, Islam KM and Krishnasastry VM. 2007. Side chains of Taxol and 10-DeacetylbaccatinIII induce distinct changes in the 'kiss and Run' dynamics of caveolae. FEBS Letters.

15. Pelkmans, L. and Zerial, M. 2005. Kinase-regulated quantal assemblies and kiss-and-run recycling of caveolae. Nature. 436, 128-133.
16. Rose CW. 1992. Taxol; a review of its preclinical in vivo antitumor activity. Anti-cancer drugs 3, 311-321.
17. Rowinsky EK, Cazenave LA, Donehower RC. 1990. Taxol: a novel investigational antimicrotubule agent. J. Natl. Can. Inst. 82, 1247- 1259.
18. Sheikh SH, Abela BA and Mulchandani A. 2000. Development of a fluorescence immunoassay for measurement of paclitaxel in human plasma. Analytical Biochem. 283, 33-38.
19. Suffiness M. 1993. Taxol: from discovery to therapeutic use. In: Bristol JA, (Ed), Annual reports in Medicinal Chemistry, Vol: 28, Michigan, USA.

Chapter 6

Effect of Rhodamine-taxol conjugate on Caveolin dynamics

1. Summary

In the present study, Rhodamine- taxol conjugate treatment resulted in a transient recruitment of Caveolin-1 to the cell surface followed by internalization. Conjugate accumulation on the cell surface was predominantly seen in cell lines expressing Caveolin-1-GFP such as HeLa and A431, while cells such as 293T which have very less expression of Caveolin-1 did not show any sign of accumulation. Further these interactions were supported by localization studies of the conjugate and Caveolin-1-GFP by confocal microscopy. Localization was observed as early as 5 minutes and reached saturation by 9 h. These observations thus infer that there is some interaction between taxol and Caveolin-1.

2. Introduction

Taxol, a diterpene, first isolated from *Taxus brevifolia*, is a promising drug against various human cancers (Magri and Kingston, 1998). In a recent report it is shown that taxol induces expression of Caveolin-1, a marker protein of the caveolae in MCF-7 cells and also that the Caveolin-1 phosphorylation at tyrosine-14 is necessary to enhance taxol mediated cytotoxicity (Shajahan et al, 2007). With respect to earlier studies, taxol's mode of action involves binding to microtubules, stabilizing them further and inducing apoptosis (Manfredi and Horwitz, 1984), but its role in enhancing Caveolin-1 expression in not clear. Moreover, Caveolin-1 is a dynamic entity, as the caveolae undergo a continuous cycle of 'kiss and run' dynamics with the plasma membrane (Pelkmans and Zerial, 2005). Hence in this study, we examined the dynamics of caveolae, their distribution and change in dynamics of taxol vis-àvis cytotoxicity in HeLa cells expressing Caveolin-1-GFP when treated with Rhodamine-taxol conjugate by total internal reflection fluorescence microscopy (TIRFM) and also compared the accumulation of taxol fluorescent conjugate signal on cells with low expression of Caveolin-1. Most importantly to observe any interaction between taxol and Caveolin-1 confocal study was done to see localization.

3. Materials

HeLa cells were cultured in DMEM medium supplemented with 10 % (v/v) fetal calf serum and penicillin and streptomycin. Rhodamine-taxol conjugate treatment was done at 60-70 % cell confluency. HeLa cells were transfected with Caveolin-1-GFP construct (gifted by Dr. A. Helenius) after seeding them at a density of $2x10^5$ cells/ml in 35mm culture dish with fuGENE 6 kit using 1 µg of plasmid at 6:1 reagent to plasmid ratio. After 6 h of transfection, the medium was replaced with complete medium.

4. Methods

To study the interactions, two taxol conjugates having FITC and Rhodamine as labels were synthesized. Preliminary studies to find the compatibility between taxol conjugate signals and GFP signals using TIRFM system filters was done. These studies showed that FITC-taxol conjugate could not be used as it is not suitable for TIRF single spot study. Thus, further studies were done using Rhodamine-Taxol conjugate (RTc).

4.1. TIRFM (Total Internal Reflection Fluorescence Microscopy)

4.1.1. Studies on HeLa with and without GFP transfection

HeLa cells, grown on coverslips, were mounted in an Atto chamber containing DMEM medium without phenol red and 1 mg/ml BSA. The total internal reflection angle was adjusted to observe the dynamics of Rhodamine-taxol in regions of the cells in an Olympus IX-81 microscope equipped with a 532 nm laser line. All recordings were performed with 100X-TIRFM, 1.45NA, objective with Cascade 512B camera at 10 hertz at 10 ms exposure time for about 90 frames for each recording. The data were recorded before treatment and after the indicated drug treatment. All the videos examined were recorded with 25 frames per second. Rhodamine-taxol concentrations used for the study were ranging from 1-10 nM. Various concentrations were used to study the change in the dynamics. In contrary to non transfected cells, Caveolin-1-GFP dynamics and Rhodamine-taxol signals were recorded simultaneous using respective filters in transfected cells.

4.1.2. Studies on A431 and 293T cell lines

Dynamics of RTc were recorded on both the cell lines under the same conditions as described above. None of these cell lines were transfected with Caveolin-1-GFP as these studies would act as control systems. However, recordings on 239T cell lines were taken even after 3 h while in case of A431 they were taken up to 2 h.

4.2. Confocal microscopy

HeLa cells, after 12 h of transfection, were treated with RTc for a given time followed by washing with PBS. Cells were then fixed with 3.7 % paraformaldehyde (pH 7.4) in PBS, pH 7.4, for 10 min and permeabilized with 0.1 % Triton X-100 for 20 min. Non-specific binding was blocked by pretreatment with 3 % BSA in PBS for 30 min. RTc concentrations used were 2-7 nM. The cells were then visualized in Zeiss LSM 510 Confocal microscope. Fluorescence emission was detected in 0.5 μm optical sections.

4.3. MTT assay

To assay the viability of cell after treatment with RTc, HeLa cells were seeded at a density of $5x10^3$ cells per well in a 96 well plate and treated with various concentrations of RTc for 48 h in triplicates. At the end of the treatment, the media was removed and 50 μl of MTT (1 mg/ml) in DMEM (without phenol red) was added to each well and incubated for another 4 h at 37 ^{0}C. Formazan crystals were solublized in 50 μl of iso-propanol with shaking at room temperature for 10 min. Absorbance was measured at 570 nm using 630 nm filter. Absorbance given by cells treated with DMSO was taken as 100 % viability.

5. Results

The aim of the present work is to understand the role and dynamics of Taxol with respect to the dynamics of Caveolin-1 to examine any possible direct interactions involved between the two. Cytotoxicity against HeLa and A431 cell line was found to be similar with the treatment of unlabeled taxol and RTc.

5.1. TIRFM

5.1.1. HeLa cells without GFP transfection

RTc (at concentration 2-7 nM) signal appeared on the cell surface within 5 minutes and the intensity increased with the increase in time. Fluorescence appeared as single bright spots with dynamic movement throughout the membrane. The tiny bright fluorescence spots firstly formed clusters and diffused into membrane with increase in time. Fluorescence appeared to be unevenly distributed i.e. spots did not appear evenly spread throughout the membrane, instead, were seen dense at the periphery and sparse at the center. After about 30 minutes the fluorescence reached saturation and these spots started appearing diffused. Cell membrane and morphology did not change with treatment at these concentrations (1 nM and 2.5 nM) of RTc, but when high concentration (7 nM) was used membrane appeared damaged and fluorescence appeared immediately on the cell surface (FIG 1).

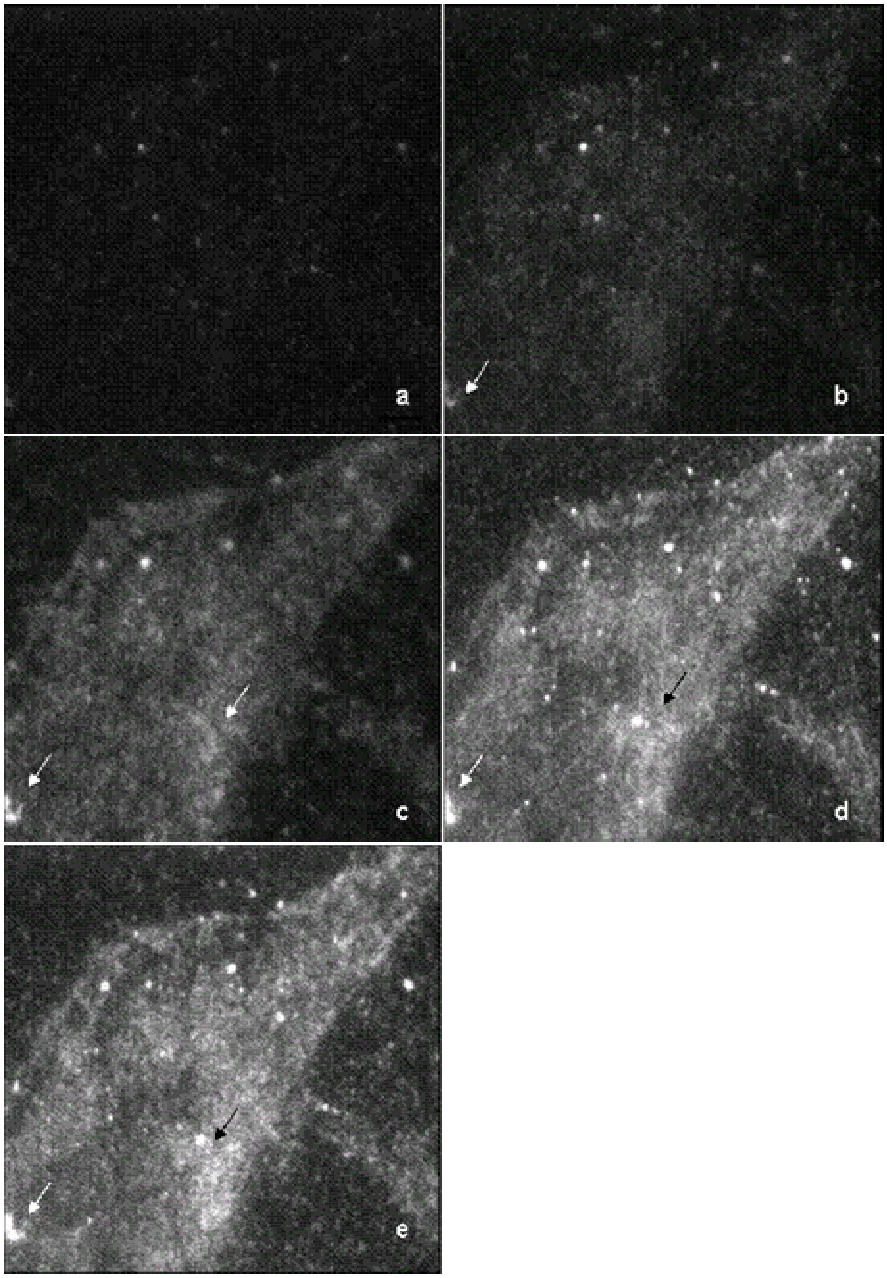

FIG 1: TIRFM images of Rhodamine-taxol conjugate on HeLa cells. Still frame images from videos showing the distribution pattern at 2.5 nM concentration. Arrows showing cluster formation which was seen after treatment with RTc. a) Immediately after the addition of Rhodamine- taxol, b) after 5 min, c) after 10 min, d) after 20 min and e) after 30 min of addition.

5.1.2. HeLa cells with GFP transfection

HeLa cells after Caveolin-1-GFP transfection showed very high and moderate expression of Caveolin-1-GFP. For TIRFM studies, moderately expressed Caveolin-1-GFP cell which showed distinct bright spots with dynamic movement were selected. Fluorescence of Caveolin-1-GFP and Rhodamine-taxol conjugate was recorded simultaneously using the respective filters. Signal spillage and leaking was fool proofed by observing GFP signal using Rhodamine filter and vice versa. With the addition of RTc, Caveolin-1-GFP cell surface recruitment was clearly seen. Kiss and run dynamics of Caveolin-1-GFP was observed. New cluster of Caveolin-1-GFP appeared with progression of time which was not seen before treatment. The other most important observation was the velocity with which the spots appeared to move through out the membrane after the treatment, which was very less before treatment. After about 30 minutes the Caveolin-1-GFP withdrawal from the cell surface was seen (FIG 2).

RTc fluorescence on the other hand also showed similar dynamics in terms of amount of signal appearing on the cell surface and the time taken to appear. RTc distribution appeared exactly as that of the Caveolin-1-GFP confining its density towards the periphery of the cell membrane or to some areas on the surface. Wherever clusters of Caveolin-1-GFP appeared clusters of RTc were also seen indicating the possible interactions involved between the two. The signal strength appeared to increase and then diffuse with increase in time. Saturation in the fluorescence was observed by 1 h after which diffusion of the signal was seen (FIG 2).

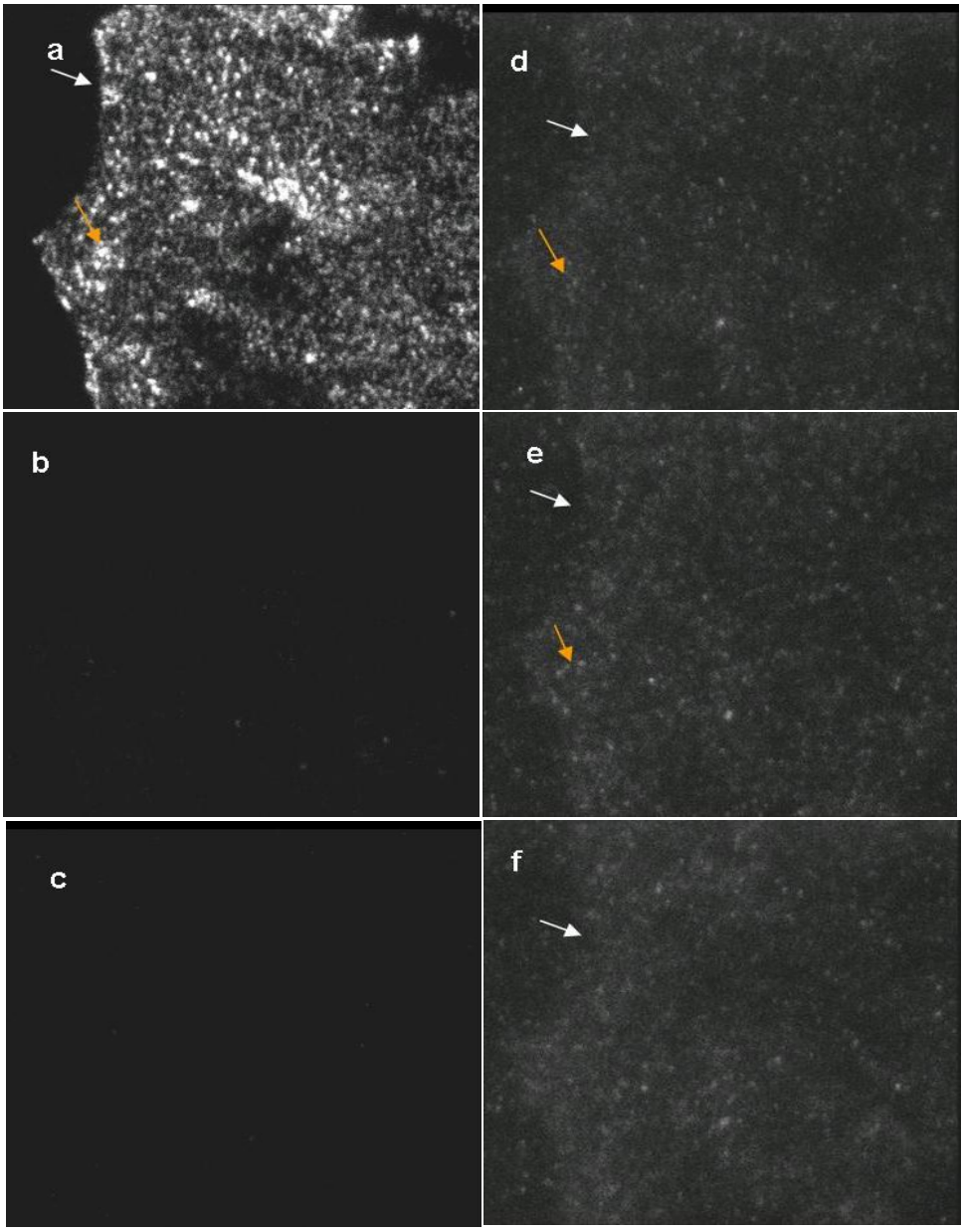

FIG 2: TIRFM images showing distribution of Rhodamine-taxol conjugate on the HeLa cell surface (Arrows in white). Clusters formation was seen at many points on the cell membrane (shown by orange arrows). a) Caveolin-1-GFP distribution on HeLa cell. b) Immediately after the addition of Rhodamine-taxol. c) Rhodamine-taxol signal under GFP filter. d), e) & f) Rhodamine-taxol conjugate localization at 5, 15 and 30 min.

5.1.3. A431 and 293T cell line

Caveolin-1-GFP and Rhodamine-taxol conjugate dynamics appeared very similar with A431 cell, as observed incase of HeLa cells. But the dynamics observed on 293T cell line were very interesting. With the treatment of 1 nM RTc the cells did not show any fluorescence spots on the surface even after 20 minutes (FIG 3) and with the treatment of 2.5 nM concentrations RTc signal was seen but was not confined to the cellular area (FIG 4). Indeed the RTc signal appeared diffused throughout the focused area without any discrimination between cellular and non cellular area. Even when treated with high concentrations such as 7 nM there was no significant localization of RTc was seen on the cell surface (FIG 5), while HeLa cells when treated with same concentrations showed an immediate localization of RTc on cell surface.

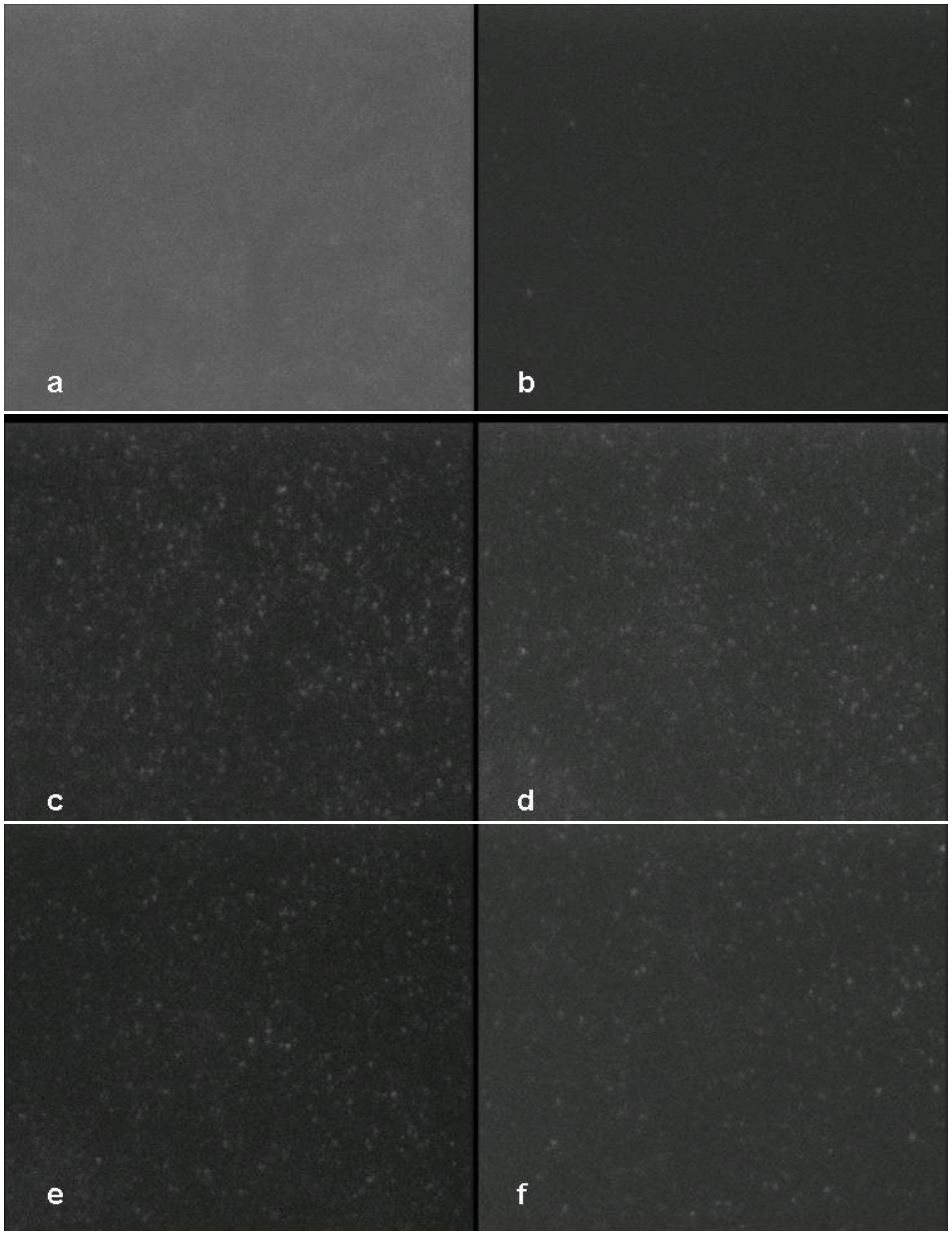

FIG 3: TIRFM images showing even distribution of Rhodamine-taxol conjugate through out the cover slip not being confined to cellular area. This did not increase with increase in time. a) Phase contrast micrograph of 293T cells, b) Before addition of RT conjugate (1nM), c) Cells after addition at zero minutes, d), e) & f) after addition, at 10 min, 20 min and 2 h respectively.

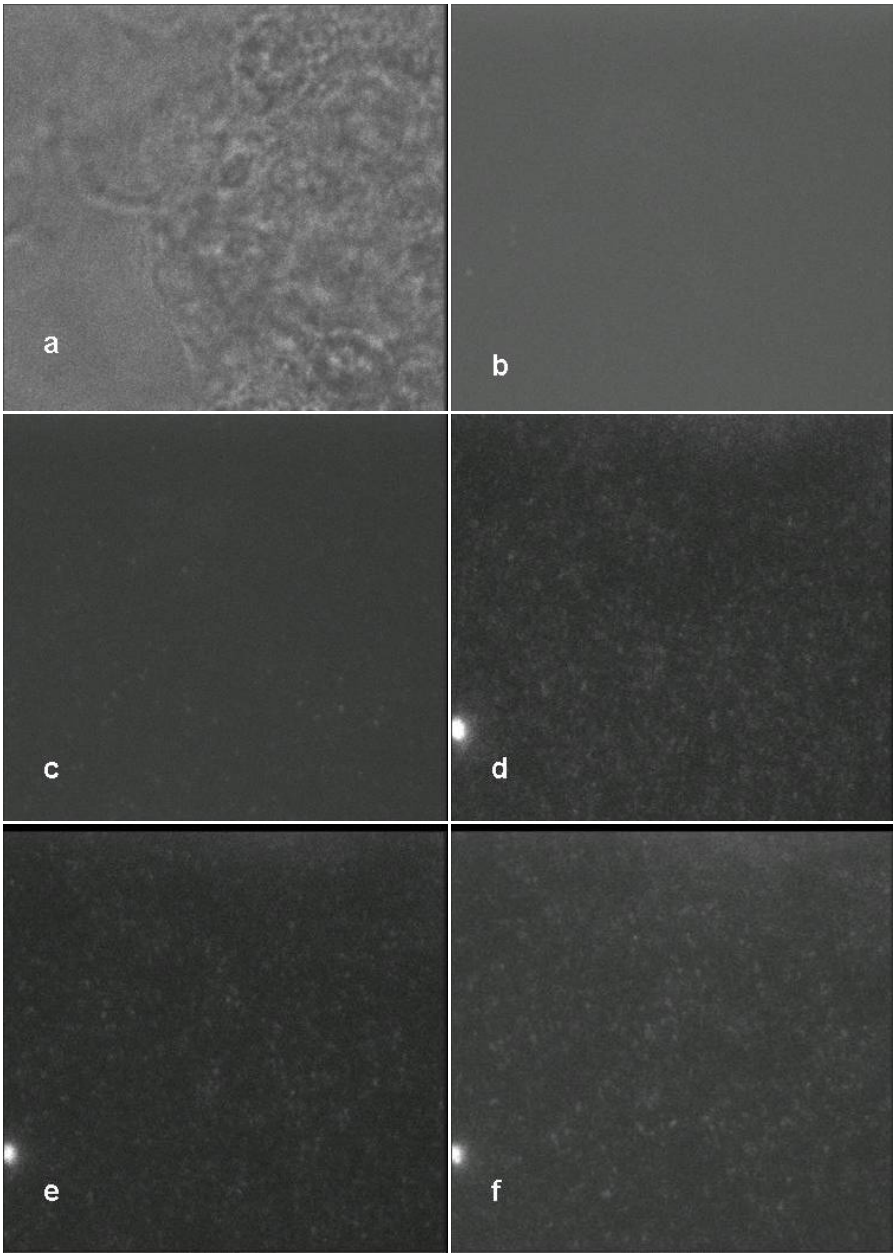

FIG 4: TIRFM images showing 293T cells with no prominent localization of Rhodamine-taxol conjugate on cell membrane with concentration (2.5 nM). a) Phase contrast micrograph, b) Before addition of Rhodamine-taxol conjugate, c), d), e), & f) at 10 min, 20 min, 1 h and 2 h after addition.

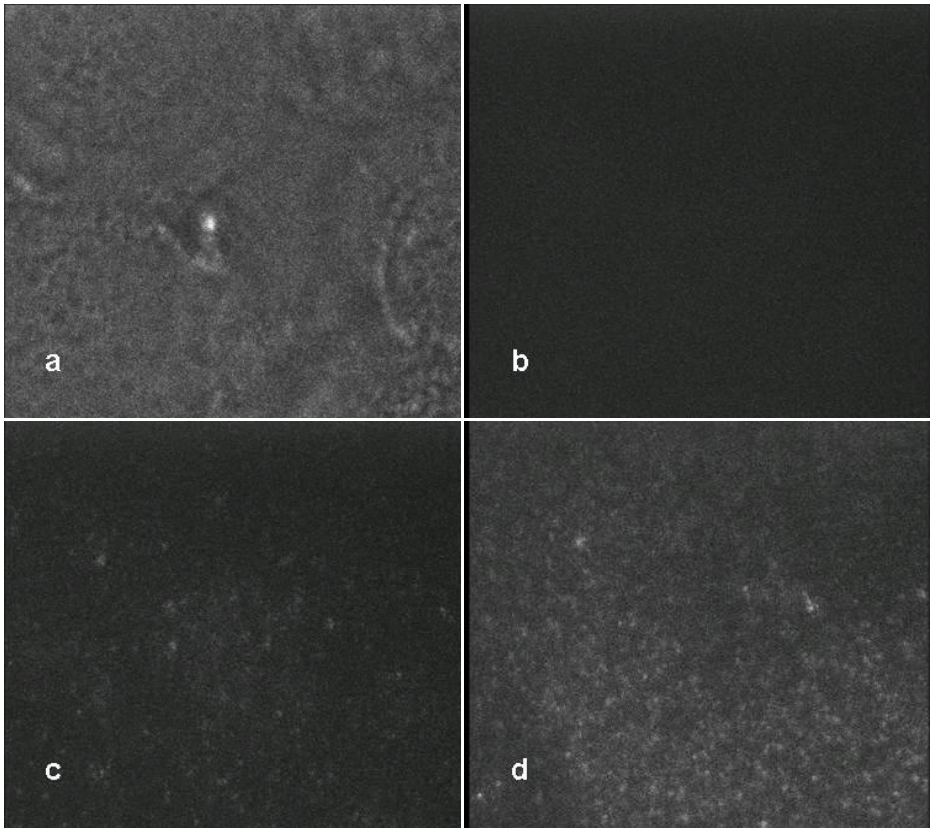

FIG 5: TIRFM images showing 293T cells with no prominent localization of Rhodamine-taxol conjugate on cell membrane even with high concentration such as 7 nM. a) Phase contrast micrographs of 293T cells, b) Before addition of Rhodamine-taxol conjugate, c) & d) after addition of RT conjugate at 10 min and 1 h.

5.2. Confocal studies:

RTc and Caveolin-1-GFP localization was clearly studied using confocal microscopy. With the treatment of RTc, Caveolin-1-GFP started forming clusters within 5 minutes and RTc started localizing on the cell surface with respect to Caveolin-1-GFP localization (FIG 6). Clusters of RTc were seen prominently than that of the individual spots. This probably infers the early recruitment of Caveolin-1 and internalization of the caveolae. However the intensities of RTc observed were not that prominent as that of the Caveolin-1- GFP.

After about 1 h RTc localization was seen very prominently through out the periphery of the cells wherever Caveolin-1-GFP was localized. An important observation found in confocal imaging was the cluster formation which was prominently seen even after 3 h and receded after 9 h (FIG 6). This probably infers the surface recruitment of Caveolin-1-GFP followed by internalization. RTc reached saturation after 3-4 h which was inferred by the diffused state of signal.

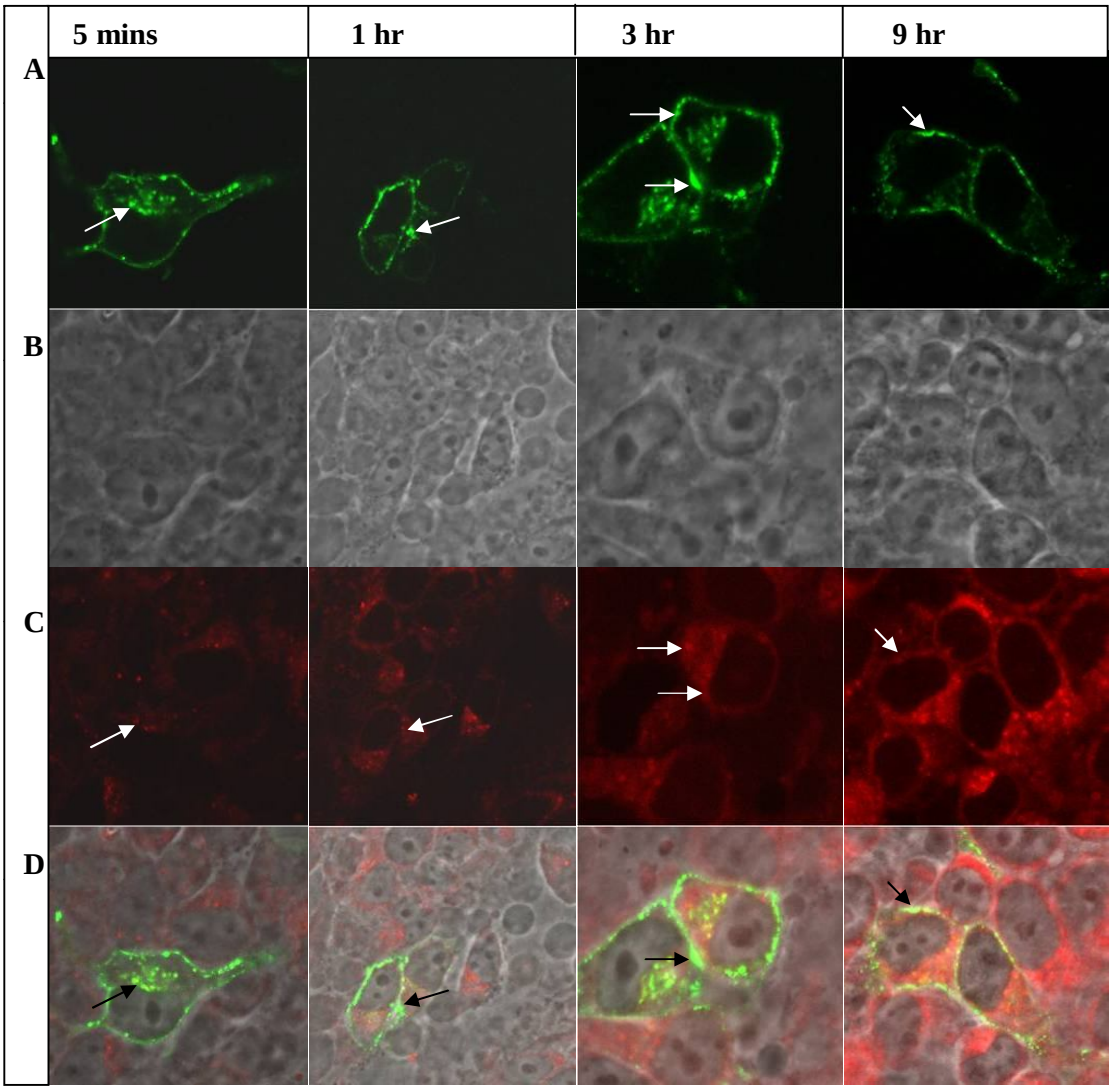

FIG 6: Localization of Caveolin-1-GFP and Rhodamine-taxol conjugate on HeLa cells as examined by confocal microscope. Panel A shows Caveolin-1-GFP localization, Panel B shows phase contrast images, Panel C shows RTc localization and Panel D shows merged images of Caveolin-1-GFP signal and RTc signal.

6. Discussion

Our studies suspected a possible interaction between taxol and Caveolin-1 and probably suggest that the taxol side chain may play a role in these interactions (Neesar et al, 2008). It is reported that taxol side chain can interact with the aromatic amino acids of Caveolin-1 (97YWFYRL102) which have been projected to insert into cytoplasmic side of the cell membrane. Thus the present study was to extend more focus on the interactions. The modifications done on the taxol molecule to couple with Rhodamine were exclusively done on OH group at 7^{th} carbon (Magri and Kingston, 1998; Mellado et al, 1984). These modifications did not result in any change in its cytotoxic activity and its ability to interact with Caveolin-1 which was quite evident by the localization of Rhodamine-taxol conjugate on cell surface. The cell lines used for the study were chosen based on their expression abilities of Caveolin-1. As HeLa cell show high expression of Caveolin-1, in A431, it is moderately expressed and in 293T cell line, its expression is very low (Koleske et al, 1995). This helped us to understand the role of Caveolin-1 in taxol mediated cytotoxicity.

Previous studies showed that taxol upregulates the expression of Caveolin-1 in MCF-7 cell line (Yang et al, 1998). Further our studies also showed that Caveolin-1 surface recruitment is seen when HeLa cells were treated with taxol followed by withdrawal, which infers the internalization of caveolae. With these studies it is known that there is some peculiar Kiss and Run dynamics seen when the cells are treated with taxol and the possible interactions involved between taxol and Caveolin-1. With the treatment of low concentrations of RTc (2-7 nM) similar dynamics of Caveolin-1 was seen on cell membranes of HeLa and A431 cell lines as studied by TRIF microscopy. The method employed is a good tool to examine the events that occur at/beneath plasma membrane. RTc started localizing on the cell surface after about 5 minutes and reached saturation after 2-3 h. New cluster formation of the RTc was seen similarly as observed in Caveolin-1 forming caveolae. A large amount of Rhodamine-taxol seems to accumulate at cell membrane.

The HeLa cells expressing Caveolin-1-GFP, before treatment, exhibited characteristic K&R events which are identical to the observations reported by Pelkans and Zerial. With the addition of RTc there was immediate surface recruitment Caveolin-1-GFP. As

the RTc started localizing on the cell surface, it was interesting to see the formation of Caveolin-1-GFP clusters and RTc clusters simultaneously using respective filters. These RTc clusters, however, were seen diffusing with increase in time inferring the possible internalization of RTc by caveolae.

Interesting observations were acquired when 293T cells were treated with Rhodamine-taxol conjugate. There was no defined accumulation of RTc on the cellular surface of 293T cells. Even with high concentrations of RTc, there was no localization on the cell membrane and we could not observe any clusters on the cell surface after about 3 h of treatment. This clearly indicates that in localization of taxol on the cell surface there is a definite role played by Caveolin-1. This also suggests that taxol enhances expression of Caveolin-1 and might be engulfed through caveolae showing the "Kiss and Run" dynamics before it actually triggers the apoptosis. These observations helped us understand the interactions involved between taxol and Caveolin-1. These observations lead to the conclusions that Taxol probably interacts with Caveolin-1, caveolae helps in the internalization of taxol and the amount of taxol binding to the cell surface is greater than the cytotoxicity shown.

7. References

1. Koleske AJ, Baltimore D and Lisanti MP. 1995. Reduction in caveolin and caveolae in oncogentically transformed cells. Proc. Natl. Acad. Sci. USA. 92, 1381-1385.
2. Magri NF and Kingston DGI. 1998. Modified taxols, 4. Synthesis and biological activity of taxols modified in the sidechain. J. Natl. Prod, 51, 298.
3. Manfredi JJ and Horwitz SB. 1984. Taxol: an antimitotic agent with a new mechanism of action. *Pharmacol. Ther.*, 25, 83-125.
4. Mellado W, Magri NF, Kingston DGI, Garcia AR, Orr GA and Horwitz SB. 1984. Preparation and biological activity of taxol acetates. Biochem. Biophys. Res. Commun. 124. 329.
5. Neesar A, Sreekanth D, Saumya SS, Amita S, Absar A, Islam KM and Krishnasastry VM. 2007. Side chains of Taxol and 10-DeacetylbaccatinIII

induce distinct changes in the 'kiss and Run' dynamics of caveolae. FEBS Letters.

6. Pelkmans L and Zerial M. 2005. Kinase-regulated quantal assemblies and kiss-and run recycling of caveolae. Nature. 436, 128-133.
7. Rowinsky EK and Donehower RC. 1995. Paclitaxel (taxol). N. Engl. J. Med. 332, 1004-1014.
8. Shajahan AN, Wang A, Decker M, Minshall RD, Liu MC and Clarke R. 2007. Caveolin- 1 tyrosine phosphorylation enhances paclitaxel-mediated cytotoxicity. J. Biol. Chem. 282, 5934-5943.
9. Yang CPH, Galbiate F, Volonte D, Horwitz SB and Lisanti MP. 1998. Upregulation of caveolin-1 and caveolae organelles in taxol- resistant A549 cells. FEBS letters. 439. 368- 372.

Chapter 7

General Discussion and Conclusions

Endophytic microbes from *Taxus baccata* (stem, bark and needles), growing at higher altitudes of West Bengal, India were isolated and exploited for taxol production. Methods employed to isolate microbes resulted in successful isolation of mostly fungal endophytes (Moutia and Dookuna, 1999). Majority of endophytes isolated were slow growing, which is one of the characteristic feature of endophytes and were unusual fungi representing different genera. Forty endophytic fungal strains were isolated and after attaining purity, were screened immunologically for taxol production. Among the fungal cultures, one strain designated as AAT-TS-4_1 was detected to be taxol producing. The media containing precursors such as benzoic acid, sodium benzoate, phenylalanine and pyridoxine was found to be very suitable for the fungus to grow and synthesize the taxol molecule. Taxol production increased exponentially with an increase in growth of the fungal culture (21 days), indicating that taxol is produced maximally at late log phase or early stationary phase of the fungal growth, which is quite often seen in secondary metabolites production. However, taxol could be estimated in culture as early as two days in low concentrations but these concentrations were much higher than reported after 21days (Strobel et al, 1993). Taxol production was estimated to be high in culture broth as compared to fungal mycelium indicating that the metabolite is secreted into the medium. Production was also observed to be maximum in 2 L flasks indicating the requirement of plenty of oxygen and surface area. As the fungus has some industrial and biotechnological importance, it was characterized based on the morphological and molecular evidences. The culture on solid media took more than a week for its optimum growth, which is quite evident of it being an endophyte (Petrini, 1996). Microscopic analyses show the mycelia to be hyaline, septate bearing conidiophores which are verticillium-like, a characteristic feature of *Gliocladium* sp. Phialides are solitary or produced in a group of 2-5, straight, smooth, and are verticillium-like. Conidia are produced in a small moist cluster apically and are smooth, oval to cylindrical to curved, hyaline, single celled, and variable in shape and size which is typically seen in *Gliocladium* sp (Hans et al, 1999). All the mentioned characteristics are identical to those described for the fungus *Gliocladium* sp. (Barnett et al, 1998), hence fungus AAT-TS-4_1 can be referred as *Gliocladium* sp.

In sequence analyses using BLAST and ClustalW, both ITS region sequences (0.2 kb and 0.3 kb sequences) and 18S rRNA sequence (1.1 kb) show highest similarity with genera- *Gliocladium, Bionectria*, and *Clonostachys*. All the three genera indicated share similarities in morphological and molecular characters. However *Bionectria* (anamorph) and *Clonostachys* (teleomorph) belong to imperfect fungi and family Bionectriaceae, while *Gliocladium* belongs to family Hypocreaceae. The phylogenetic studies of ITS region sequences indicate that the nearest relative of the fungus AAT-TS-4_1 is either from genus *Gliocladium* or *Clonostachys*, while 18S sequence indicate the closest relative to be *Nectria* sp. which is a teleomorph of *Gliocladium* sp. Considering the morphological characters we identify the fungus as *Gliocladium* sp. as the fungus does not show any asci formation which is very often seen in *Bionectria* and *Clonostachys* genera. The sequence analyses and phylogenetic analyses do support the identification. However in recent reports, many species from genus *Gliocladium* are classified under *Clonostachys* (anamorph) and *Bionectria* (teleomorph) based on morphological and molecular similarities (Hans et al, 1999).

Gliocladium sp., for the first time, has been isolated from any *Taxus* sp. producing taxol and this would be the second report to find *Gliocladium* sp as an endophyte. Strobel, et al and others have however isolated taxanes from different endophytic fungal species (*Taxomyces andreanae, Pestalotiopsis, Pestalotia, Fusarium, Alternaria* and others) obtained from *Taxus* sp. that are common to Europe, Asia and North America. The isolation of taxol from the culture of *Gliocladium* sp. is the first demonstration of its occurrence in fungi isolated from Indian Yew tree *Taxus baccata* also. In conclusion, we have isolated an endophytic fungus *Gliocladium* sp. producing taxol, extra /intracellularly.

Further studies on the isolation of the taxanes produced by *Gliocladium* sp. indicate that the fungus produces 10 DAB III in the culture broth. Compound isolated and purified on TLC and HPLC showed similar spectroscopic and chromatographic properties as that of the 10 DAB III. In addition to 10 DAB III and taxol, this fungus also produces few unidentified taxanes, although in trace amounts. This study probably has its importance

in isolating 10 DAB III from fungus as there are many reports of baccatin III isolation but not 10 DAB III isolation.

The ability of *Gliocladium* sp. to make taxol was confirmed by isolation of a compound having chromatographic properties similar to those of standard taxol in three solvent systems A, B and C which showed a single dark bluish violet spot on TLC when sprayed with anisaldehyde reagent or vanillin sulfuric acid reagent. Putative taxol on HPLC C18 symmetry column showed a single symmetrical peak at retention time of 25.5 min that confirmed its homogeneity. Absorption maximum of the purified fungal taxol was found to be at 227 nm as reported earlier (Chan et al, 1994). In ESI-MS, molecular ions at *m/z* 854 attributing to the $(M+H)^+$ and at *m/z* 876 attributable to $(M+Na)^+$ confirmed its molecular weight to be 853 (Edward et al, 1994). MS/MS showed fragment ions at *m/z* 570 attributable to taxane ring substructure and at *m/z* 286 for the side chain substructure which are usually seen as taxol fragment ions (Thomas, 1992). ^{1}H NMR spectrum was identical with that of the standard taxol spectrum (Chmurny et al, 1992). Taxol obtained per liter of culture was estimated to be approximately 10 µg. The concentration of taxol produced is neither low nor high when compared with the other reports (Guo et al, 2006; Strobel et al, 1996), however, this is the first report on taxol from an endophyte of yew tree growing in India. Anti-tumor activity of taxol was checked against HL-60 (Leukemia) cell line, A431 (Epidermal carcinoma) cell line, and MCF-7 (Breast cancer) cell line, showing 58 %, 53 % & 46 % with 30 µM, 3.65 µM & 3.65 µM fungal taxol respectively. Taxol showed less cytotoxicity on HL-60 cell line, however in case of MCF-7 and A431, the cell-growth inhibition was significantly high even at low taxol concentration. A number of *Taxus* sp. has been reported to produce 10 DAB III (Xueli et al, 1998) and we have also isolated this compound from a 14-day old fungal culture. ESI-MS showed a molecular ion at *m/z* 545 and at *m/z* 567 attributable to $(M+H)^+$ and $(M+Na)^+$, inferring its mass to be 544 (Edward et al, 1994). 10 DAB III produced was 65 µg / L culture.

The other major study *viz*: the microbial transformation of taxol precursor molecules 10 DAB III and Side chain into biologically active taxanes was successfully achieved by using *Gliocladium* sp. The study was aimed to witness whether this fungus, which has all the machinery required to synthesize taxol, can couple the abundantly present 10

DAB III and easily synthesized side chain to biologically active taxanes. As postulated we did the transformation using fungus *Gliocladium* sp. which resulted in two major novel compounds. Further study was focused on these two major compounds which show high concentrations on TLC. The transformed compounds were purified by preparative TLC and HPLC. The homogeneity of the purified compound was determined by TLC using solvent systems A, B, and C. Of the two compounds seen on TLC one of the compound showed similar R_f values as that of the standard taxol (0.5) while the other compound has R_f value of 0.7. Complete transformation of the precursor molecules was not seen which was evident by presence of 10 DAB III on TLC and HPLC. However side chain (N-benzoyl-(2R, 3S)-3-phenylisoserine) could not be detected in either of them. Maximum conversion of the precursors was seen when 10 DAB III and Side chain were taken in 1:5 ratio respectively. The UV absorption analysis showed a peak showing absorption maxima at 225 nm (Theodoridis et al, 1998). Depending on the R_f values observed on TLC in different solvent systems and U.V absorbance it was postulated that the biotransformed molecule could have similar structure as that of taxol, although not exact. Further, our study was focused on the compound which showed similar R_f values as that of taxol as the other compound did not show proper molecular mass.

The formation of 10 Deacetyl paclitaxel using precursors 10 DAB III and side chain with the help of fungus *Gliocladium* sp. was authenticated when the LC-MS analysis and MALDI-TOF analysis showed peak at *m/z* 811 attributing to the M^+ ion of 10 Deacetyl paclitaxel (Kerns et al, 1994). Further fragment ion of 10 Deacetyl paclitaxel at *m/z* 568 attributing to taxane sub structure was also seen. However the peak obtained was considerably unstable and undergoes fragmentation easily, which is quite evident in spectrum. A peak at *m/z* 870 attributing to $(M+NH_4+CH_3CN)^+$ of 10 Deacetyl paclitaxel was consistently seen constituting to its stability. Proton NMR analysis of the purified compound showed that the signals caused by the acetate group at 2.5 ppm was missing *(which is seen in taxol) indicating the compound to be 10 Deacetyl paclitaxel. Further analysis of the fractions obtained showed that taxol was also formed but in low concentrations. 10 Deacetyl paclitaxel does mimic the mode of activity as that of the taxol and its derivatives in terms of it showing affinity to bind to tubulin and polymerizing them which is evident by turbidity assay (Kumar, 1981). Cytotoxicity of

10 Deacetyl paclitaxel against A431 does prove the above statement. MIC of the compound was determined to be 6.7 µM against THP1 cell line.

In conclusion, we can say that the above biotransformed, purified molecule showing chromatographic and spectroscopic similarities to taxol is confirmed to be 10 Deacetly paclitaxel. This report on its own is a novel discovery of converting abundantly present taxol precursor 10 DAB III and easily synthesized side chain into biologically active 10 Deacetyl paclitaxel, a taxane molecule using taxol producing fungus *Gliocladium* sp.

Synthesis of fluorescent taxol conjugates using different fluorescent compounds and using CdS nanoparticles was achieved by derivatizing taxol chemically. The objective behind the synthesis was to study the interactions of these taxol conjugates with cell membrane moieties, to explore the fluorescent properties of CdS-taxol conjugate and to study the caveolin dynamics with taxol treatment and taxol fluorescent conjugates. Taxol was derivatized chemically to 2'-glutaryl hexanediamine taxol and 7-succinyl taxol with a free amino and carboxyl group respectively. These modifications have eased the mechanism of coupling fluorescent molecules to taxol. Ideally none of the fluorescent molecules should give any toxic effect on the samples treated as they are used for many *in vitro* and *in vivo* studies. In our studies, the FITC and Rhodamine dyes which we used are conventionally used for many cell based studies and were observed that both of them do not have any toxic effect on cells.

FITC- taxol conjugate was successfully synthesized and purified using TLC and HPLC. UV-Vis absorbance spectrum of the purified compound reveals that a hump at 430 nm attributes to FITC absorbance. However it is not similar as that of plain FITC which shows absorbance maxima at 488 nm. The shift in the λ max might be because of coupling with the taxol moiety which is usually seen in many cases. Emission spectrum obtained when the conjugate was excited at 488 nm shows that there is a shift in the λ max, this also might be a reason as described above. However, the spectrum was broad which was same with plain FITC as well. Higher cytotoxicity shown by conjugate than plain taxol could be because of the increased hydrophilicity of the conjugate. Plain taxol is highly hydrophobic but when modified with glutaric anhydride, the resulting glutaryl taxol is hydrophilic because of the free carboxylic group conferred on it. Further on

treatment with hexanediamine, the product glutaryl-hexanediamine taxol gets an additional amino group which also contributes to the hydrophilic nature. These derivatives are more potent as cytotoxic molecules than the plain taxol. FITC-taxol conjugate thus synthesized could not be used for further *in vivo* studies because of its spectroscopic disadvantages in using along with GFP.

To exploit the CdS nanoparticles fluorescent properties, CdS nanoparticles were coupled with taxol. Taxol was successfully derivatized to hexanediamine taxol and the free amino group of it was targeted to couple with the carboxyl group of capping protein present on CdS nanoparticles (Ansary et al, 2007). CdS-taxol conjugate on HPLC showed absorbance on both the wave lengths attributing to taxol and CdS absorbance maxima. The fluorescence spectrum of the conjugate showed a very sharp emission spectrum with λ max at 398 nm. The emission spectrum also infer that even after CdS coupling with taxol it did not lose its fluorescence properties and showed similar intensities as seen in plain CdS nanoparticles. The conjugate also showed cytotoxicity greater than plain taxol against THP1 cell line. In many of recent reports it is indicate that CdS nanoparticles do show cytotoxicity. Thus the increase in cytotoxicity might account from CdS nanoparticles apart from increased hydrophilic nature of the drug. Fluorescent microscopic studies reveal that the conjugate starts accumulating on the cell surface after about 15 minutes and the signal intensify by 30 minutes. Fluorescence appears homogenous throughout the cell surface and does not accumulate on non cellular area. This indicates the probable interaction between conjugate and some moiety on cell membrane. These results do support our studies on taxol and its interactions with caveolin (Neesar et al, 2007), a marker protein on cell membrane (Pelkmans et al, 2005). The fluorescence signals were diffused and did not appear as bright spots. This could be because of size of nanoparticles which may not be the size of quantum dots (2-5 nm) which can be used for imaging or could be because of the use of inefficient light source. However, our studies revealed that biologically synthesized nanoparticles can not only be used for fluorescence imaging but can also be easily coupled with drugs. These studies also infer that CdS nanoparticles indeed can be used, in addition to an anticancerous drug as anticancerous agents (Li et al, 2007).

Coupling of taxol with rhodamine was successfully carried out by derivatizing taxol to 7-succinyl taxol. Further absorbance spectrum of the conjugate shows two peaks at wave length 227 nm and 550 nm attributing to λ max of taxol and rhodamine. Respectively, fluorescence spectrum of the conjugate showed emission spectrum with a smooth and sharp peak with λ max at 580 nm (Sheikh et al, 2000). Cytotoxicity of the conjugate did not increase as was seen in case of other conjugates in comparison with plain taxol. Further, this compound was used for *in vivo* studies to understand taxol interactions with that of caveolin on cell membrane.

HeLa cells when treated with Rhodamine-taxol showed that taxol accumulates on the cell surface and increases the recruitment of Caveolin-1. It was found that the amount of taxol binding to the cell membrane is greater than the resulting cytotoxicity shown. Dynamics of Rhodamine-taxol and Caveolin-1-GFP changed with the increase in time. As seen incase of Caveolin-1-GFP, which shows sudden recruitment onto the cell surface followed by time depended withdrawal. Rhodamine-taxol also showed similar dynamics, the increase in amount of taxol binding to the cell surface increases with time, but taxol internalization was found to be very slow. Probably this slow internalization process might account for the low cytotoxicity shown in contrary to the greater amounts of taxol binding to the cell surface. It was interesting to see no significant accumulation of Rhodamine-taxol on the cell surface of 293T cell line which has very low expressions of Caveolin-1. These observations lead to the conclusions that Taxol probably interacts with Caveolin-1 and caveolae helps in the internalization of taxol.

In conclusion we state as following:-

- Endophytic fungi were successfully exploited from *Taxus baccata* growing at higher altitudes of West Bengal, India.
- These fungi were screened for taxol production immunologically, out of forty tested, one designated as AAT-TS-4_1 was found to produce taxol.
- Fungus AAT-TS-4_1 was classified as *Gliocladium* sp. based on its morphological and molecular characters.

- Taxol produced by the fungus at different flask volumes, time intervals and localization of taxol was quantified immunologically.
- Putative taxol and 10 DAB III was purified by using column chromatography, preparative TLC and HPLC.
- Homogeneity of fungal taxol was determined by TLC on three different solvent systems. Fungal taxol R_f was found to be 0.5.
- Taxol produced by fungus was quantified to be 10 µg/ L and 10 DAB III to be 65 µg/ L.
- Molecular mass of the fungal taxol and 10 DAB III was determined to be 854 *m/z* (M+H), 876 *m/z* (M+Na) and 545 *m/z* (M+H), 567 *m/z* (M+Na) respectively by ESI-MS. MS/ MS showed fragments at 570 and 286 *m/z* attributing to taxane and sidechain substructure.
- Further characterization was done by comparison of standard taxol proton spectrum with that of fungal taxol proton spectrum and was found to be similar.
- Cytotoxicity of fungal taxol was determined against three different cell lines (A431, HL-60 and MCF-7) and found to inhibit 58 % cell proliferation with 30 µM fungal taxol against HL-60 (leukemia) cell line, 46 % with 3.65 µM fungal taxol against MCF-7 (breast cancer) cell line and 53% with 3.65 µM fungal taxol against A431 (epidermal carcinoma) cell line.
- Antibacterial potential of the commercially available taxol, 10 DAB III and Baccatin IIII against eight pathogenic bacteria (*Staphylococcus aureus, Proteus vulgaris, Streptococci group D, Bacillus, Escherichia coli, Klebsiella pneumoniae, Pseudomonas aeruginosa, Serratia morganii*) was determined by microtiter plate assay. Out of eight bacteria tested five of them were found to be susceptible to taxol, 10 DAB III and Baccatin IIII.
- Microbial transformation of taxol precursors, abundantly present 10 DAB III and easily synthesized side chain into biologically active taxanes was done using fungus *Gliocladium* sp.
- Two novel biotransformed compounds were observed on TLC, one with similar R_f value to that of the taxol (0.5) and other one with R_f value 0.7.
- These putative taxanes were purified by preparative TLC and HPLC. Taxanes were quantified using immunoassay.

- Molecular mass of taxane was determined to be 811 *m/z* (M^+) by LC- MS and MALDI-TOF attributing to the molecular mass of 10 Deacetyl paclitaxel.
- Proton NMR spectrum showed similar proton profile as that of 10 Deacetyl taxol.
- 10 Deacetyl taxol showed affinity for tubulin and showed activity against A431 and THP1.
- Taxol was successfully modified into hexanediamine taxol and succinyl taxol to couple with FITC, Rhodamine and CdS.
- Fluorescent conjugates FTIC-taxol, Rhodamine-taxol and CdS-taxol were characterized based on spectroscopic and fluorescence properties.
- HL-60 cells and THP1 cells when treated with CdS-taxol conjugate showed accumulation of CdS signals on the cell surface.
- All the conjugates showed cytotoxicity greater than plain taxol.
- HeLa cells when treated with Rhodamine-taxol conjugate showed differences in the dynamics of Caveolin-1 and taxol which was time and concentration dependent. Confocal microscopic studies revealed the possible taxol interactions with Caveolin-1.

Reference

1. Ansary AA, Anil SK, Krishnasastry MV, Majid KA, Sulabha KK, Absar A and Khan MI. 2007. CdS quantum dots: Enzyme mediated in vitro synthesis, characterization and conjugation with plant lectins. J. Biomed Nano. 3, 406-413.
2. Barnett HL, Hunter BB. 1998. Illustrated genera of imperfect fungi (Fourth edition). APS Press, USA.
3. Chan KC, Alvarado AB, McGuire MT, Muschik GM, Issaq HJ, Snader KM. 1994. High-performance liquid chromatography and micellar electrokinetic chromatography of taxol and related taxanes from bark and needle extracts of *Taxus* species. J. Chrom. B. 657: 301-306.
4. Chmurny GN, Hilton BD, Brobst S, Look SA, Witherup KM, Beutler JA. 1992. ^{1}H- and ^{13}C-NMR assignment for taxol, 7-epi-taxol and cephalomannine. J. Nat Prod. 55: 414-423.

5. Edward KH, Kevin JV, Susan EH. 1994. Profiling taxanes in Taxus extracts using LC/MS and LC/MS/MS techniques. J. Nat Prod. 57: 1391-1403.
6. Guo BH, Wang YC, Zhou XW, Hu K, Tan F, Miao ZQ, Tang KX. 2006. An endophytic taxol-producing fungus BT2 isolated from *Taxus chinensis* var. *mairei*, Afr. J. Biotec. 5: 875-877.
7. Hans JS, Gary JS, Keith AS, Walter G. 1999. Classification of the mycoparasite *Gliocladium roseum* in *Clonostachys* as *C. Rosea*, its relationship to *Bionectria ochroleuca*, and notes on other *Gliocladium*- like fungi. Mycologia. 91(2): 365- 385.
8. Kerns E, Volk KJ, Hili SE and Lee MS. 1994. Profiling of taxanes in *Taxus* extracts using LC/MS and LC/MS/MS techniques. J. Nat. Prod. 57, 1391-1403.
9. Kumar N. 1981. taxol induced polymerization of purified tubulin, J. Biol. Chem. 256, 10435-10441.
10. Li J, Wu C, Dai Y, Zhang R, Wang Xuemei, Fu D, and Chen B. 2007. Doxorubicin-CdS nanoparticles: A potential anticancer agent for enhancing the drug uptake of cancer cells.
11. Moutia M and Dookuna A. 1999. Evaluation of surface sterilization and hot water treatments on bacterial contaminants in bud culture of sugarcane. Expl Agric. 35: 265-274.
12. Neesar A, Sreekanth D, Saumya SS, Amita S, Absar A, Islam KM and Krishnasastry VM. 2007. Side chains of Taxol and 10-DeacetylbaccatinIII induce distinct changes in the 'kiss and Run' dynamics of caveolae. FEBS Letters.
13. Noh MJ, Yang JG, Kim KS, Yoon YM, Kang KA, Han HY, Shim SB, Park HJ. 1999. Isolation of novel microorganism, *Pestalotia heterocornis,* producing paclitaxel. Biotech and Bioeng. 64: 620-623.
14. Pelkmans, L. and Zerial, M. 2005. Kinase-regulated quantal assemblies and kiss-and-run recycling of caveolae. Nature. 436, 128-133.
15. Petrini O. 1996. Ecological and physiological aspects of host-specificity in endophytic fungi. In: redline S. C., Carris L. M., eds, Endophytic fungi in grasses and woody plants, APS Press, St. Paul (USA), pp. 87-100.
16. Sheikh SH, Abela BA and Mulchandani A. 2000. Development of a fluorescence immunoassay for measurement of paclitaxel in human plasma. Analytical Biochem. 283, 33-38.

17. Stierle A, Strobel G, Stierle D. 1993. Taxol and taxane production by *Taxomyces andreanae*, and endophytic fungus of pacific yew. Science. 260: 214-216.
18. Strobel G, Yang X, Sears J, Kramer R, Sidhu RS, Hess WM. 1996. Taxol from *Pestalotiopsis microspora*, an endophytic fungus of *Taxus wallachiana*. Microbiology. 142: 435-440.
19. Strobel GA, Hess WM, Ford E, Sidhu RS, Yang X. 1996. Taxol from fungal endophytes and the issue of biodiversity. J. Industrial microbiol. 17: 417-423.
20. Suffiness M. 1993. Taxol: from discovery to therapeutic use. In: Bristol JA, (Ed), Annual reports in Medicinal Chemistry, Vol: 28, Michigan, USA.
21. Theodoridis G, Laskaris G, De Jomg CF, Hofte ATP and Verpoorte R. 1998. Determination of paclitaxel & related diterpeniods in plant extracts by high performance liquid chromatography with U. V detection in high performance liquid chromatography- mass spectrometry. J Chrom A. 802, 297- 305.
22. Thomas D., Clure Mc, Karl HS. 1992. The mass spectrometry of taxol. J Am Soc Mass Spectrom. 3: 672-679.
23. Wang J, Li G, Lu H, Zheng Z, Huang Y, Su W. 2000. Taxol from *Tubercularia* sp. strain. TF5, an endophytic fungus of *Taxus mairei*. FEMS Microbiol. Let. 193: 249-253.
24. Xueli C, Yu T, Tian ZY, Yoichiro I. 1998. Separation and purification of 10-deacetylbaccatin III by high-speed counter-current chromatography. J. Chrom A. 813: 397-401.

Author's Publications

1) Neesar. K, **Sreekanth. D**, Amitha, Khan. M. I, Ahmad. A, Krishnasastry. M. V. 2008. Caveoline dynamics with respect to Taxol, 10 Deacetlybaccatin III and Baccatin III treatment in Hela cells. FEBS Letter. 582. 3595-3600.

2) **D. Sreekanth**, S. K. Gupta, A. Syed, B. M. Khan, M. I. Khan, A. Ahmad Molecular and morphological studies of a Taxol producing endophytic fungus, *Gliocladium* sp from *Taxus baccata*. (Communicated).

3) **D. Sreekanth**, A. Syed, S. Sarkar, D. Sarkar, B. Santhakumari, M. I. Khan, A. Ahmad. Production, purification and characterization of taxol and 10DAB III from a new endophytic fungus *Gliocladium* sp. isolated from the Indian yew tree, *Taxus baccata*. (Communicated).

4) **D. Sreekanth**, A. Syed, M. I. Khan, A. Ahmad. Transformation of taxol precursors 10 Deacetly baccatin III and side chain into biologically active taxane by fungus *Gliocladium* sp. (Manuscript under preparation).